Introduction

The mammalian heart is the first functional organ in vertebrate embryos. In humans, it beats spontaneously by the fourth week of development. Its development begins with the formation of two endocardial tubes which merge to form the tubular heart (primitive heart tube). It loops and become separated into four chambers and paired arterial trunks. (Moorman, *et al*., 2003). According to Moorman and Christoffels (2003) and van den Hoff *et al.* (2004) the heart development started when the first mesodermal cells migrated anterolaterally and formed the bilateral heart-forming primordia during gastrulation. The main walls of the heart were formed between day 27 and day 37 of the development of the embryo. Growth began with two tissue masses which were actively growing towards each other until they finally merged and split into two separate tubes (Fernández, 2002).

The topographical anatomy, conducting system and blood supply of the heart of adult camel are considered similar to those of other domestic mammals (Kanan, 1971; Smuts and Benzuidenhout, 1987; Taha and Abdel-Magied, 1996; Nawal, *et al.*, 2002; Marwa-Babiker and Taha, 2015).

Myocardial bridges (MBs) are cardiac abnormalities in which segments of coronary artery penetrated the myocardium. However, MBs were considered normal in adult dromedary camels (Marwa-Babiker, *et al.*, 2013). They were studied in adult camel by Taha and Abdel-Magied, (1996), Erden, *et al*. (2006) and Marwa-Babiker and Taha (2013). The presence of gross MBs in camel foetuses was reported previously in the third trimester (Marwa-Babiker and Taha, 2013).

Prenatal studies on the morphological changes in the development of the heart and the myocardial bridges of the camel appeared to be virtually

1

lacking. Hence, the present investigation is undertaken to study the morphology and morphometry of camel foetal hearts.

Objectives

General objective:

To study the morphology and morphometry of the pre-natal development of dromedary heart.

Specific objectives:

1. The development of the cardiac muscles.
2. The occurrence and structure of the myocardial bridges.
3. Histogenesis of the prenatal cardiac conducting system.
4. The ultrastructure of the whole heart, the cardiac muscles and myocardial bridges using scanning and transmission electron microscopy.
5. The ultrastructural morphometry of the cardiac muscles and myocardial bridges.

CHAPTER ONE
LITERATURE REVIEW

1.1. Histology

1.1.1. The Cardiac Muscle

The heart is the first organ to form during embryogenesis and its early circulatory function is critical for the viability of the mammalian embryo. Hence, the developmental mechanisms which coordinate the formation and morphogenesis of this organ had received much attention among classical and molecular embryologists. Due to the evolutionary conservation of many of these processes, major insights had been gained from the studies of a number of vertebrates and invertebrate embryos (Zaffran and Frasch, 2002).

Cardiomyocyte formation was extensively studied during the development of chicken (Stalsberg and de Haan, 1969). This is due to the easy accessibility to the embryo and the extended developmental period during which the initial phase of development occurs. The cardiac progenitor cells are among the first mesodermal cells to form during gastrulation at stage 3 in chicken or at Carnegie stage (CS) 6 in human (O'Rahilly and Müller, 1987; Redkar, *et al.*, 2001).

Balogh and Sótonyi (2003) studied the early cardiac development in rabbit. They have stated that on the 9th day of gestation the embryonic disc appeared, on the 10th day the single cardiac tube was formed, on the 11th day the bulboventricular loop was formed and the heart consisted of three chambers. On the 12th day the partitioning of atria and ventricles was close to its end. On the 13th day the heart consisted of four chambers and on the 14th day the developmental stage of the heart was very similar to that seen in the newborn. In rabbits the most intensive development of the heart took place in the period between the 10th and the 13th day.

The smooth zones of the interventricular septum and the pulmonary and aortic roots, compared to the trabeculated parts of the right and left ventricles, were recognizable. The transition zone between compact and trabeculated tissues was called the spongy layer and it was recognized as a network of fine trabeculations, the different layers of the ventricular myocardium. Non-compaction of the myocardium was associated with heart failure and sudden cardiac death (Savolainen, *et al.*, 2009).

Norman *et al.* (2000) undertook a longitudinal study to define the cardiac morphology and physiology of the developing zebra fish. Their studies included 48-hrs, 5-days, 2-weeks, 4-weeks, and 3-months post-fertilization of zebra fish eggs. They measured ventricular and body wet weights, and performed morphologic analysis on the heart with H&E and MF-20 antibody sections. Ventricular and body weight increased geometrically with development, but at different rates. Until maturity, the atrium showed extensive pectinate muscles, and the atrial wall increased two to three cell layers. The ventricular wall and the compact layer increased from three to four cell layers, while the extent and complexity in trabeculation continued. Further thickening of the heart wall was mainly indicated by an increase in cell size. These data defined the parameters of normal cardiac morphology and ventricular function in the developing zebra fish.

1.1.2. The Cardiac Conduction System

The first description of the anatomy of the nodes and atrioventricular conduction system appeared nearly 100 years ago. Since then the subject has been controversial, possibly because of the early researchers' imprecise knowledge of histology. The components and structure of the specific conduction system in humans are similar to those found in commonly used

laboratory animals. The conduction system is composed of specialized myocytes. Its atrial components, sinus node and atrioventricular node, are in contact with atrial myocardium. The bundle of His penetrates the right fibrous trigone, then divides into two specialized ventricular branches (right and left), which are also surrounded by a fibrous sheath that separates the specialized myocytes from the ordinary myocardium. Only at the distal ramifications of the bundle branches the fibrous sheaths disappear allowing continuity with the ventricular myocardium (Sánchez-Quintana and Yen Ho, 2003).

Miquerol *et al.* (2010) stated that the ventricular conduction system controlled the prevalence of electric activity through the heart to coordinate cardiac contraction. This system was composed of specialized myocytes organized in defined structures including central components and a peripheral Purkinje fibre network. A biphasic mode of development, lineage limitation followed by limited outgrowth underlied establishment of the mammalian ventricular conduction system.

The sinus node of yak has been studied using the histological methods. The sinus node artery of yak is also determined by the injection-corrosion casting technique, the angiographic and histological methods (Duan *et al.,* 2012).

Serial histological sectioning revealed that the sinus node in camel was located 0.5 mm beneath the epicardium, near the junction between the cranial vena cava and the right atrium at the sulcus terminalis. Its shape was elongated, and oblong; 28.25 mm in length, 5.75 mm in width and 5.38 mm in thickness. The maximum section area was 101.66 mm^2. The central artery of the node originated from the circumflex branch of the left coronary artery,

and throughout its length in the substance of the sinus node, it had an internal elastic membrane (Ghazi and Tadjalli, 1996).

Histologically, the sinus node of the camel contained a central artery and a framework of collagen fibres, which were distributed around the central artery. The nodal cells were irregularly organized around the central artery in two types, namely (p) cells and transitional cells. The (p) cells had a perinuclear clear zone but the transitional cells contained more myofibrils. The intercalated discs were not present. At the periphery of the sinus node there were many nerve fibres and a ganglion. The purkinje fibres were present within the atrial myocardium as well as within the ventricular myocardium (Ghazi and Tadjalli, 1996).

The anatomy and histology of the atrioventricular bundle (AVB) and sinus node was studied in the heart of the dromedary camel (Ghazi and Tadjalli, 1993 and 1996). They stated that the trunk of the atrioventricular bundle (Bundle of Hiss) was a direct continuation of the atrioventricular (AV) node with no sharp line of demarcation between the node and the bundle. The atrioventricular bundle ran through the fibrous trigone and entered the lower part of the interventricular membranous septum beneath the right endocardium. They lay then over or slightly to the side of the centre of the muscular interventricular crest. The AVB of camels measured 4.12±1.00 mm in length, 3.66±1.13 mm in width and 1.13±1.85 mm in thickness, its maximum sectional area being 12.68±6.13 mm^2 (Ghazi and Tadjalli, 1993 and 1996).

Histologically, the AVB in the heart of camels comprised multiple strands of Purkinje cells separated by collagen fibres and surrounded by connective tissue. It resembled that in humans and dogs except that, in

camels, intercalated discs were present at the intercellular connections in the AVB (Ghazi and Tadjalli, 1996).

The development of the atrioventricular bundle (AVB) and ventricular Purkinje system and their innervation has been studied in sheep foetuses from 27 to 140 days of gestation (term is 147 days) (Canale, *et al.*,1987).The AVB initially consisted of a primordium, which lacked innervation and was composed of small, relatively undifferentiated myocytes. Differentiation of Purkinje-like cells within the AVB began near its distal end and extended towards the atrioventricular node (AVN). Differentiation of the ventricular Purkinje system extended distally from the region of bifurcation of the AVB from cells that were indistinguishable from the working myocardium and continuous with the AVB primordium. Differentiation of Purkinje-like AVB cells was complete by 46 days gestation but Purkinje fibres were still differentiating within the ventricular wall at 60 days of gestation. The main morphological changes included a large increase in cell size and organization into strands, development of characteristic glycogen-filled regions containing many intermediate filaments and early development of myofibrillar M lines compared to the working myocardium. The differentiation of AVB cells and the ventricular Purkinje system preceded their innervation.

Canale *et al.* (1987) stated that in sheep the AVB became innervated earlier than ventricular Purkinje fibres. Intimate contacts between proximal AVB cells and nerve axons were present at 60 days of gestation. Nerve fibres were observed in the septomarginal band at this time. Although the AVB and ventricular Purkinje system of adult sheep composed morphologically of similar cells, they differed in origin and their mode of differentiation as well as timing and intimacy of innervation. Innervation

7

was not part of the developmental mechanism leading to the differentiation of Purkinje fibres (Canale, *et al.,* 1987).

1.1.3. Myocardial Bridges (MBs)

The myocardial bridges (MBs) are considered as an anomaly characterized by intramyocardial paths of an epicardial coronary artery segment. They were found during autopsies in the year 1737 and were described angiographically in 1960 (Darius, 2014). MBs were also defined as a congenital coronary abnormality in which a branch of a coronary artery passes intramurally through the myocardium (Kosinski and Grzybiak, 2001; Chen, *et al*., 2004; Singh, *et al*., 2005; Alegria, *et al*., 2005; Demirsoy, *et al*., 2006). They were also considered as structures consisting of heart muscle which passed above the coronary arteries or their branches (Chen and Lin, 2003; Kosinski, *et al.*, 2004; Aytan, *et al.*, 2006). The coronary arteries might dip into the myocardium for varying lengths and reappear on the heart's surface; this muscle overlying the segment of the epicardial coronary artery was termed a myocardial bridge (Loukas, *et al*., 2006; Bharambe and Arole, 2008).

Iuchi *et al*. (2013) stated that the anatomical properties of MBs, especially of its length and thickness, played decisive roles as regulators of atherosclerosis in the left anterior descending coronary artery regardless of the amount of adipose tissue around it.

In bovines, the histological appearance of the pre-myocardial bridge segments differed from the other segments with or without a myocardial bridge in that the intimal layer was well-developed (Shinjo, *et al.,* 2004).

Little work has been done on the myocardial bridge in camel and other domestic animals. A rare morphological research which has been conducted by Marwa-Babiker and Taha (2013). Marwa-Babiker and Taha (2015)

studied the histology of myocardial bridges in adult camel. Large amount of adipose tissue infiltrated the cardiac muscles of the bridge. The cardiac muscles distal to the bridges showed no signs of myocardial infarctions. Marwa-Babiker *et al.* (2013) and Marwa-Babiker and Taha (2015) considered the myocardial bridges as a normal feature in adult dromedary camel. However, to the best of our knowledge, there is no study of the myocardial bridge in the prenatal life of dromedary camels except the morphological research mentioned above.

1.2. Hitometry

There are very few reports on the cardiac histometry or the thickness of MBs in the available literature.

Qureshi *et al*. (2013) studied the effects of age and sex on the histometric values of blood pressure related organs including heart in teddy goats. Mean diameters, volumes and intramural connective tissue contents of right atrium, left atrium, right ventricle and left ventricle were recorded from cardiac specimens. Age affected none of the parameters mentioned before of the heart significantly. It is conceivable from these findings that the development of heart showed an increase parallel to the advancing age to adjust with the increasing blood pressure due to physiological development process. Sex, however, played a secondary role.

1.3. Ultrastructure

The internal cellular structures of the ventricular myocardium had been comparatively studied by transmission and scanning electron microscopy in sheep (Sybers and Ashraf, 1975). The scanning electron microscopy demonstrated the relationships between organelles like mitochondria, sarcoplasmic retiuclum, and nuclear envelope better than can be obtained by other methods (Sybers and Ashraf, 1975).

The studies carried out by Myklebust *et al.* (1975) SEM and TEM of the intracellular structure in sheep heart muscle cells revealed very good conformity, and it was evident that the described preparation procedure for SEM had preserved the fine structures of myofibrils, mitochondria, T-tubules and sarcoplasmic reticulum in an excellent life-like pattern. The three-dimensional demonstration of triads was of special interest and circumferentially arranged T-tubules.

Sheldon *et al.* (1976) have undertaken SEM in foetal and postnatal period in sheep between 90 days gestational age and 36 days postnatal age. Development of the transverse tubular system was visible as early as 90 days gestational age. Myofibrils in the 90-days foetus showed elongated mitochondria with constrictions and the mature myofibrils in later stages became oval and assumed their adult position in the perinuclear and interfibrillar regions. Myofibrillar development was sparse at 90 days and was most apparent in the subsarcolemmal region. Gradually the lateral addition of fibrils resulted in central displacement of the older myofibrils causing the sarcolemma to be drawn inward at its point of attachment at the Z-lines to form the T-tubules. At birth however, they resembled the adult configuration.

The embryonic development of the heart of rat was greatly dependant on the myocytes proliferation, which continued postnatally (Xavier-Vidal, *et al.*, 1997). The myocardium regeneration during postnatal period varied directly with the potential of cell proliferation. The electron microscopy showed myocytes well fixed with well-developped sarcomers disposed in an irregular form in the myocyte cytoplasm. The cardiac interstitium showed fibroblasts with characteristics of a great proteic synthesis. It suggested a

large number of binucleate cardiomyocytes during fetal period in the rat (Xavier-Vidal, *et al.*, 1997).

Kim *et al.* (1992) studied the ultrastructure of 44 normally developed human foetal hearts aged from 17 to 40 weeks gestation. Myofibril formation occurred by attachment of thin filaments into amorphous Z materials which were present in sarcolemmal plaques, sarcoplasmic condensations, desmosomes and in Z lines. Myofibrils radiated from these Z centers in many directions and branched and anastomosed with further development. This pattern of myofibrillar development continued throughout the whole foetal period. A transverse tubule system was clearly evident in later foetal development. It occurred by invagination of sarcolemma into myocardial cells and by the formation of subsarcolemmal caveolae. Mitochondria, well-developped Golgi complexes, glycogen granules and well-developped microvessels were found throughout the whole foetal period. Binucleated myocytes appeared by 32 weeks gestation and this suggested that myocyte hyperplasia might cease before birth in humans. Development of the myocyte was an ongoing process which may be continued in the postnatal period.

Chacko (1976) studied the ultrastructural differentiation of myocardium of Sprague-Dawley rat's embryos. Both thick (myosin) and thin (actin) filaments became identifiable for the first time in the tenth-day myocardium when the heart was pulsating but circulation was not established. The appearance of the myofilaments and synthesis of Z lines was concomitant. There was a rapid proliferation and differentiation of most of the organelles by the eleventh day of gestation and during the subsequent days. The myofilaments became organized into fully formed striated fibrils. Intercalated discs appeared as small wavy lines on the eleventh-day and

became plicated in later stages and served as cell boundaries and points of attachment for myofilaments and fibrils. There was a tangible change in the number and morphology of mitochondria from the tenth to eleventh day and during later stages of development when the heart became functional. Similarly, there was a rapid proliferation and differentiation of granular endoplasmic reticulum and Golgi complexes. Large quantities of free ribosomes were dispersed in the cytoplasm of tenth-days myocardium. However, in later stages there was a progressive reduction in the distribution of these organelles. An intimate assembly of ribosomes and polysomes with the developing myofibrils was discernible.

The T-system and sarcoplasmic reticulum began to appear in myocytes at eleventh-day. The embryonic myocardium displayed intense mitotic activity throughout its development. A unique feature of embryonic myocardial cells was the simultaneous occurrence of myofilament synthesis and mitotic activity within the same cells (Chacko, 1976).

1.4. Morphometry

Barth *et al*. (1992) studied the ultrastructural quantitative composition of normal myocardial cells in 9 different species: dog, pig, cat, rabbit, guinea-pig, rat, mouse, ferret, bat, and man. Volume densities of mitochondria, myofibrils, and cytoplasm were determined using morphometry. It was found that the percentage of mitochondria differed in various species ranging between 22.0-37.0%. It was a very specific and constant value for any particular species, the smallest species having the highest percentage. The myofibrillar volume density showed no species variability. It was about 60.0% in all species.

The volume densities of mitochondria, myofibrils, and unspecified cytoplasm in myocardium of dogs, rats, hamsters, mice, and in biopsied

tissue from human hearts were measured using ultrastructural morphometry (Schaper *et al.*, 1985). Human myocardial cells composed of 23% mitochondria, 59% myofibrils, and 18% cytoplasm. Volume densities for mitochondria were 22%, 32%, 28% for dogs, mice, rats and hamsters respectively. Myofibrillar volume densities were highest in dogs (63%) than rats and hamsters (57%), and mice (49%). An extensive analysis of canine myocardium revealed that the quantitative composition of tissue from the left ventricular wall (anterior, lateral, posterior) and the papillary muscles was identical. There were also no differences between subepicardium and subendocardium as well as midmyocardium. Volume densities from longitudinal sections were identical to those from transverse sections. There were no differences between volume densities in samples from the left ventricular wall (anterior, lateral, and posterior) in rats, hamsters, and mice (Schaper, *et al.*, 1985).

Sheridan *et al.* (1977) studied the quantitative ultrastructure of the right ventricular papillary muscles of cat in three age groups. The weight of animals was determined. Volume fractions were calculated for myofibrils, sarcoplasm, mitochondria, lipid, sarcoplasmic reticulum (SR), Golgi complex, and nuclei. The myofibril content of neonatal fibres was significantly less than that of the infant or adult groups (P<0.05 and 0.005 respectively). In addition, the infant fibres contained a smaller volume of myofibrils than that of adult ones (P<0.001). The mitochondrial content of the neonatal fibres was also significantly less than that of either the infant (P<0.005) or adults (P<0.001). These data provided an anatomical basis for the progressive age-related increase in mechanical performance of the cat myocardium in postnatal life.

Olivetti *et al*. (1980) measured morphometrically the differential growths of the capillary network of myocytes in the left and right ventricular walls from 1 to 5 days and from 5 to 11 days in rats postnatally. Capillary length, luminal volume, luminal surface area, and endothelial cell volume each increased two-three times more rapidly than myocardial mass or myocyte mass in each ventricle. Mean intercapillary distance and the transverse cross sectional area of the capillary decreased markedly. The mean number of capillaries across the ventricular walls increased from 16 to 79 in the left ventricle and 14 to 22 in the right ventricle. Maturation of the cytoplasm of left and right ventricular myocytes from 1 to 11 days included increment in the volume percentage of myofibrils, mitochondria and smooth endoplasmic reticulum.

According to Anversa *et al*. (1980) the mean cell volume, cell length, and percent binucleation of cardiac myocytes were similar in both ventricles. During this period, average myocyte length increased and the percentage of binucleate myocytes also increased. No differences were observed in the characteristics of epicardial and endocardial myocytes in either ventricle.

Xavier-Vidal *et al.* (1997) made a qualitative electron microscopic study to determine the volumetric density values of myocytes, (including nuclei), myocyte nuclei alone and connective tissue (including vessels). The study gave the following values 69.3%, 6.5%, and 30.7% respectively. The myocyte nuclei had a mean surface density equivalent to 0.073 μm^2. The diameter of myocyte nuclei was 3.7 μm.

Johnston *et al*. (1983) measured the volume densities of mitochondria and myofibrils of ventricular myocytes in haemoglobin-less icefish (*Chaenocephalus aceratus*), which gave 0.47% and 0.25% values respectively. The values for mitochondrial volume density were higher and

those for myofibrillar volume density were lower than for most vertebrate hearts.

CHAPTER TWO
MATERIALS AND METHODS

2.1. Histology

Thirty hearts of camel foetuses obtained from Al-Ssalam and Tamboul slaughter houses, Sudan, were used in this study. Depending on the age, the foetuses were divided into three equal groups: first trimester 0.1-23.5 cm CVRL (65-130 days), second trimester 24-71 cm CVRL (131-260 days) and third trimester 71.5-132 cm CVRL (261-426 days). The age of foetus was determined by using the equation of crown vertebral-rump length (CVRL) GA = (CVRL + 23.99)/0.366] GA (Gestational Age) in days as described by Elwishy *et al.* (1981).

The histological samples which were fixed in 10% buffered formalin included the entire hearts from the first and early second trimesters and 1cm^3 thick specimens from the late second and third trimesters. Specimens were taken from myocardial bridges and related arteries (paraconal or subsinuosal interventricular branches), sinoatrial node, atrioventricular node, atrioventricular bundle and purkinje fibres. Specimens were prepared by routine histological procedures (Bancroft and Stevens, 2008). General histological stains (H&E) and some special stains including Van Geison's and Masson's Trichrome for collagenous fibres, Verhoff's and Gomori's Aldehyde fuchsin for elastic fibres, Gordon and Sweet for reticular fibres were used in this study (Bancroft and Stevens, 2008).

2.2. Histometry

H&E sections (5 µm thick) from 16 foetal hearts (8 hearts from second trimester and 8 hearts from third trimester) were used for histometric measurements.

Measurements of the thickness of central and peripheral parts of the MB as well as the thickness of tunica intima, tunica media and tunica adventitia of the interventricular branch of coronary artery were done. Olympus microscope (CH20-Japan) with ocular micrometer lens X6 was used in this study. The objective lens X40 and X10 were used to measure the thickness after calibrating the ocular scale of the microscope (Thienpont, *et al.,* 1986). Nine measurements of each section were taken from each heart and the mean value was calculated. Data of the different histometric parameters were statistically analyzed by the Student's t-test, and the difference was considered statistically significant at $p < 0.05$.

2.3. Ultrastructure

A total of 18 foetal hearts were used. Samples were collected from Tamboul slaughterhouse, Gezira, Sudan. The entire heart and/or small pieces of tissue were taken for electron microscopy. Either the whole heart or $1cm^3$ thick sections were used for scanning microscopy and $1 mm^3$ thick sections for transmission electron microscopy. Tissues were taken from atrial myocardium, ventricular myocardium and myocardial bridges. The age of foetuses was determined using the equation of crown-vertebral rump length (CVRL) (Elwishy, *et al.*, 1981).

Samples were fixed in 2.5% glutaraldehyde in cacodylate buffer (pH 7.4) for 48 hours at 4°C. Samples were then, washed in 3 changes of cacodylate buffer and post fixed in osmic tetroxide for 90 minutes. They were then washed in 3 changes of cacodylate buffer for 4 hours and dehydrated in ascending grades of alcohol (30%, 50%, 70%, and 90%) for 2 hours each and in absolute alcohol for 2 days (Bancroft and Stevens, 1990). The samples were then either processed for scanning or transmission electron microscopy.

17

For scanning electron microscopy specimens were immersed in amylacetate for 1-2 days and then dried using critical point drying process. Specimens were furtherly dehydrated using graded series of amyl acetate/ absolute alcohol followed by absolute amyl acetate for 5 min each. The soaked specimens were then quickly moved to a cooled high pressure chamber (Polliack, *et al*., 1973). Finally the specimens were coated by a very thin layer of gold and examined by JEOL JSM-6390LA analytical scanning electron microscope.

For transmission electron microscopy specimens were embedded in epon-araldite mixture. Semi-thin sections were cut with Leica Ultracut UCT ultramicrotome. These sections were stained with toluidine blue, and then examined by light microscope. Ultrathin sections were prepared and were stained with uranyl acetate and lead citrate, then examined by JEOL (JEM-1400 TEM) transmission electron microscope.

2.4. Morphometry

A total of 16 camel foetuses of different ages were used in this study. Small pieces of heart tissue about 1 mm^3 thick were taken from myocardium and myocardial bridges in the three gestational stages of pregnancy. Samples were collected from Tamboul slaughterhouse, Gezira, Sudan. Samples were conventionally prepared using ultrastructural techniques (Bancroft and Stevens 1990), examined by JEOL (JEM-1400 TEM) transmission electron microscope.

Measurements were done using the electron microscope processing software that included the dimensions of myofibrils nuclei, nuclei of connective tissue cells between myofibrils at (X3000), mitochondria of myofibrils at (X10000). Sarcomeres (space between two Z lines) were also measured at (X3000). The nuclei being oval or semi oval in shape were

measured at the longest line (length) and the vertical line at the narrowest region (width).

2.5. Statistical analysis

Statistical analysis was done using Statistical Package for the Social Science (SPSS) and Student's t-test analytical program.

CHAPTER THREE

RESULTS

3.1. Histological Development of Myocardium and Conduction System

3.1.1. First Trimester

3.1.1.1. Pericardium

At the stage of 71 days of gestation (2 cm CVRL) the pericardium surrounded the future embryonic heart and it consisted of three layers of mesodermal origin; a thick outer layer which showed a moderate cellular content, a middle layer with a few cellular content and an inner layer which was thin and contained a few but closely packed cells (Fig. 1, A).The outer layer is the future fibrous pericardial layer, the middle layer is the future parietal layer of serous pericardium and the inner layer is the future visceral layer of the serous pericardium (epicardium). Between the visceral and parietal layers of serous pericardium a large pericardial cavity was observed. The thickness of the pericardial layers, blood supply and fibrous content increased gradually with the increase in the embryonic age (Fig. 2, A, B and C). The pericardium was attached to diaphragm, liver and thoracic vertebrae (Figs. 1 and 2).

3.1.1.2. Heart wall

At the stage of 71 days of gestation (2 cm CVRL) the atrial outlines irregularly showed many perforations, whereas the ventricular outlines were relatively regular (Fig. 1, A, B and C). The atria and ventricles were surrounded by a thin layer of epicardium followed by layers of cardiac muscle cells. The cardiac muscle layer consisted of trabeculae and cardiac jelly which was rich in nucleated red blood cells (Fig. 1, B and C). Some pectinate muscles of different shapes and sizes extended from atrial wall to the atrial lumen (Fig. 1, B). The ventricular mass was covered by a thicker

epicardial layer compared to that in the atrium. Its wall was formed of a relatively thick layer of myocardial fibres and contained many trabeculae of cardiac muscle with many blood filled spaces (Fig. 1, C).

At 73-79 days of gestation (2.8-5 cm CVRL) thin atrial and thick ventricular epicardiam was observed continuous with the myocardial layer (Figs. 2 and 3). Some cardiac muscle fibres were arranged in the form of small bundles in the right and left atria. The wall of left ventricle was thicker than that of right one and the ventricular trabeculation was increased in 5 cm CVRL (79 days) in comparison to that of 71 days of gestation (Fig. 4, B and C). The ventricular trabeculae were highly branched and anastomosing with each other forming spaces filled with oval nucleated red blood cells (RBCs). At this stage the atrioventricular (AV), atrioventricular and interventricular septa were observed (Fig. 2, A and B). The inter-atrial cushion grew down from the roof of the primitive atrium towards the AV tissue forming the left and right atria (Fig. 2, A). The atrioventricular septum was formed at the lower end of the AV canal (Fig. 2, B). The interventricular septum started as a ridge of muscular tissue arising from the wall of the future left ventricle and right ventricle (Fig. 2, A). At this stage the free leaflets of the atrioventricular valves were observed with their distal ends attached to the atrioventricular cushion tissue and ventricular wall (Fig. 4, A and C).

At 85-96 days of gestation (8.5-11 cm CVRL) the atrial size became larger and it appeared with some compact layers of cardiac muscle fibers which showed reticular fibres in between (Fig. 5, B and C). The atrium was lined by a simple squamous epithelium (Fig. 4, A, B and C). In the heart of the 11 cm CVRL embryo (96 days of gestation), the ventricles had highly trabeculated thick walls and narrow lumina (Fig. 6, A). The muscle bundles

increased in number and size and they were surrounded by a thin layer of connective tissue which was followed by the endothelium (Fig. 6, A and B).

During the stage of 98-112 days of gestation (12-17.5 cm CVRL) the atrial and ventricular epicardium was formed of a thin layer of loose connective tissue. The endocardium was formed of an endothelium supported by a subendothelial layer of loose connective tissue (Figs. 7, A and 8). The atrial myocardium presented scattered and thick cardiac muscle bundles (Fig. 7, A and B). The ventricular myocardium was in the form of compact layers of cardiac muscle fibres rich in connective tissue and blood vessels with decreased trabeculation and wide luminae (Fig. 8, A, B and C). The right ventricle at this stage showed long septomarginal trabeculae, which mainly contained connective tissues. The left ventricle had a thick layer of myocardium, the walls of the left and right ventricles showed a considerable amount of connective tissue, which contained a large number of lymphocytes and many blood vessels especially in the right ventricle (Fig. 8, A and B). Many cardiac muscle fibres were closely surrounding the endocardium and some others were transformed from myofibroblasts to myocytes (Fig. 8,A, B and C).

3.1.1.3. Conduction System

Conduction system of the heart of the camel foetus was shown in (Fig. 9). The atrioventricular node (AVN) was first observed at the stage of 13 cm CVRL (101 days of gestation) as a group of large-sized and lightly stained cardiac muscle cells, which were located between the right atrium and right ventricle (Fig. 10, A and B). The node was close to the right atrioventricular opening and it was surrounded by an accumulation of fibroblasts and separated from the surrounding ordinary cardiac muscles by a loose connective tissue which contained reticular fibres (Fig. 10, B). The cells had

22

large, oval or spherical and centrally located nuclei and they were located in rich connective tissue. In one section at this stage (17 cm CVRL; 112 days of gestation) the AVN appeared as scattered three groups of cells separated from each other by connective tissue rich in fibroblasts (Fig. 11, A).

Purkinje fibres appeared in 18 cm CVRL (115 days of gestation) embedded in cardiac muscle fibres close to the ventricular endocardium. They had a large size and lightly stained cytoplasm with oval and eccentric nuclei; these fibres were surrounded by small cells which were eosinophilic and had oval nuclei (Fig. 11, B).

Myocardial bridges were not observed in the first trimester.

3.1.2. Second Trimester

3.1. 2.1. Heart Wall

In 24.5 cm CVRL (133 days of gestation), the three cardiac layers that formed the heart wall became thicker compared to that in the first trimester (Fig. 12, A and B). The epicardium was covered by a mesothelium (simple squamous epithelium) under which there was submesothelium that was formed of a thick connective tissue layer in which the interventricular branches of coronary artery and their branches were embedded. The coronary artery walls were thin and they were formed of an endothelium and a thin layer of 1-2 smooth muscle fibres followed by a thin adventitia (Fig. 12, A and B).

At the stage of 29 cm CVRL (145 days of gestation), the interventricular branch of the coronary artery was embedded in the epicardial connective tissue of the right ventricle which showed many blood vessels (Fig. 13).

At the stage of 30 cm CVRL (148 days of gestation) there was a large amount of adipose tissue in the epicardium in which the interventricular

23

branches of coronary artery and their branches were embedded (Fig. 14 and Fig. 15).

The atrial endocardium was formed of endothelium and a thin layer of connective tissue (subendothelium), at 24.5 cm CVRL (132.5 days), 29 cm, CVRL (145 days), 33 cm (146 days), 38 cm CVRL, (169 days) and 41 cm (177.5 days) (Fig. 16, A, B, D, E and F).

The atrial myocardium at the stages of 30 cm CVRL (145 days), 33 cm CVRL (156 days), 38 cm CVRL (169 days) and 41 cm (177.5 days) (Fig. 16, C, D, E and F) was formed of bundles of cardiac muscle fibres; RBCs infiltrating in spaces between these muscle bundles (Fig. 16, A, B and F). In the stage of 30 cm CVRL (148 days) pectinate muscles were well developped (Fig. 16, C).

At the stage of 60 cm (230 days of gestation) the atrial muscle bundles were separated from the endocardium by a thin layer of connective tissue. These bundles consisted of large amounts of connective tissue between the muscle fibres especially reticular fibres (Fig. 17, A). In the late stage of the second trimester (68 cm, CVRL 251 days) a thick layer of adipose tissue (Fig. 17, B) covering the atria was observed.

The differentiation of ventricular myocardium from embryonic connective tissue (mesenchyme) was very clear at the stage of 24.5 cm CVRL (133 days of gestation). There was an accumulation of lightly stained myofibroblasts having oval nuclei. The myocardial muscle fibres were characterized by the presence of small blood vessels and blood spaces of different sizes (Fig. 18).

In 60 cm CVRL (230 days) cardiac muscles were separated by a large number of reticular fibres and the myocardium had the same structure in left and right ventricles (Fig. 19).

24

3.1. 2.2. Conduction System

3.1.2.2.1. Sinoatrial Node (SAN)

The sinoatrial node (SAN) appeared at the early and late stages of the second trimester of gestation; 38 cm CVRL (169 days) (Fig. 20, A) and 68 cm CVRL (251 days) (Fig. 20, B) as a group of spherical cells, which had dark cytoplasm and peripheral nuclei and embedded in connective tissue.

3.1.2.2.2. Atrioventricular Node (AVN)

At the early stage of the second trimester 38 cm CVRL (169 days of gestation), the AVN consisted of a group of spherical cells which had oval and central nuclei. These cells were surrounded by cardiac muscle fibres which were followed by connective tissue formed mainly of elastic fibers (Fig. 21, A and B). At the late stage of the second trimester the AVN appeared as a group of cells with the same structure but they were embedded in rich amounts of connective tissue (Fig. 22, A and B).

3.1.2.2.3. Atrioventricular Bundle (AVB)

The atrioventricular Bundle (AVB) appeared at the stage of 61 cm CVRL (232 days of gestation) as a bundle of lightly stained fibres that were embedded in the myocardium (Fig. 23, A).

At the stage of 68 cm CVRL (251 days of gestation) AVB was in the form of a group of lightly stained fibres which were covered by connective tissue. The fibres were spherical or oval and they had spherical and central nuclei and their cytoplasm was dark peripherally and light centrally and it had clear striation (Fig. 23, B and C).

3.1.2.2.4. Purkinje Fibres (PF)

The formation of Purkinje fibres was very clear in the ventricular myocardium in 24.5 cm CVRL (132.5 days of gestation) (Fig. 24). The fibres had different sizes and shapes and very dark cytoplasm laterally with

large empty vacuoles in the centre. They had central, spherical nuclei and some of the fibres contained two nuclei. The striation was clear in peripheral parts of some fibres. Some Purkinje fibres were found embedded in the connective tissue (Fig. 24). At the stage of 33 cm CVRL (156 days of gestation) the Purkinje fibres appeared as bundles embedded in the connective tissue with large amounts of collagenous fibres extending from the epicardium to the myocardium. The fibres were irregular in shape with peripheral nuclei; their cytoplasm was dark peripherally (Fig. 25, A and B).

At the stage of 41 cm CVRL (178 days of gestation) Purkinje fibres appeared as lightly stained fibers embedded in the myocardium. The fibres had light cytoplasm with spherical and central nuclei. Most of these fibres contained two nuclei and the cytoplasm around the nuclei was light (Fig. 26).

At the stage of 60 cm CVRL (230 days of gestation) Purkinje fibres were embedded in the myocardium as oval or spherical cells. Their cytoplasm was very light centrally and dark peripherally (Fig. 27, A).

In late stages of second trimester, 71 CVRL (259.5 days of gestation) Purkinje fibres appeared as bundles of fibres embedded in the connective tissue of the myocardium (Fig. 27, B). In some sections at the same stage (71 cm CVRL) Purkinje fibres were found in the subendocardium (Fig. 28).

3.1.3. Third Trimester
3.1.3.1. Heart Wall

The atrial structures were well developed in the third trimester. In the early stages of the third trimester 74 cm CVRL (268 days of gestation) the atria were having pectinate muscle fibres in the form of bundles which were covered by a thin layer of connective tissue (Fig. 29).The endocardium was

in the form of endothelium and thick subendothelial connective tissue extended between the muscle bundles (Fig. 30). Elastic fibres were also observed (Fig. 31) between the cardiac muscle bundles and in the wall of blood vessels. The amount of collagen and reticular fibres were large in the late stages of the third trimester (Fig. 32, Fig. 33 and Fig. 34).

The histological structure of the ventricular cardiac muscles in the third trimester of gestation was similar to that in the adult; the cardiac muscle cells were joined end to end and each cell was usually branched (Fig. 35, A and B). Infiltration of Purkinje fibers was also observed between the muscle fibers in the left and right ventricles (Fig. 35, B). Elastic and collagen fibers were found between the cardiac muscle fibers (Fig. 36, A and B).

3.1.3.2. Conduction System

3.1.3.2.1. Sinoatrial Node (SAN)

In the early stages of the third trimester 71-132 cm (261-426 days), SAN appeared as a group of darkly stained fibres. It was embedded in fair amounts of connective tissue that contained adipose cells and collagenous fibres. At stages of 74 cm CVRL (268 days) and 76 cm (273 days) of gestation the cells were surrounded by a circular and very light area and they had different shapes and sizes (Fig. 37, A). Their nuclei were large and were peripherally located. The nuclear chromatin was peripherally distributed (Fig. 37, B). The connective tissue surrounding SAN was rich in blood capillaries and collagenous fibres. An arteriole and a venule were embedded between ordinary cardiac muscles and SAN connective tissue (Fig. 37, A).

At the late stages of the third trimester 71.5-132 cm CVRL (261-426 days) SAN became elongated in shape with long peripheral tapering ends (Fig. 38, A and B).

A ganglion associated with SAN was observed in the third trimester specimens at 76-79.5 cm CVRL (273-283 days of gestation). It was located in the subepicardial area near the cardiac muscles embedded in connective tissue rich in adipose tissue, blood vessels and nerves (Fig. 39, A, B and C). The ganglion was surrounded by a thin connective tissue capsule that enclosed large scattered irregular neurons characterized by large nuclei and prominent nucleoli. Satellite cells were observed around the neurons (Fig. 39, D).

Two types of SAN cells could be identified; the first type had dark cytoplasm and large spherical lightly stained nuclei. The chromatin was peripherally distributed (Fig. 40, A and B). The other cells were small and spindle shaped with dark small nuclei. Blood capillaries were found in between these cells (Fig. 40, A and B).

3.1.3.2.2. Atrioventricular Node (AVN)

At the early stages of the third trimester 76 cm CVRL, 273 days of gestation AVN consisted of a group of dark stained cells (modified cardiac muscle cells). These cells had oval and central nuclei and were surrounded by connective tissue. The connective tissue consisted of a large amount of fibroblasts followed by cardiac muscle fibres (Fig. 41, A and B). At the middle and late stages of the third trimester, AVN was embedded in connective tissue containing large amounts of adipose tissue (Fig. 42, A, B and C).

3.1.3.2.3. Atrioventricular Bundle (AVB)

At the early stages of the third trimester of gestation represented by 76 cm CVRL (273 days of gestation), AVB appeared as groups of fibres which were covered by connective tissue between the endocardium and myocardium. The fibres nuclei were lightly stained centrally, and darkly

stained peripherally (Fig. 43, A). They were also observed as bundles of light stained fibres with spindle shaped and oval pale nuclei in the epicardium and between the myocardium (Fig. 43, B).

At 89 cm CVRL (309 days of gestation) and 91 cm CVRL (314 days of gestation) AVB appeared as bundles of spindle shaped fibres with oval central nuclei. They were separated by connective tissue (Fig. 44). At the stage of 97 cm CVRL (331 days of gestation), the AVB appeared as bundles of fibres between the myocardial muscles near the endocardium (Fig. 45, A, B and C). They had a light cytoplasm and pale central nuclei. They were either separated from the myocardium by loose connective tissue or directly attached to it. AVB fibres at this stage possessed clear striation (Fig. 45, C).

3.1.3.2.4. Purkinje Fibres (PF)

At the early stages of the third trimester as shown at the stage of 74 cm CVRL (268 days of gestation) and 76 cm CVRL (273 days of gestation), Purkinje fibres appeared as oval fibres. They had a light cytoplasm and one or two oval, centrally located nuclei (Fig. 46, A and B). The fibers were found near the epicardium or in-between the myocardial muscles and were either attached to the myocardium or separated from it by connective tissue.

The fibres were embedded in the connective tissue (Fig. 47, A, B and C) in the apical part of the left ventricle at the stage of 79.5 cm CVRL (283 days of gestation). In this stage Purkinje fibres had dark cytoplasm. At the stage of 88 cm CVRL (306 days of gestation) the Purkinje fibres had light cytoplasm than that of the cardiac muscle. However, it was darker than that of Purkinje fibres in other stages (Fig. 48, A and B). These Purkinje fibres were found as separate fibres, as small groups of fibres or as bundles embedded in connective tissue.

At the stage 89 cm CVRL (309 days of gestation), Purkinje fibres and myocardial muscles appeared as parallel bundles (Fig. 49, A). In other sections they were embedded in connective tissue beside blood vessels branching in the myocardium and epicardium (Fig. 49, B). The fibres which were also observed directly attached to the myocardium, contained one or two nuclei (Fig. 49, C).

At the stages of 91 cm CVRL (314 days of gestation) and 97 cm CVRL (330.5 days of gestation), Purkinje fibres appeared as bundles of fibres parallel to myocardial muscles. They were also embedded in the endocardial connective tissue as groups or separate fibres (Fig. 50, A and B).

At the late stages of pregnancy, 131 cm CVRL (423.5 days of gestation) Purkinje fibres were also embedded as groups of fibres parallel to myocardial muscles and in the myocardial connective tissue around a number of blood vessels (Fig. 51, A and B).

3.2. Myocardial Bridges and Related Arteries

The myocardial bridges (MBs) were observed in the second and third trimesters (Fig. 52, A and B). MBs were not detected in the first trimester of gestation. In the second trimester of gestation the MBs first appeared at the age of 132.5 days and also in other different ages of the second trimester in eight hearts out of ten. At this stage the bridge was in the form of a bundle which consisted of parallel cardiac muscle fibres (Fig. 53, A). The bundles passed above the interventricular branch of the coronary artery. It was thin at the centre and thick at the periphery (Fig. 53. B). In some sections, the bridge was completely covering the interventricular branch of the coronary artery, (Fig. 53, A, C and F) whereas in others it was partially covering the artery (Fig. 53, B, D and E).

The interventricular branch of the coronary artery in the early stages of second trimester of gestation was irregular in shape and it consisted of about two layers of smooth muscle fibres in the tunica media followed by a layer of elastic fibres internally and collagenous fibres externally (Fig. 53, A, B, C and D). Sometimes the interventricular branch of coronary artery was attached to the medial aspect of the myocardium without any connective tissue fibres (Fig. 53, C). Collagenous fibres were observed in the tunica adventitia of the artery and epicardial connective tissue (Fig. 53, E).

MBs were observed in eight hearts out of ten from the early stage of the third trimester of gestation (74 cm, 268 days of gestation), the interventricular branch of coronary artery in this stage was oval in shape in cross section (Fig. 54, A). There were fair amounts of connective tissue separating the artery from the bridge (Fig. 54, B, C, D and F).

The interventricular branch of coronary artery in the late stages of the third trimester was irregular in shape. It consisted of about 2-6 layers of smooth muscle fibres in tunica media depending on its location in the interventricular groove followed by layers of elastic fibres and collagenous fibres in tunica adventitia (Fig. 54, D and F). Sometimes the interventricular branch of coronary artery was attached to the medial aspect of the myocardium without any connective tissue fibres (97 cm CVRL, 330.5 days of gestation) (Fig. 54, E).

3.3. Histometry

Histometric measurements of the MBs in the second and third trimester of gestation are shown in tables 1 and 2. The thickness of the MBs in its extremities gave higher values than that in the centre of the bridge. The mean thickness of the central part of the MB in the second trimester was 41.06±25.39 µm and that of its extremities was 58.79±36.26 µm. The mean

thickness of the centre of the MB in the third trimester was 153.98±108.39 μm and it was 190.59±147.54 μm in the extremities.

The mean thickness of tunica intima and tunica media of the interventricular branch of the coronary artery in the second trimester was 19.78±8.89 μm and that of tunica adventitia was 36.96±27.48 μm. The mean thickness of tunica intima and tunica media of the interventricular branch of the coronary artery in the third trimester was 31.02±10.28 μm and that of tunica adventitia was 66.42±15.73 μm. The different measurements of the third trimester were significantly higher (P< 0.05) than those of the second trimester.

Table 1: Mean thickness (μm) of the myocardial bridges (MBs) and the wall of interventricular branch of coronary artery in the second trimester of gestation in camel foetuses.

Foetus No.	Animal age/days	Centre of MB	Extremities of MB	Tunica Intima + tunica media	Tunica Adventitia
1	131	14.3	16.55	12.18	12.9
2	132.5	13.75	22.58	13.98	25.8
3	145	36.95	42.83	11.18	14.62
4	177.5	53	69.5	21.5	21.5
5	229.5	38.7	66.33	15.05	35.12
6	232	53	69.5	22.22	38.22
7	251	27.2	50.2	38.22	97.47
8	259.5	91.55	132.9	23.89	50.17
Mean± SD	- -	41.06± 25.39	58.79± 36.26	19.78± 8.89	36.96± 27.48

Table 2: Mean thickness (μm) of the myocardial bridges (MBs) and the wall of interventricular branch of coronary artery in the third trimester of gestation in camel foetuses.

Foetus No.	Animal age/day	Centre of MB	Extremities of MB	Tunica intima +tunica media	Tunica adventitia
1	268	87.1	75.9	21.5	76.54
2	273	71.1	99.05	23.89	38.92
3	283	38.7	16.48	26.19	77.64
4	309	126.1	154.8	22.93	74.06
5	314	239.0	258.8	29.14	72.39
6	317	358.3	422.1	32.97	64.98
7	330.5	93.6	118.0	39.90	45.63
8	423.5	217.9	379.6	51.6	81.21
Mean± SD	- -	153.97± 108.39	190.59± 147.54	31.02± 10.28	66.42± 15.73
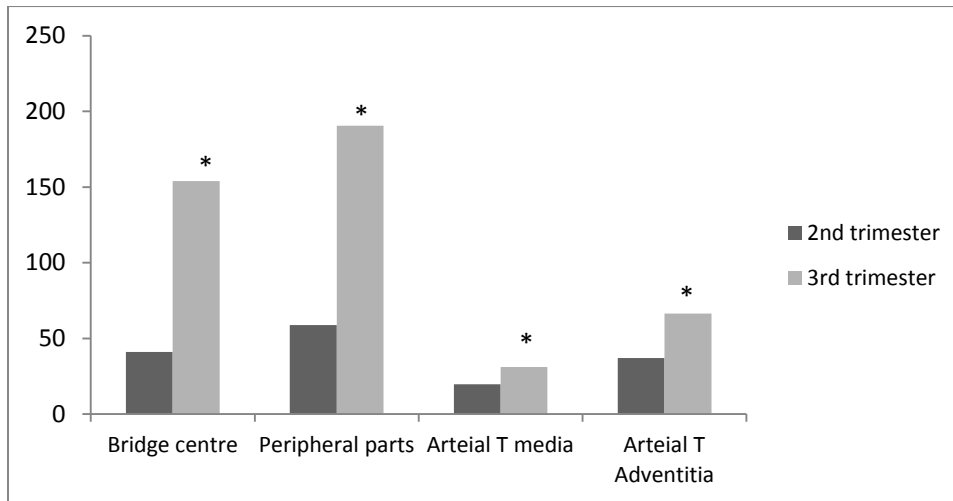
Text- Fig. 1: showing the thickness (μm) of myocardial bridges (MBs) and wall of interventricular branch of coronary artery in the second and third trimesters *Significant difference (P < 0.05).

3.4. Ultrastructure

3.4.1. Scanning Electron Microscopy

3.4.1.1. First Trimester

The heart of the camel foetus in early stages of the first trimester at 6.8-9.2 cm CVRL, (84-91 days gestation) had a semi-triangular shape (Fig. 55, A). The length from the base to the apex was about 3.67 mm and the width was about 3.33 mm in the broadest part. The coronary groove was not clear but the longitudinal groove appeared as a shallow depression at the upper part of the future longitudinal groove. Inter-ventricular branches of coronary arteries were observed in the upper part of this groove (Fig. 55, A and B). The atria were not clear at 84 days of gestation (Fig. 55, B). However; they appeared as small buds at 91 days of gestation (Fig. 56, A and B). The length of the heart in the middle of the first trimester 13 cm CVRL (101 days) was about 8.61 mm and the width was about 5.19 mm. The longitudinal groove and interventricular branches of coronary arteries were clear (Fig. 57, A and B).

At the early stages of first trimester atrial pectinate muscles had wavy appearance (Fig. 57, C and D). The length of the right ventricle was about 3.85 mm and the width was about 0.9 mm; the length of the left ventricle was about 2.80 mm and the width was about 0.7 mm. The ventricular myocardium in the upper part of the ventricular lumen showed a whirly appearance (Fig. 57, E and F). The lower part of the ventricular lumen showed well developped trabeculae carneae (Fig. 57, C and E). During the late stage of the first trimester 23 cm CVRL, 128 days of gestation the atrial pectinate muscles appeared as anastomosing branches. Each branch was in the form of a longitudinal bundle which was about 38.4 μm thick (Fig. 58, A and B). Type II myocardial bridges were clearly present in the right

longitudinal groove (Fig. 58, C and D). The interventricular branch of subsinuosal coronary artery dipped in the myocardium without reappearing (Figs. 58, C and D).

3.4.1.2. Second Trimester

Atrial pectinate muscles in the second trimester 60-65 cm CVRL (229.5-243 days) appeared as a connected plexus (Fig. 59, A, B and C). They were covered by simple squamous epithelium. The thickness of pectinate muscles was about 130.7-488.2 μm in (X75). Muscle fibres had a branched appearance in cross section of the pectinate muscle bundle (Fig. 59, C).

Ventricular myocardium in 60 cm CVRL (229.5 days) appeared as branched fibres connected to each other. A few connective tissue fibres were found between the muscle fibres (Fig. 60, A and B).

3.4.1.3. Third Trimester

Development of the right and left atrial pectinate muscles showed no significant differences. They appeared as cords covered with connective tissue (Fig. 61, A and B) in 89 cm CVRL (309 days of gestation). However, the connective tissue fibres were not clearly shown (Fig. 61, C) in 101 cm CVRL (341.5 days of gestation) and 112 cm CVRL (371.5 days of gestation). The covering epithelium was very clear (Fig. 61, B) in 89 cm CVRL (309 days of gestation). The pectinate muscle cords increased in size with the increase in foetal age. They showed a plexiform appearance. The measurements of these pectinate muscles were different in diameters. They measured about 72.05-243.03 μm in (X75) in 89 cm CVRL (309 days of gestation). However, in 101 cm CVRL (341.5 days of gestation) they also appeared as cord-like or plexiform (Fig. 62, A and B) but their covering

epithelium was groove-like (Fig. 62, C). The measurements of the pectinate muscles were about 132.06-756.9 µm in (X50).

3.4.2. Transmission Electron Microscopy

3.4.2.1. First Trimester

Transmission electron microscopy showed myofibrillar nuclei as large, central either oval or irregular in shape. They were euchromatic (Figs. 63, A). Mitochondria were numerous with different shapes and sizes. They were found around the nuclei and in the interfibrillar regions. The transverse tubular system was pale and showed irregular Z lines (Fig. 63, B). Rough endoplasmic reticulum was scattered around the nuclei.

3.4.2.2. Second Trimester

In the second trimester of gestation (131-260 days) (Fig. 64, A and B) nuclei of atrial myofibril were oval or irregular in shape. They were euchromatic. Mitochondria were scattered around nuclei and between myofibrils (Fig. 64, A and B). They were numerous and showed different shapes and sizes (Fig. 64, B). Individual mitochondrion measured about 1.12 µm in length and 0.28 µm in width at (X12000). The cell membrane was clear between myocytes and showed cell junctions (Fig. 64, A). Few connective tissue fibres were observed between myocytes. Developmental processes in the second trimester of gestation were similar to those in the first trimester of gestation. However, the transverse tubular system showed clear Z lines and pale I bands (Fig. 64, A).

Ventricular myocardium showed the myofibril structure more or less similar to that observed in atrial myocardium especially the nuclear shape and size (Fig. 65, A and B). Mitochondria were scattered around the nuclei and between myofibrils. They had large sizes when compared with those in the atrial myocytes (Fig. 65, B and B). They measured about 1.02 µm in

36

length and 0.24 μm in width (X10000). Rough endoplasmic reticulum was in the form of a few cisternae. The transverse tubular system had clear Z lines, with clear I and A bands (Fig. 65, B).

Nuclei of myofibrils of MBs were irregularly oval and the transverse tubular system had only Z lines (Fig. 66, A and B). Mitochondria were numerous having spherical or oval in shape, being scattered between myofibrils and around nuclei (Fig. 66, A and B). Numerous blood capillaries were found. Connective tissue fibres were present between myocardial fibres (Fig. 66, A).

3.4.2.3. Third Trimester

Atrial myofibrils in the third trimester of gestation in 71.5-132 cm CVRL (261-426 days of gestation) were arranged in bundles (Figs. 67, A and B; 68). Nuclei of myofibrils were euchromatic oval or irregular in shape. Mitochondria were numerous and scattered around nuclei and between myofibrils (Fig. 67, A and B). They had different shapes and sizes. Myofibrils were thin and irregular. The transverse tubular system showed clear Z lines with clear I and A bands and pale H zone (Fig. 67, B). At late stages of the third trimester, nuclei of myofibrils were elongated (Fig. 68). The transverse tubular system showed clear Z lines, clear I and A bands and pale H zones (Fig. 68).

Myocardial bridges in the third trimester of gestation were investigated (Fig. 69 and 70). Nuclei of myofibrils were semi oval or irregular in shape. The transverse tubular system showed Z lines. Intercalated discs appeared first in this stage (Fig. 69, A). Mitochondria were numerous and they were crowded between myofibrils and around nuclei. They were spherical or oval in shape (Fig. 69, B). Myofibrils appeared in transverse sections as bundles surrounded with connective tissue in 101 cm CVRL (341.5 days) (Fig. 70,

37

A). Connective tissue with many blood capillaries was observed between myocardial bundles. It contained large amounts of collagen bundles (Fig. 70, B).

3.5. Morphometry

The measurements included dimensions of the nuclei of myofibrils of myocardium in the three trimesters and of myocardial bridges in the second and third trimester, and that of connective tissue cells between myofibrils and mitochondria of myofibrils and sarcomeres of the myocardium of the three trimesters (table 3 and Appendix).

3.5.1. Measurements at the First Trimester

3.5.1.1. Myocardium

The length of myofibril nuclei was 6.69±2.30 μm and the width was 3.19±1.60 μm. The length of the nucleus of connective tissue cells was 6.23±2.18 μm and the width was 2.84±0.62 μm. The length of mitochondria of myofibril was 1.13±0.29 μm and the width 0.55±0.12 μm. The sarcomere was measuring 1.19±0.23 μm.

3.5.2. Measurements at the Second Trimester

3.5.2.1. Myocardium

The length of myofibril nuclei of the myocardium was 6.29±1.29 μm and the width was 3.11±0.37 μm. The mitochondrial length was 0.85±0.23 μm and width was 0.75±0.02 μm. The sarcomere was measuring 1.21±0.16 μm.

3.5.2.2. Myocardial Bridges

The length of myofibril nuclei was 6.71±1.52 μm while the width was 3.68±1.06 μm. The length of mitochondria of myofibril was 0.98±0.28 μm and its width was 0.83±0.23 μm. The sarcomere was measuring 1.08±0.17 μm.

3.5.3. Measurements at the Third Trimester

3.5.3.1. Myocardium

Myofibril nuclei measurements were 6.64±2.46 µm in length and 2.45±1.17 µm in width. Mitochondria of myofibril were measuring 0.45±0.25 µm for length and 0.40±0.08 µm in width. The sarcomere was measuring 1.8±0.04 µm. Connective tissue cells nuclei measured 3.79±1.86 µm and 2.02±0.45 µm in length and width respectively.

3.5.3.2. Myocardial Bridges

Nuclei measured 8.81±1.45 µm and 2.73±0.10 µm in length and width, respectively. Mitochondria were measuring 1.05±0.16 µm, and 0.77±0.14 µm in length and width respectively. The nuclei of connective tissue cells between the myocardial bridges were measuring 6.75±0.21 µm for length and 2.71±0.52 µm for width. The sarcomere was measuring 1.86±0.88 µm.

Table 3. Showing ultrastructure morphomerty of myocardium and myocardial bridges in first second and third trimesters of gestation

Foetal stage	Structure	Myofibrils Nuclei (X3000)		Connective Tissue Nuclei (X3000)		Mitochondria of myofibrils (X10000)		Sarcomere (X3000)
		Length	Width	Length	Width	Length	Width	
1st Trimester	Myocardium	6.69± 2.3	3.19± 1.6	6.23± 2.18	2.84± 0.62	1.13± 0.29	0.5± 0.12	1.19±0.23
2ed Trimester	Myocardium	6.29± 1.29	3.11± 0.37	5.95± 0.52	2.50± 0.84	0.85± 0.23	0.7± 0.02	1.21±0.16
	Myocardial Bridges	6.71± 1.52	3.68± 1.06	-	-	0.98± 0.28	0.8± 0.23	1.08±0.17
3rd trimester	Myocardium	6.64± 2.46	2.45± 1.17	3.79± 1.86	2.02± 0.45	0.45± 0.25	0.4± 0.08	1.8±0.04
	Myocardial Bridges	8.81± 1.45	2.73± 0.1	6.75± 0.21	2.71± 0.52	1.05± 0.16	0.7± 0.14	1.86±0.88

FIGURES
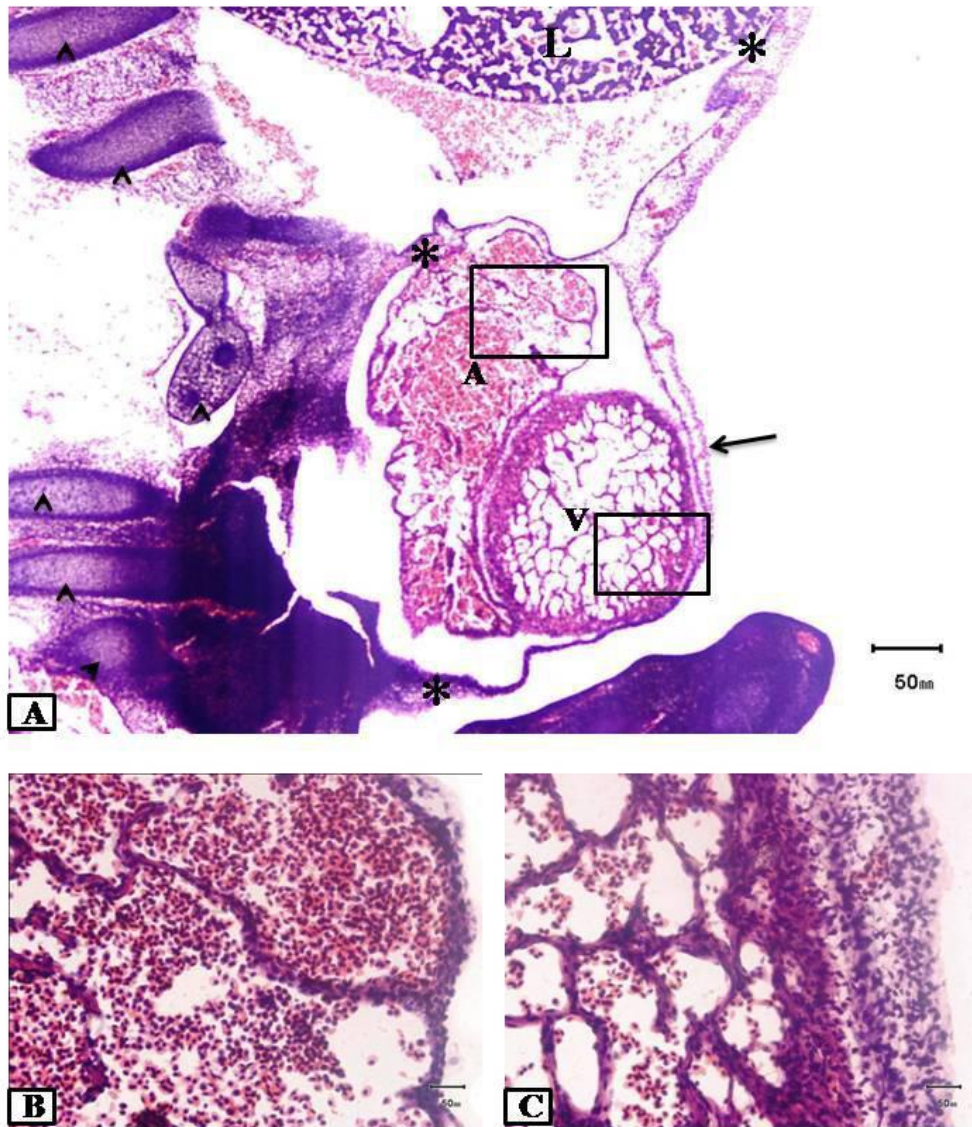
Fig. 1. A: A photomicrograph showing the heart of 2 cm CVRL camel foetus: A, right atrium, arrow, pericardium, arrowheads, vertebrae, asterisk, pericardial attachments, V, right ventricle, L, liver, H&E (X4).

B: Is a magnification of the upper rectangle in A: irregular outlines, cardiac muscle layers consisting of trabeculae and cardiac jelly with nucleated RBCs (X40).

C: Is a magnification of the lower rectangle in A: regular outlines. Showing cardiac muscle layers consisting of trabeculae and cardiac jelly with nucleated RBCs (X40).
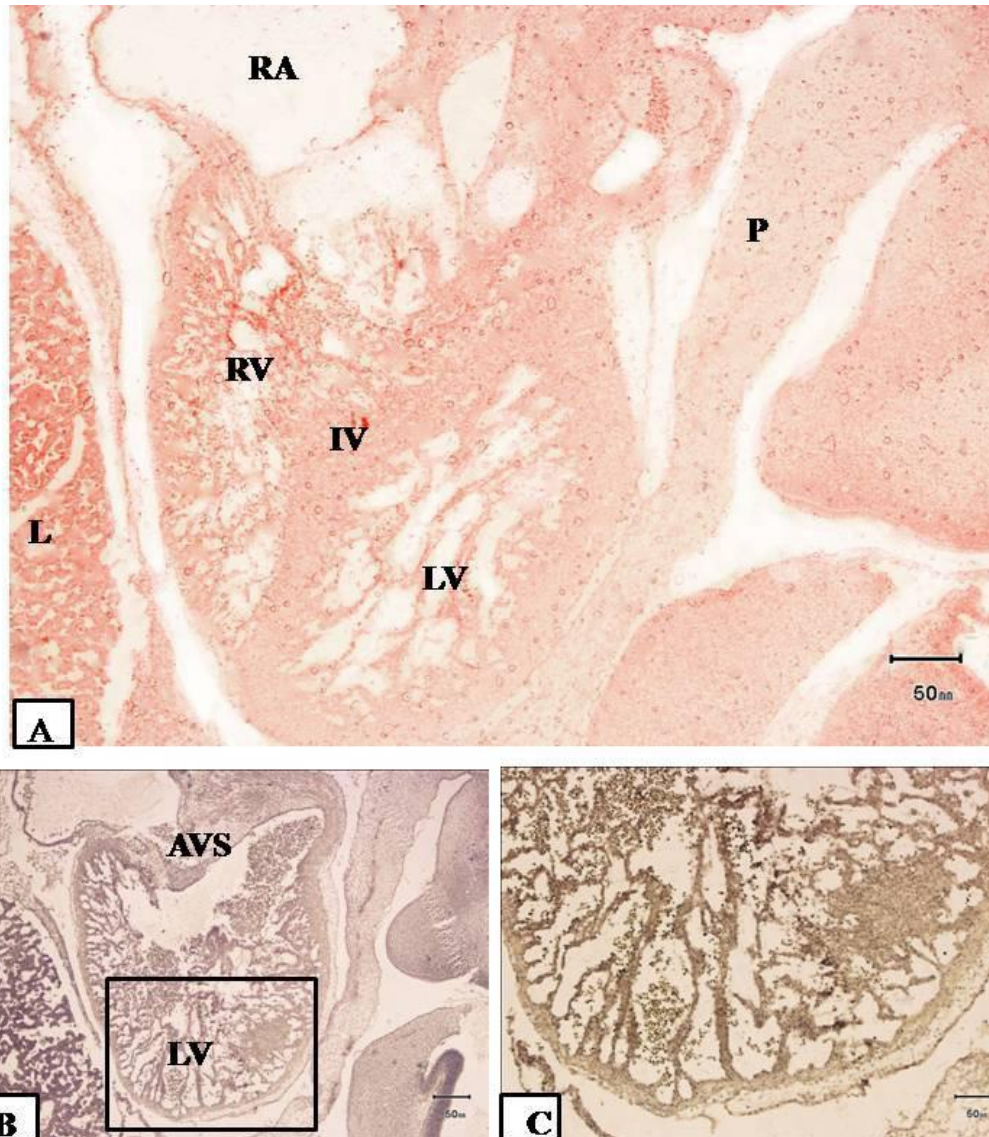
Fig. 2. A: A photomicrograph showing the heart of 2.8 cm CVRL camel foetus: IV, interventricular septum was observed, pericardium (P) attached to the Liver (L). LV, left ventricle, RA, right atrium, RV, right ventricle, H&E (X4).

B: Showing ventricular trabeculation in the same heart. Note that atrioventricular septum (AVS) was clear. Verhoff's (X40).

C: Is a magnification of the rectangle in B: showing ventricular trabeculation (X40).
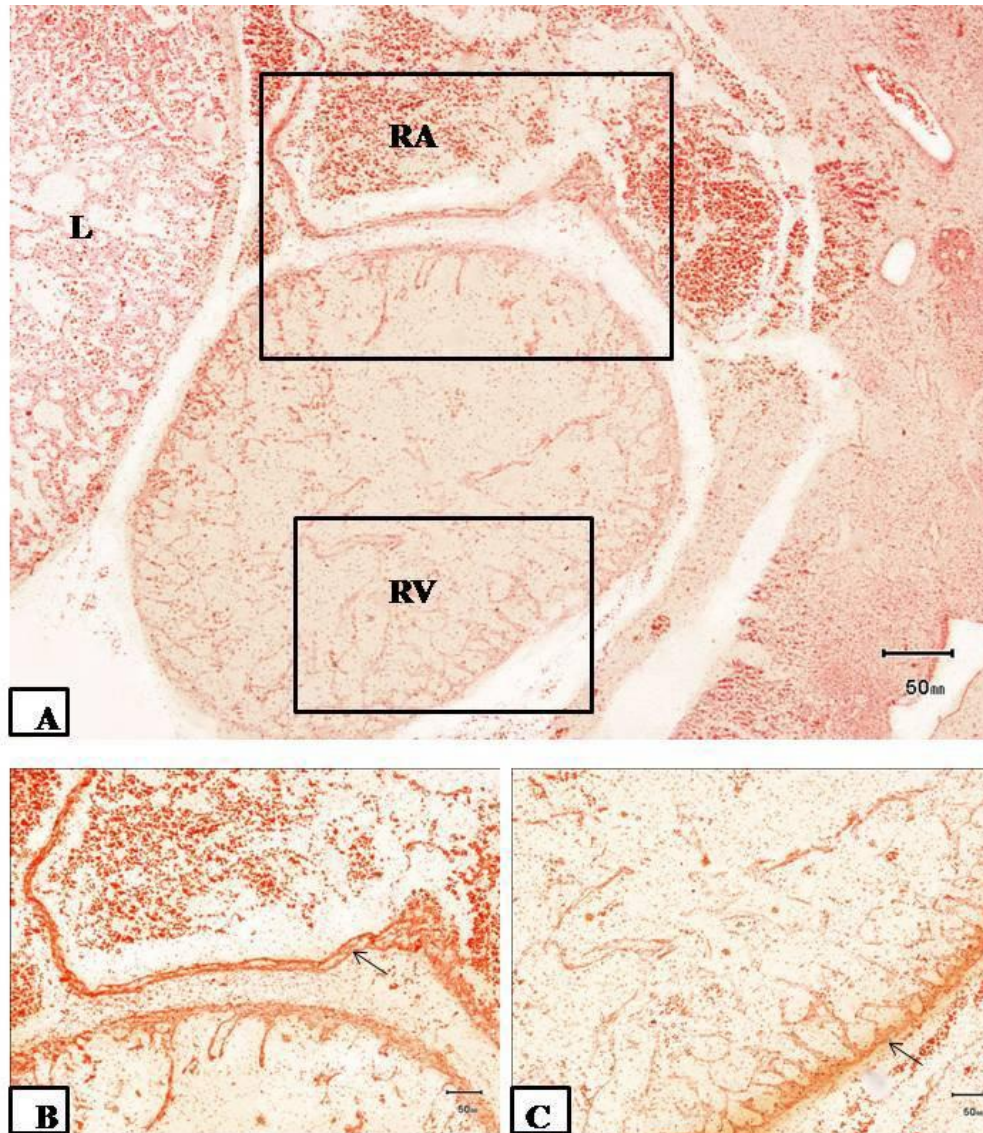
Fig. 3. A: A photomicrograph showing the heart of 3 cm CVRL camel foetus:
L, liver, RA, right atrium, RV, right ventricle. H&E (X4).
B: Is the magnification of the upper rectangle in A (X40).
C: Is the magnification of the lower rectangle in A showing the atrial and
ventricular outlines (arrows) (X40).
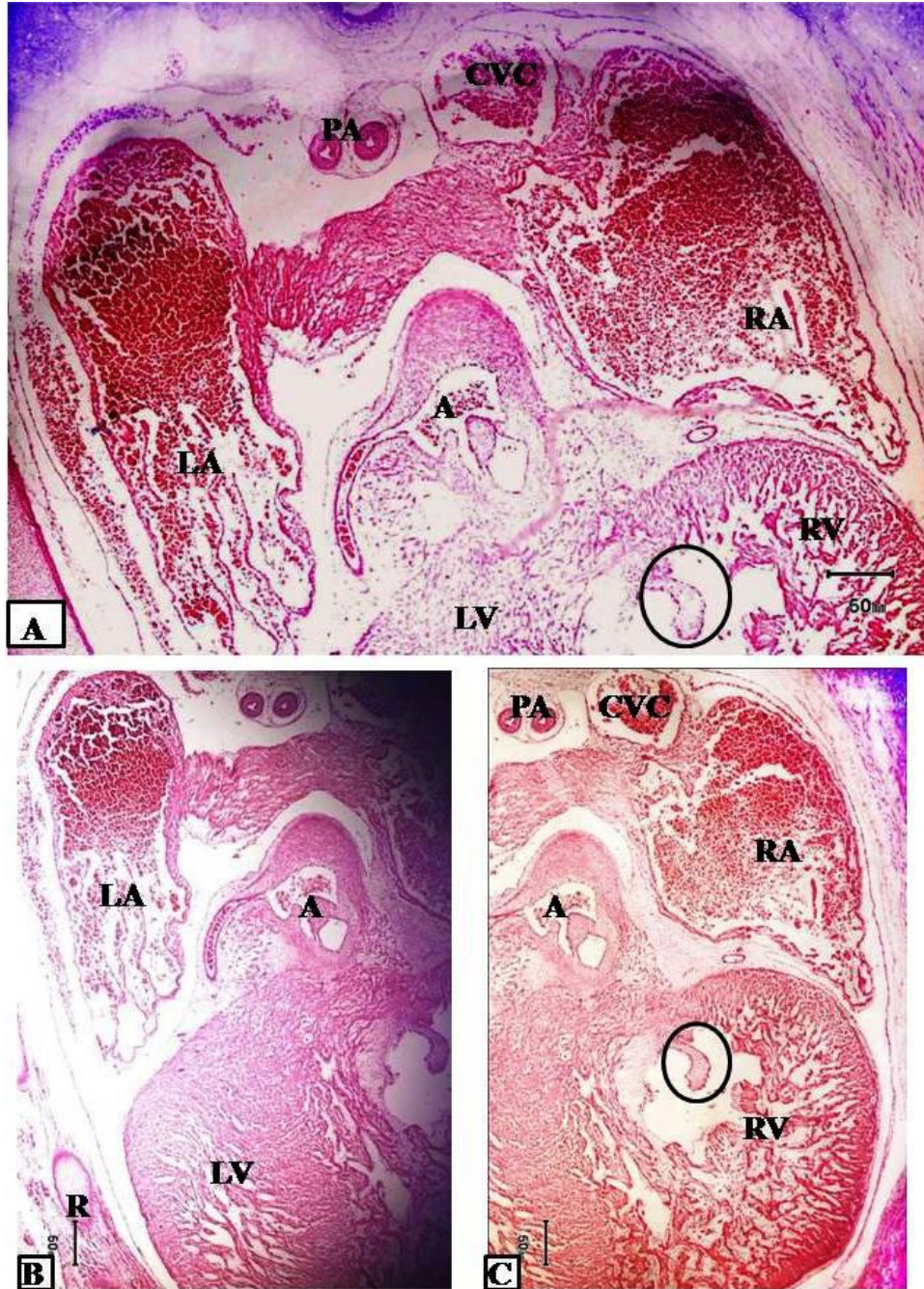
Fig. 4. A: A photomicrograph showing the heart of 5 cm CVRL camel foetus: A, aorta, circle, atrioventricular valve, CVC, cranial vena cava, LA, left atrium, LV, left ventricle, PA, pulmonary arteries, RA, right atrium, RV, right ventricle, H&E (X4).

B and C: Showing left side and right side of the same heart; the wall of the left ventricle was thicker than that of the right one. R, rib. H&E (X10).
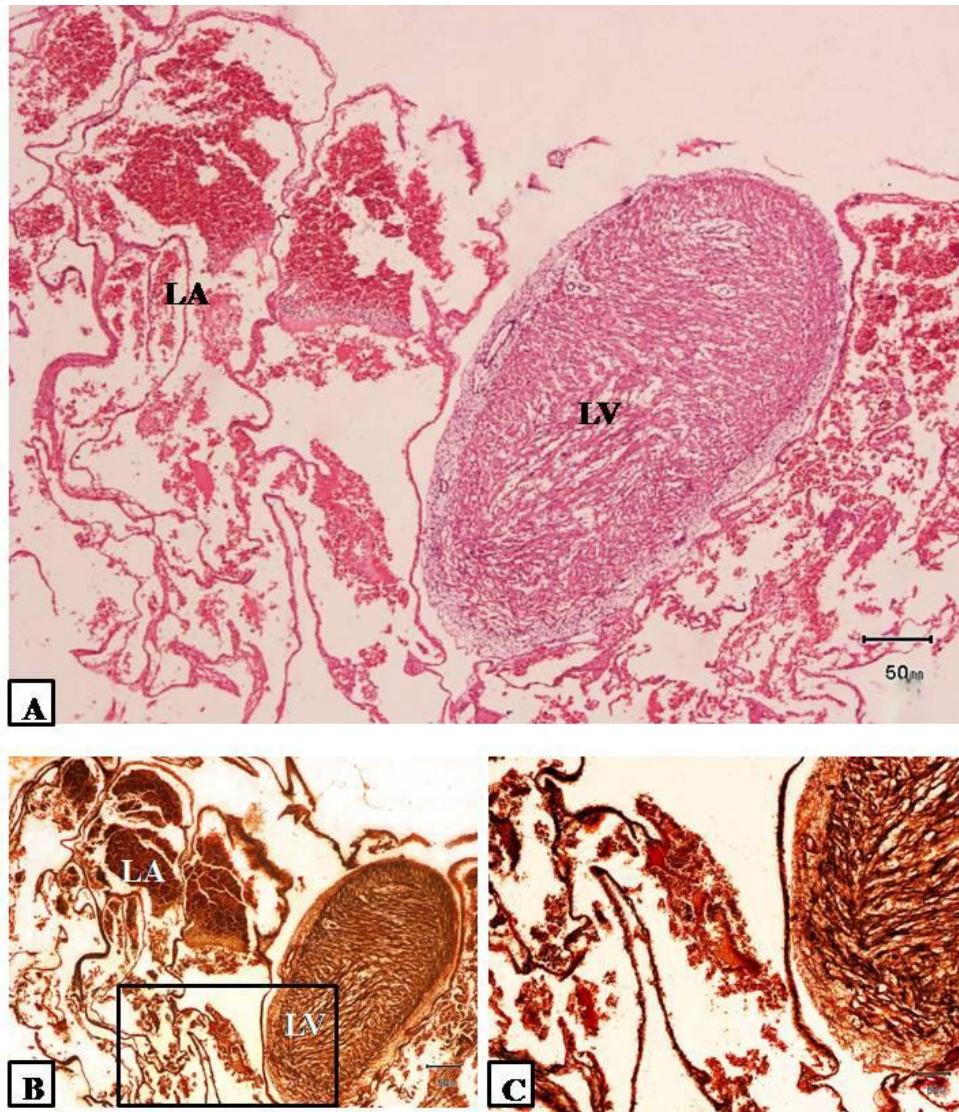
Fig. 5. A and B: Photomicrographs showing the left side of the heart of 8.5 cm CVRL camel foetus; LA, left atrium, LV, left ventricle. H&E (X4).
B: Showing distribution of the reticular fibres. Gordon and Sweet (X4).
C: Is a magnification of the rectangle in B showing reticular fibres (X10).
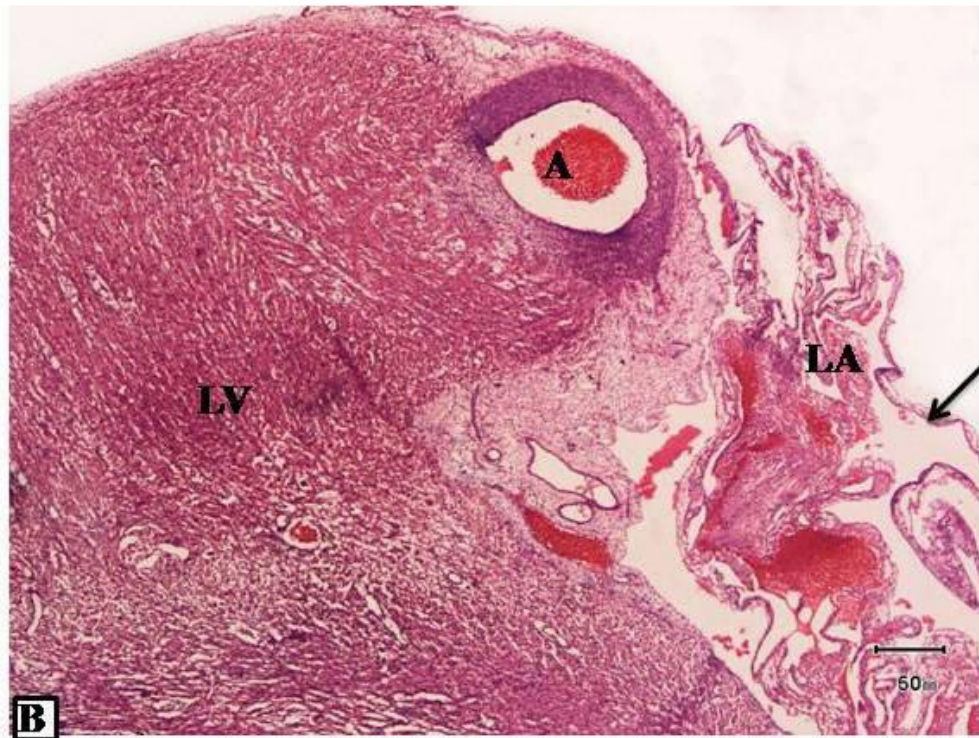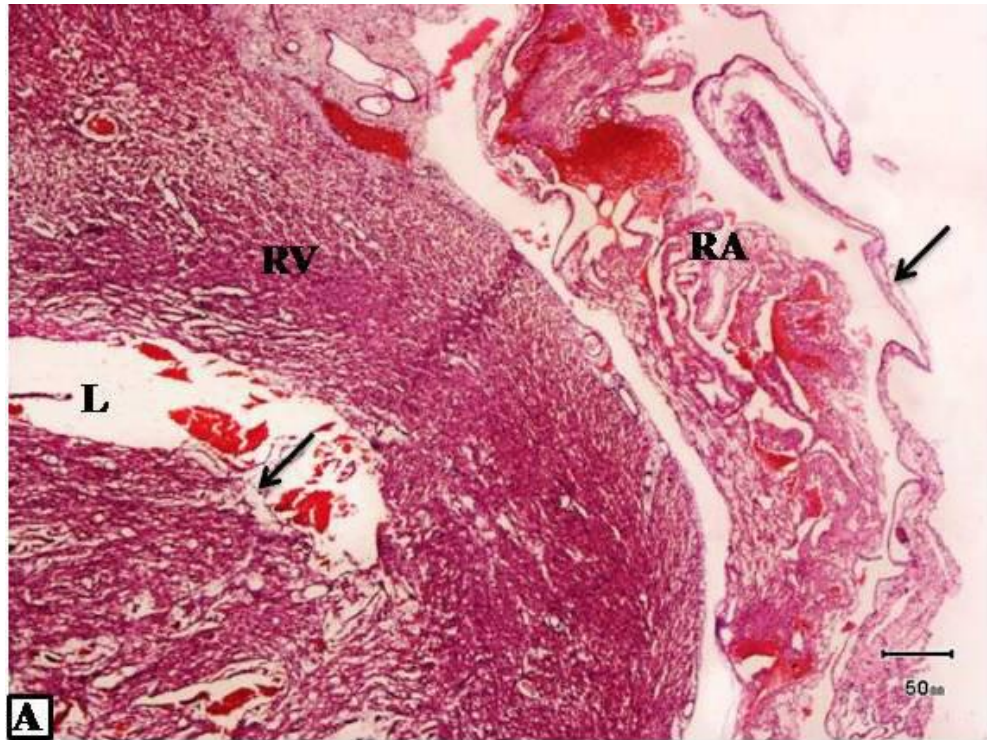
Fig. 6. A and B: Photomicrographs showing the heart of 11 cm CVRL camel foetus; the muscle bundles increased in number and size and they were surrounded by a thin layer of connective tissue (arrows) which was covered by the endothelium. A, aorta, L, lumen of right ventricle, LA, left atrium, LV, left ventricle, RA, right atrium, RV, right ventricle. H&E (X4).
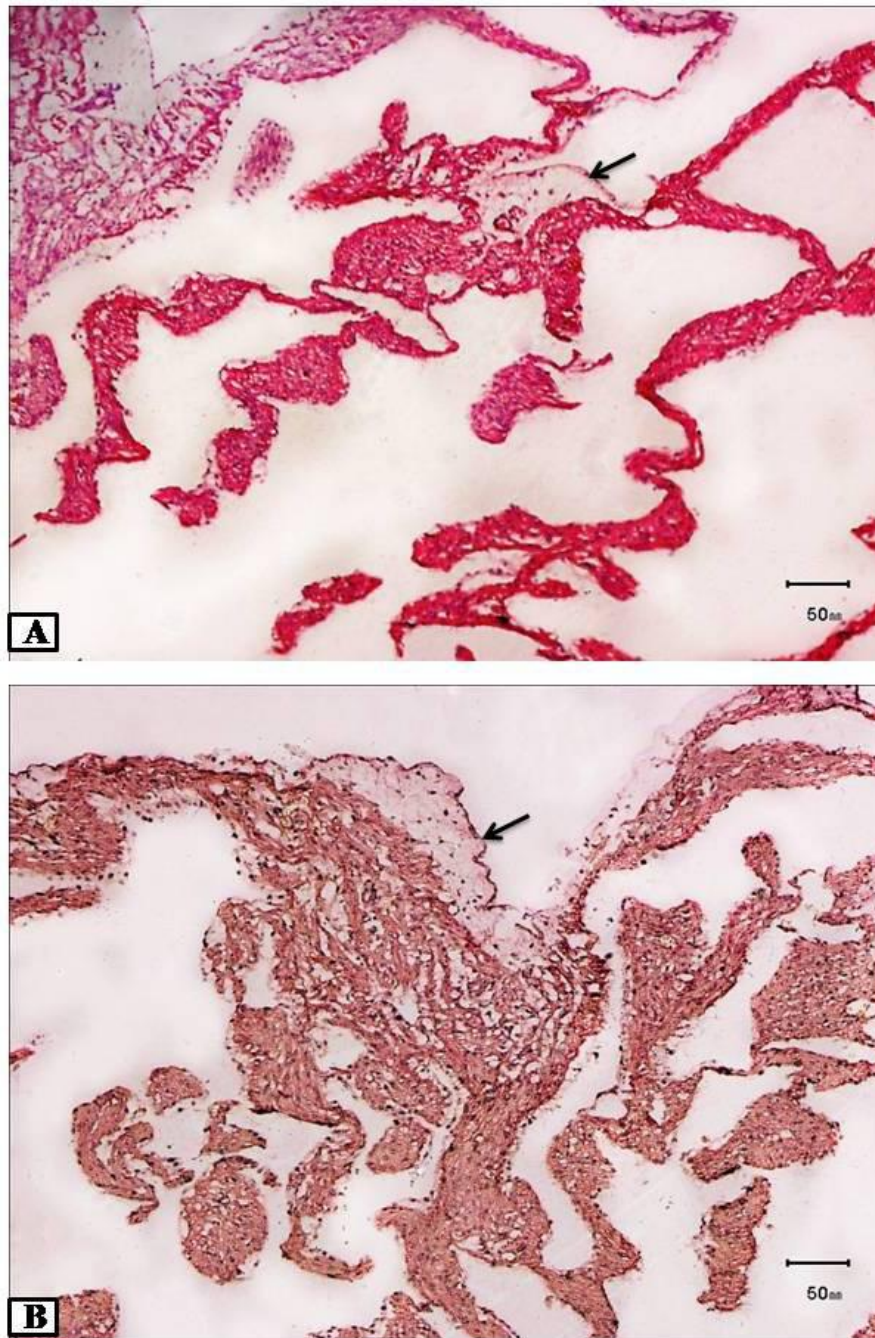
Fig. 7. A and B: Photomicrographs showing the atrium of 17 cm CVRL camel foetus; epicardium (arrow) consisting of large amount of connective tissue and lined by simple squamous epithelium. A: H&E (X10). B: Verhoff's (X10).
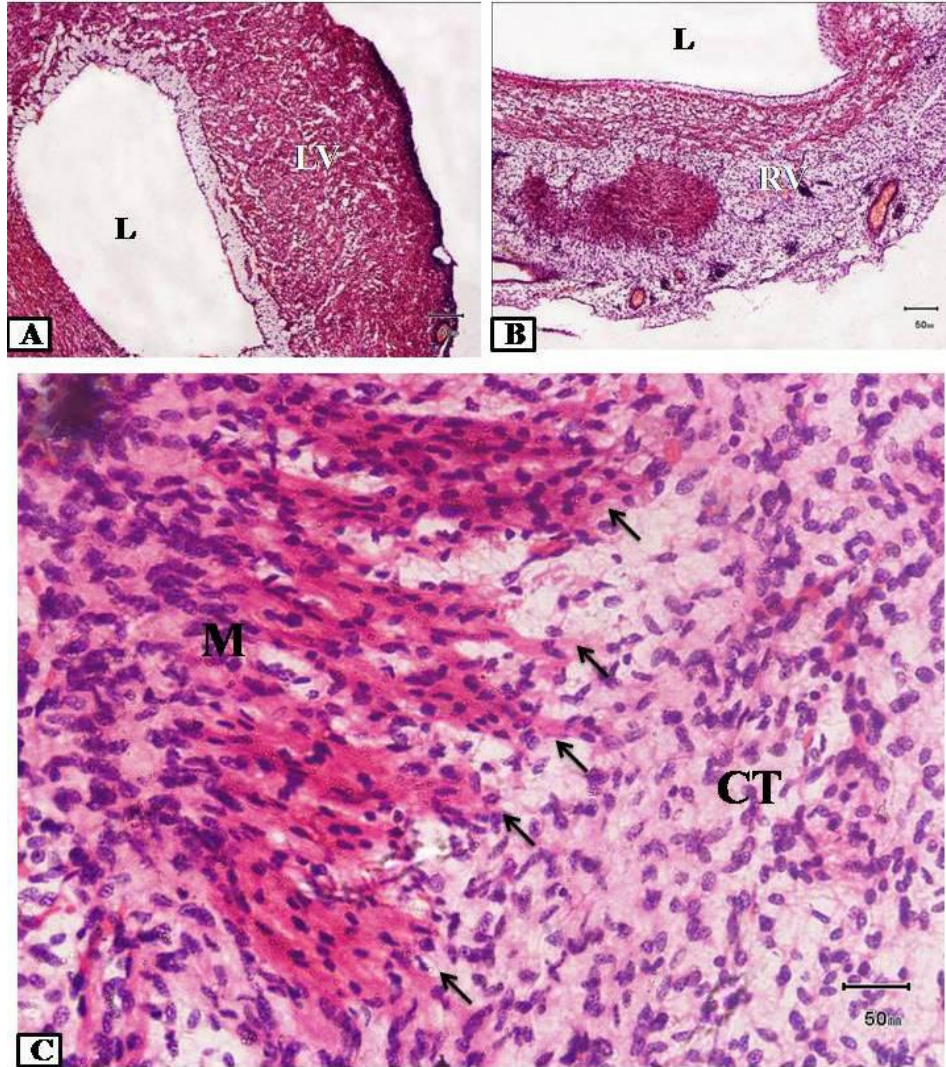
Fig. 8. A, A Photomicrograph showing histogenesis from connective tissue to muscular tissue of LV, left ventricle of 17.5 cm CVRL camel foetus. L, lumen of the left ventricle. H&E, (X4).

B: A Photomicrograph showing the right ventricle of the same heart the histogenesis was comparatively advanced than that in the left ventricle. L, lumen of the right ventricle. H&E, (X4).

C: A Photomicrograph showing higher magnification of the same section in B, histogenesis is very clear in right ventricle (arrows). CT, connective tissue, M, myocardium. H&E, (X40).
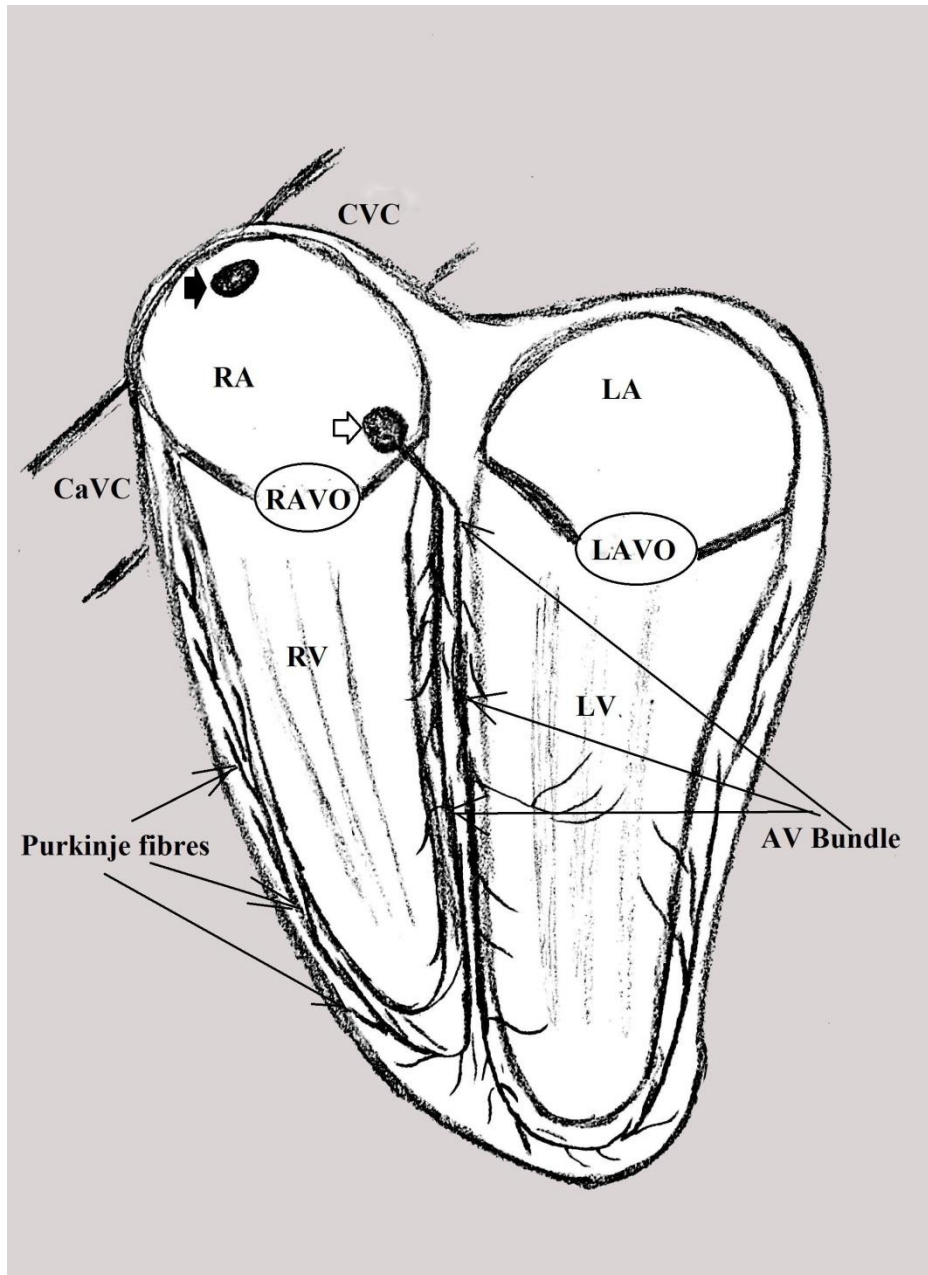
Fig. 9. A drawing showing cardiac conduction system of the camel foetus (second and third trimesters); SAN, black arrow. AVN, white arrow. AV bundle and Purkinje fibres are also shown. CaVC, Caudal vena cava, CVC, cranial vena cava, LA, left atrium, LV, left ventricle, LAVO left atrioventricular orifice, RA, right atrium, RAVO, right atrioventricular orifice.
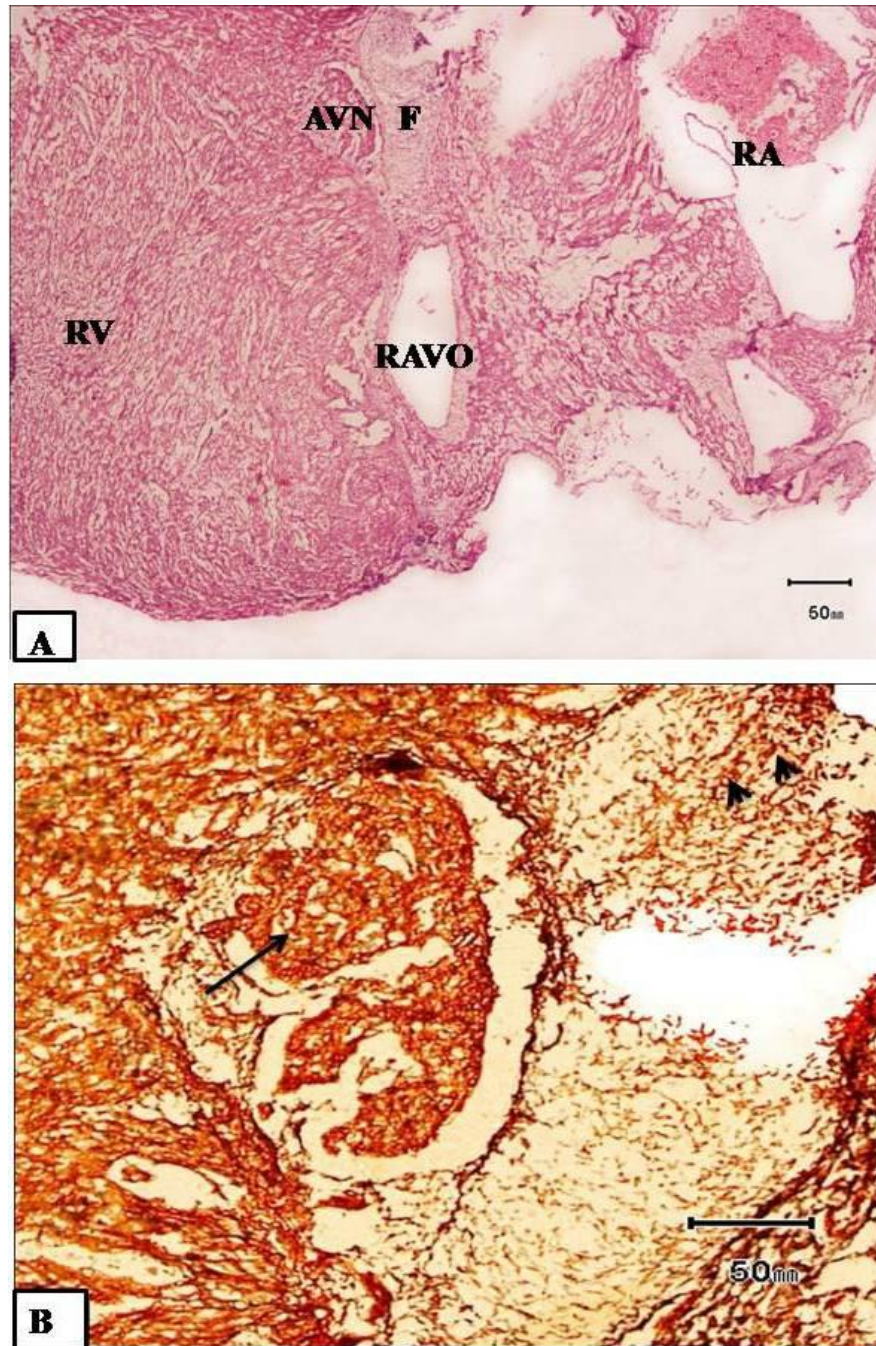
Fig. 10. A: A photomicrograph showing atrioventricular node (AVN) of 13 cm CVRL camel foetus surrounded by a large amount of connective tissue, F, fibroblasts, RA, right atrium, RV, right ventricle, RAVO, right atrioventricular opining are shown. H&E (X4).

B: A photomicrograph showing reticular fibres (arrowheads), surrounding AVN (arrow). Gordon and Sweet stain (X10).
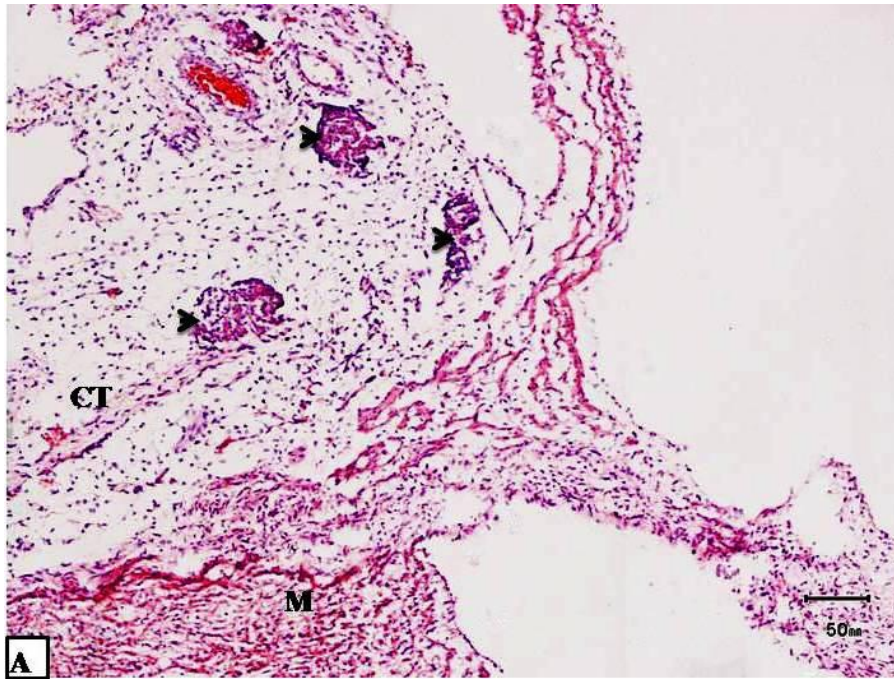
Fig. 11. A: A photomicrograph showing scattered AVN (arrowheads) of 17 cm CVRL camel foetus, connective tissue CT, myocardium M. H&E (X10).
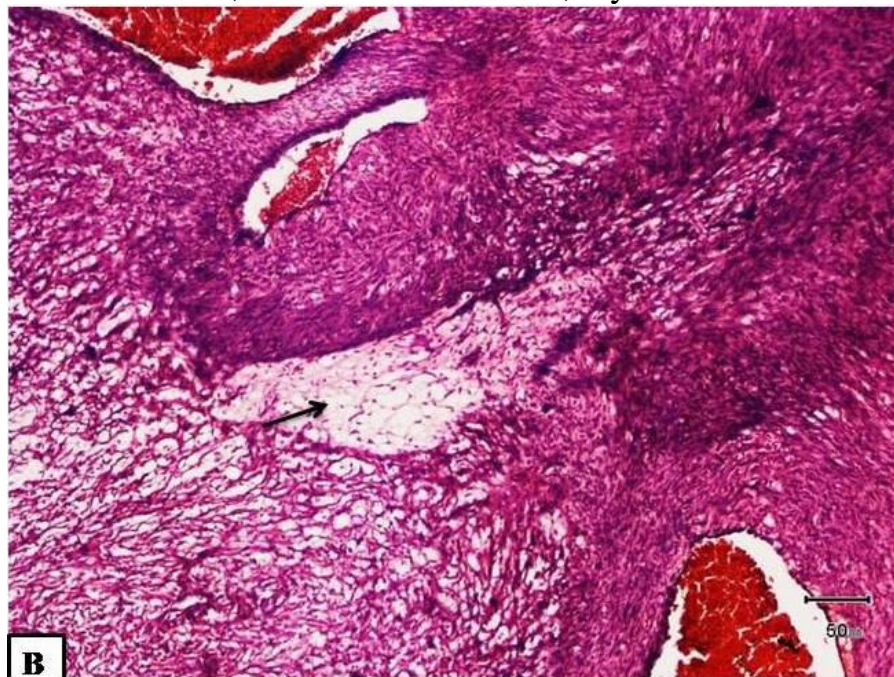
Fig. 11. B: A photomicrograph showing Purkinje fibres (arrows) embedded in myocardium of 18 cm CVRL camel foetus. H&E (X10).
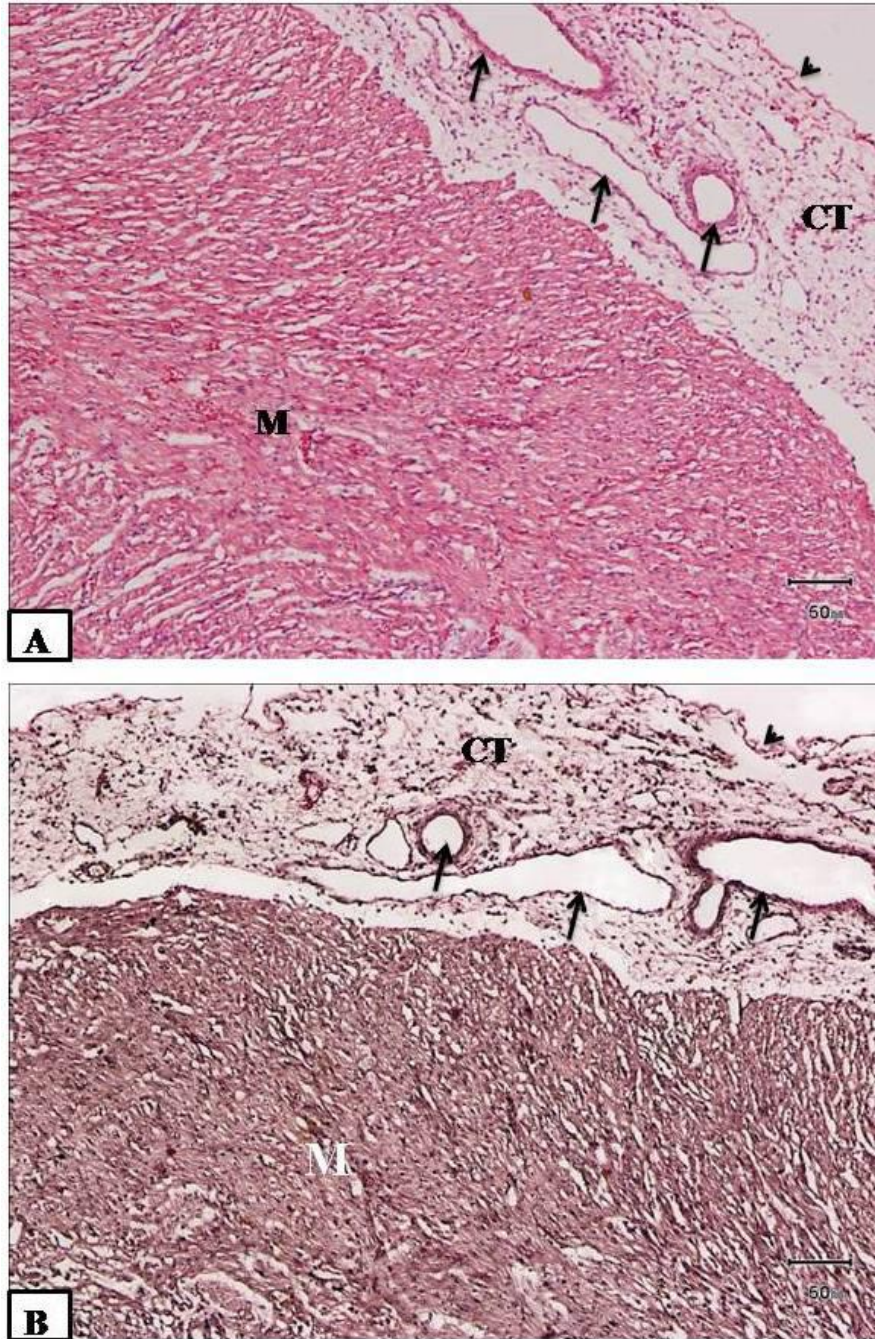
Fig. 12. A: A photomicrograph showing the heart of 24.5 cm CVRL camel foetus; showing coronary vessels and their branches (arrows), epicardial connective tissue CT, lined by simple squamous epithelium (arrowhead) myocardium M. H&E (X10).

B: Showing the same field in A; elastic fibres in the tunica media of the arteries, between cardiac muscle and in the connective tissue of subendocardium area. Verhoff's (X10).
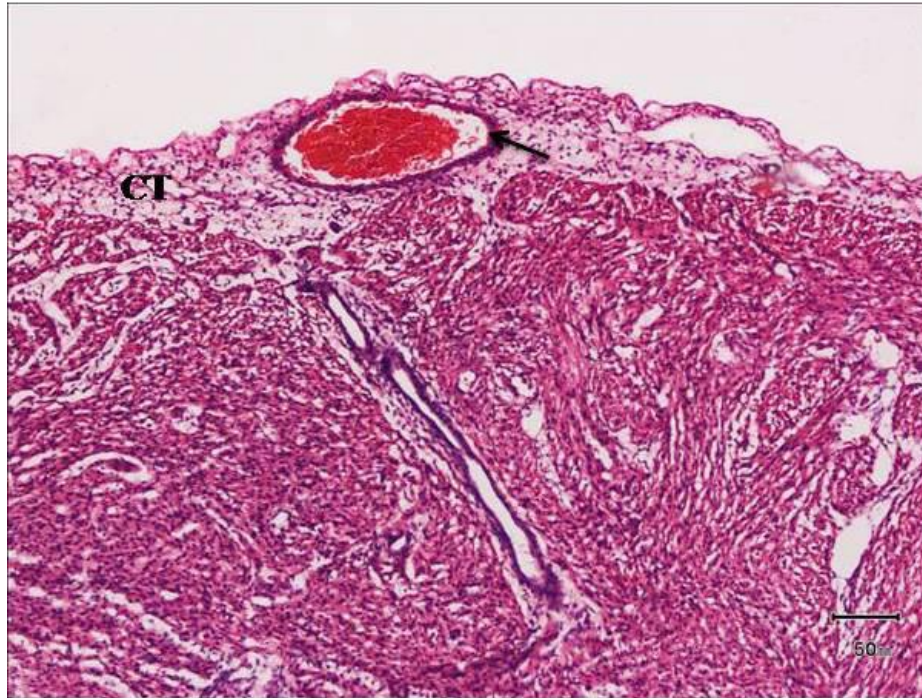
Fig. 13. A photomicrograph showing the right ventricle of the heart of 29 cm CVRL camel foetus; subsinuosal interventricular branch of coronary artery (arrow) embedded in epicardial connective tissue (CT). H&E (X10).
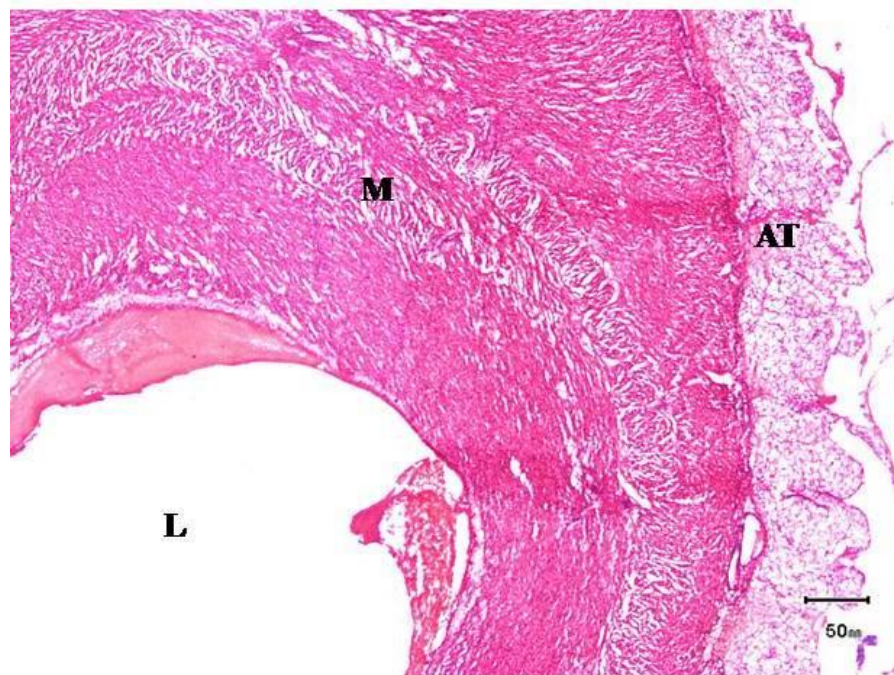
Fig. 14. A photomicrograph showing the right ventricle of the heart of 30 cm CVRL camel foetus. Epicardium lined by simple squamous epithelium and has large amount of adipose tissue (AT) attached to the myocardium (M). L, lumen of the right ventricle. H&E (X4).

Fig. 15. A photomicrograph showing the left ventricle of the heart of 30 cm CVRL camel foetus. Epicardium lined by simple squamous epithelium (arrow). Large amount of adipose tissue (AT) in the myocardium (M) and around the aorta (A). L, lumen of the left ventricle. H&E (X4).
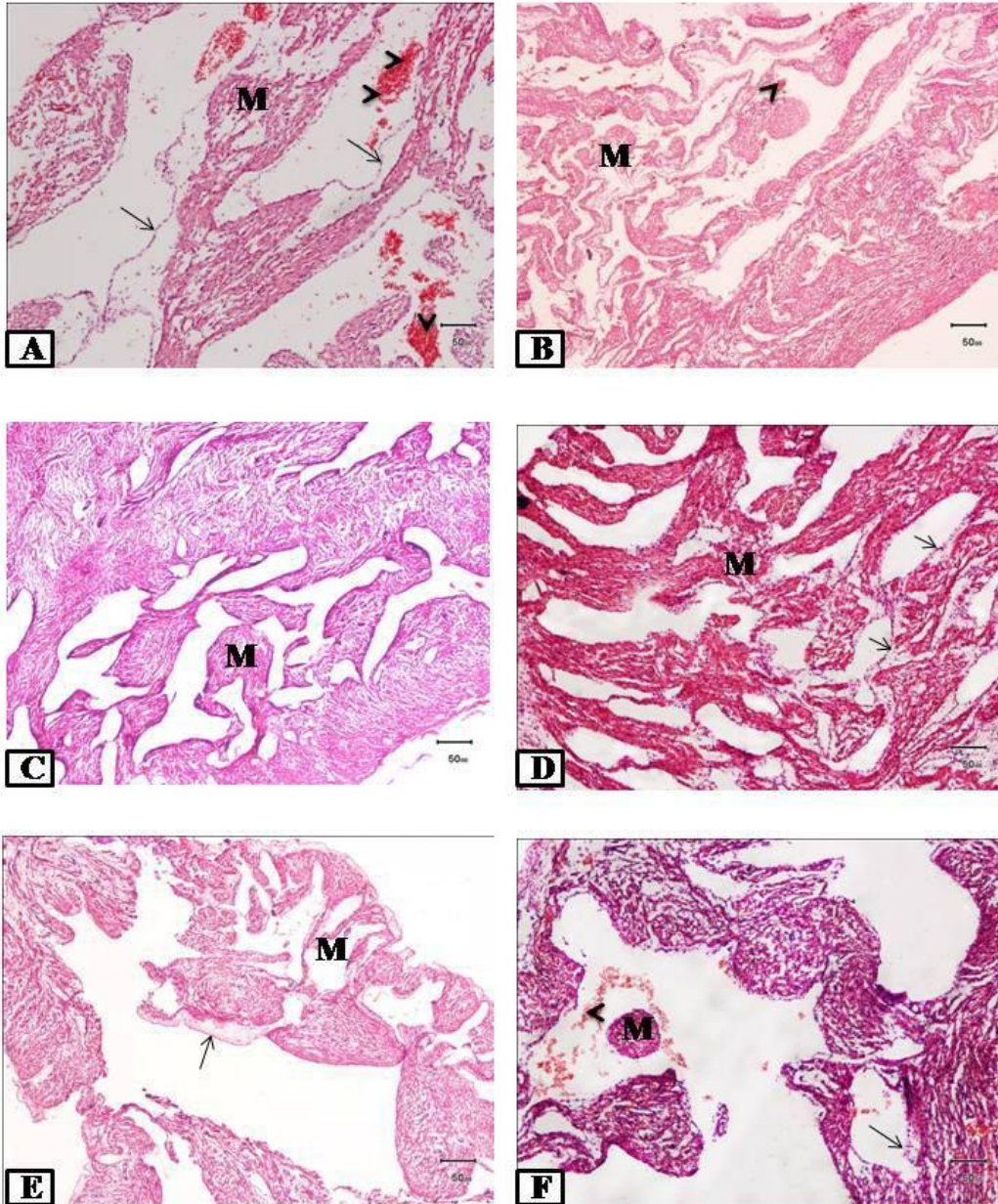
Fig. 16. Photomicrographs showing the atria of early and mid stages of the second trimester of gestation of camel foetus. A: 24.5 cm CVRL (X10), B: 29 cm CVRL (X4), C: 30 cm (X10), D: 33 cm (X10), E: 38 cm CVRL (X4), F: 41 cm CVRL (X10). Endocardium lined by simple squamous epithelium and thin layer of connective tissue is shown (arrows). M, well developped Pectinate muscles, arrowheads, red blood cells. (H&E).
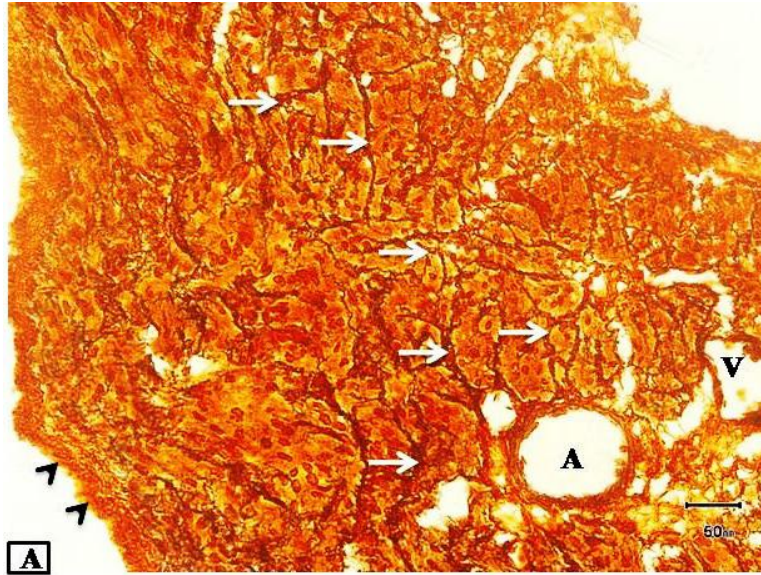
Fig. 17. A: A photomicrograph showing the atria of 60 cm CVRL of camel foetus containing large amount of reticular fibres (arrows). A, Arteriole, arrowheads, epicardium, V, venuole. Gordon and Sweet (X40).
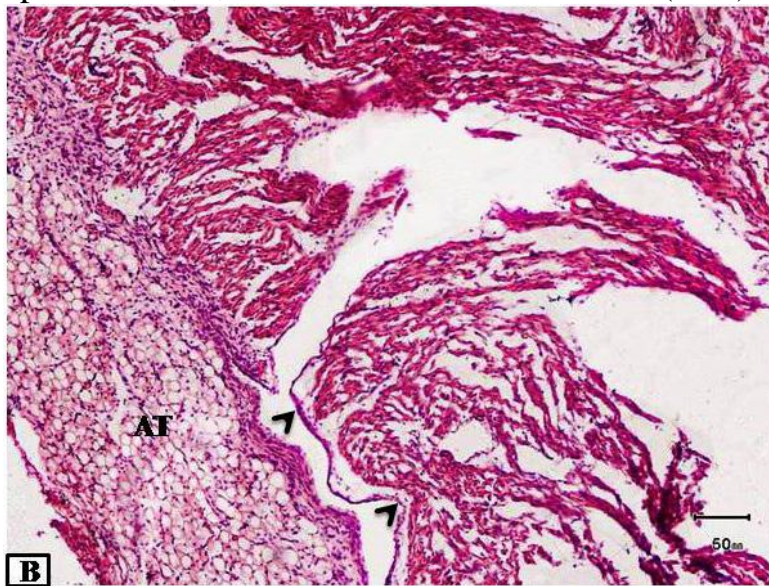
Fig. 17. B: A photomicrograph showing the atria of 68 cm CVRL of camel foetus containing large amount of adipose tissue (AT) covering epicardium (arrowheads). H&E (X4).
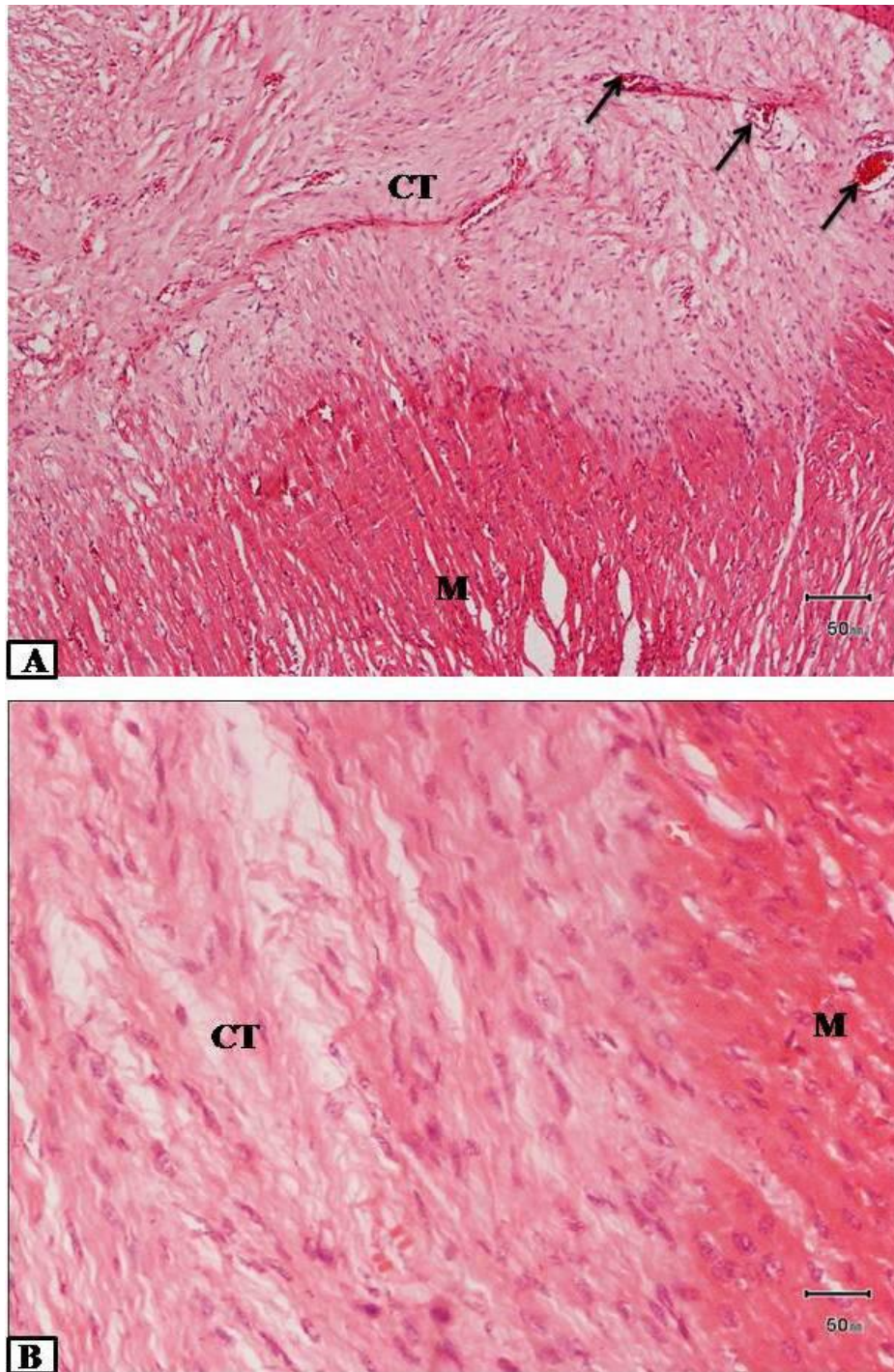
Fig. 18. A and B: Photomicrographs showing the heart of 24.5 cm CVRL camel foetus. Ventricular myocardium (M) is clearly distinguished from connective tissue (CT), blood vessels (arrows). H&E (X10), B: (X40).
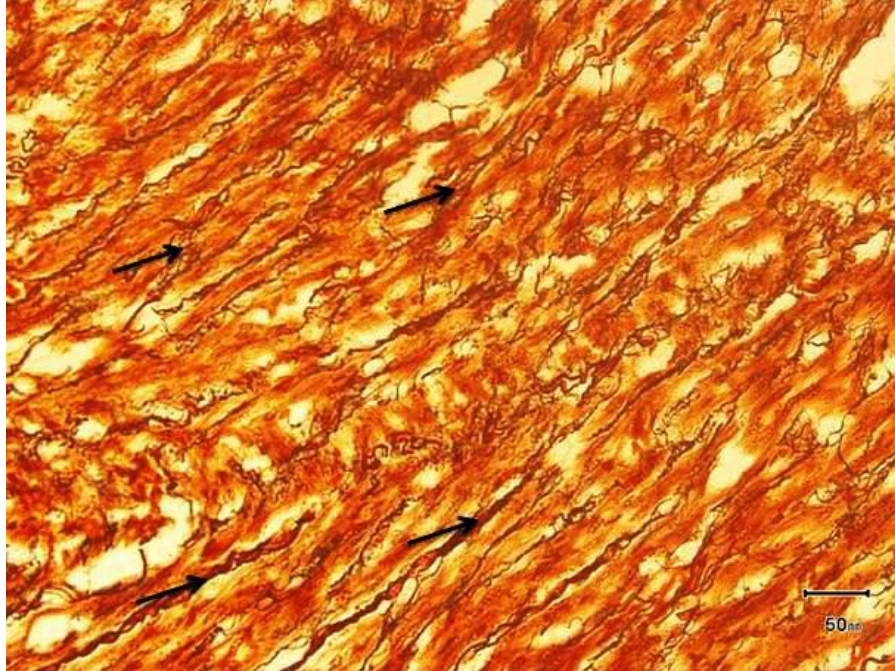
Fig. 19. A photomicrograph of cardiac muscles of 60 cm CVRL camel foetus. Note that reticular fibres (arrows) are interposed between the cardiac muscles. Gordon and Sweet (X40).
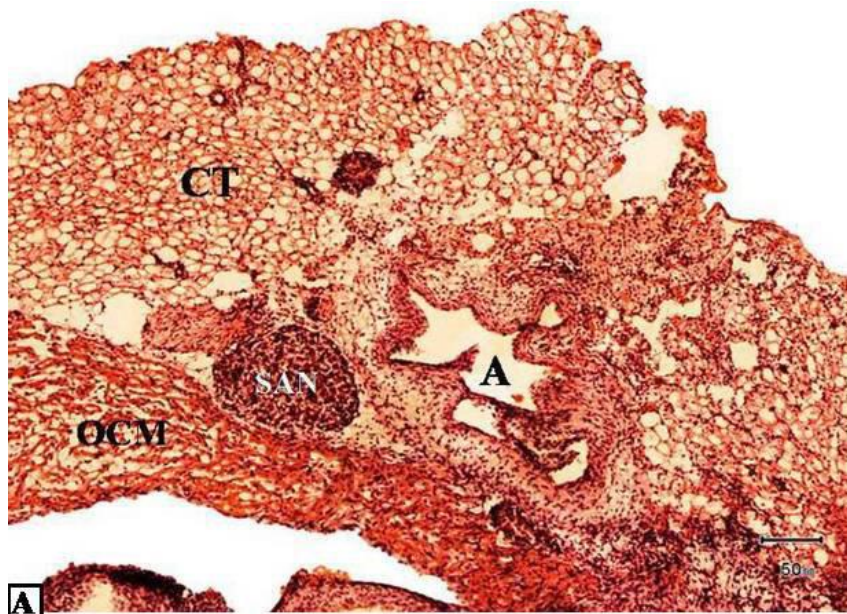
Fig. 20. A: A photomicrograph showing sinoatrial node SAN of 38 cm CVRL camel foetus embedded in large amount of connective tissue (CT) and close to the ordinary cardiac muscles (OCM). A, SAN artery. H&E (X4).
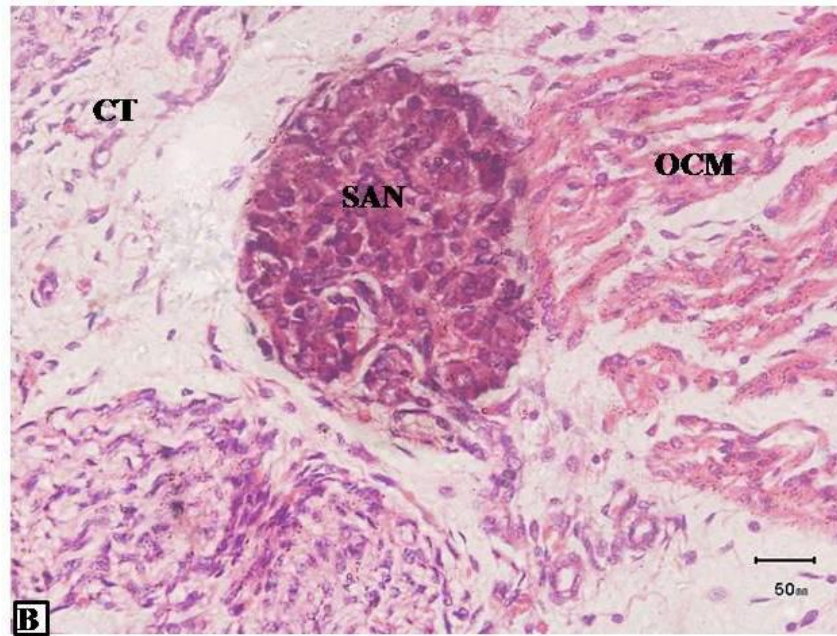
Fig. 20. B: A photomicrograph showing SAN of 68 cm CVRL camel foetus, embedded in large amount of connective tissue (CT) and close to the ordinary cardiac muscles (OCM). H&E (X40).
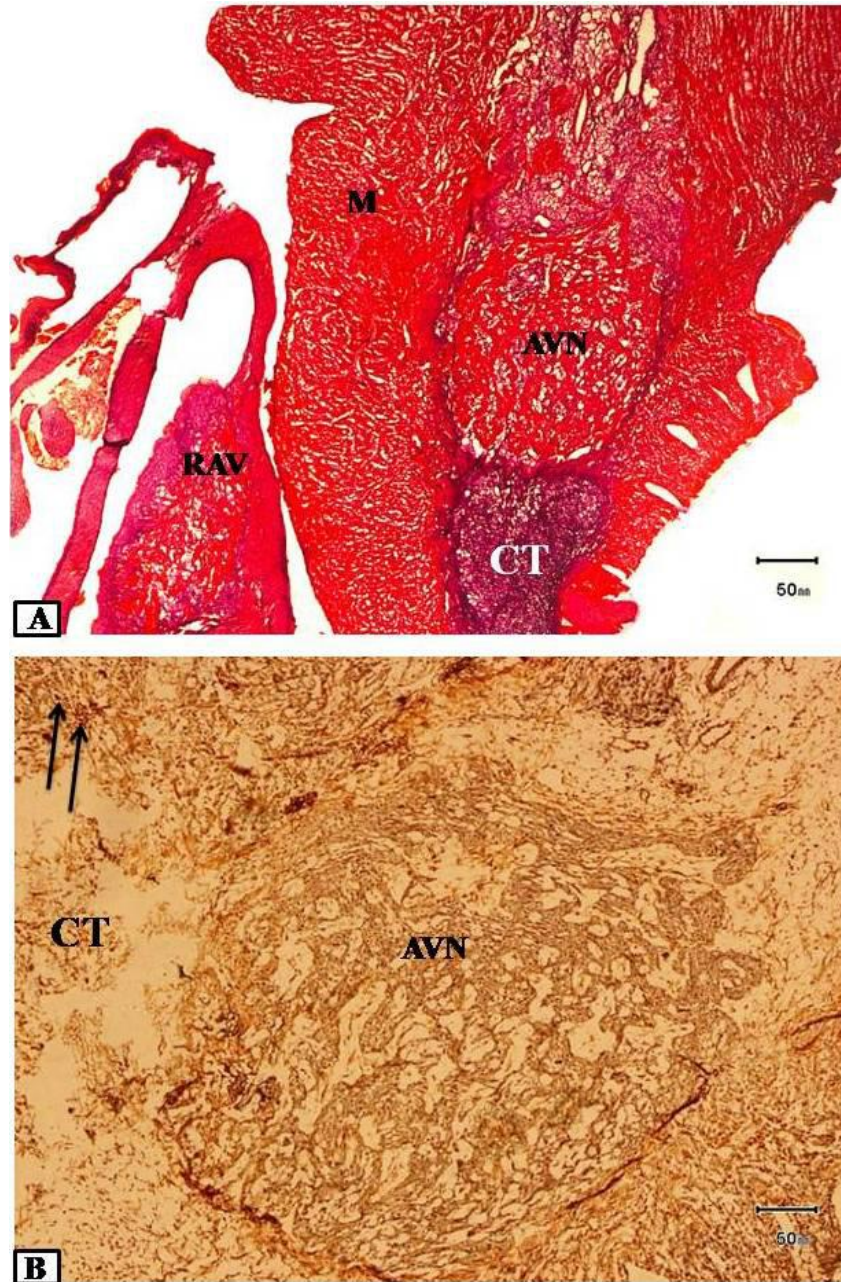
Fig. 21. A: A photomicrograph showing atrioventricular node AVN of 38 cm CVRL camel foetus close to cardiac muscle (M), surrounded by connective tissue (CT), and situated close to the right atrioventricular valve (RAV). Aldehyde fuchsin (X10).
B: The same section in A showing a few amount of reticular fibres (arrows). Gordon and Sweet (X40).
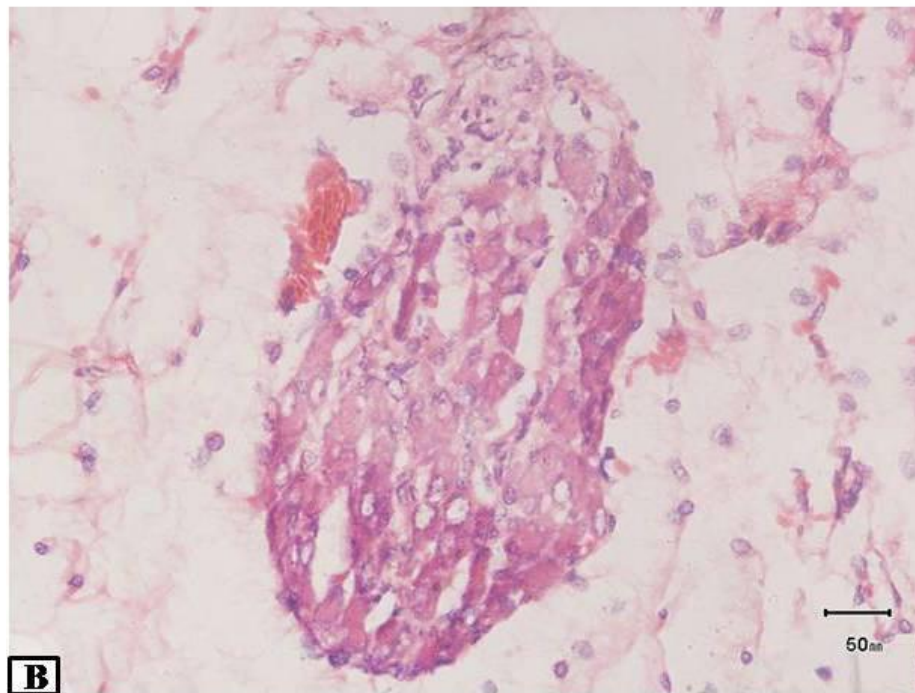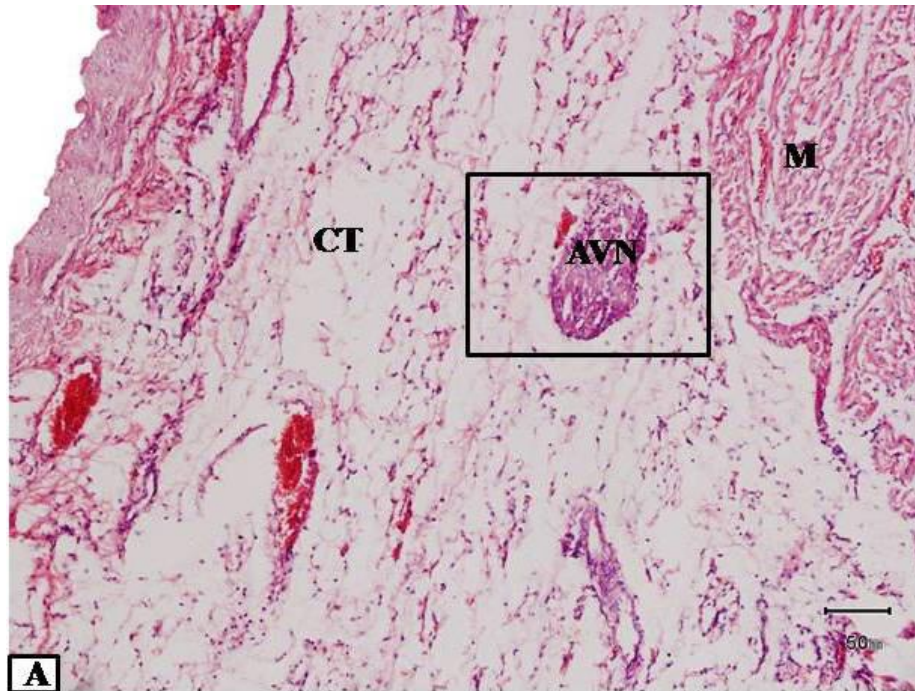
Fig. 22. A: A photomicrograph showing AVN of 71 cm CVRL camel foetus, near to the cardiac muscle (M), surrounded by a large amount of connective tissue (CT). H&E (X4).
B: Is a magnification of the rectangle in A (X40).

Fig. 23. A: A photomicrograph showing atrioventricular bundle (AVB) of 61 cm CVRL camel foetus embedded in cardiac muscle (M). H&E (X10).
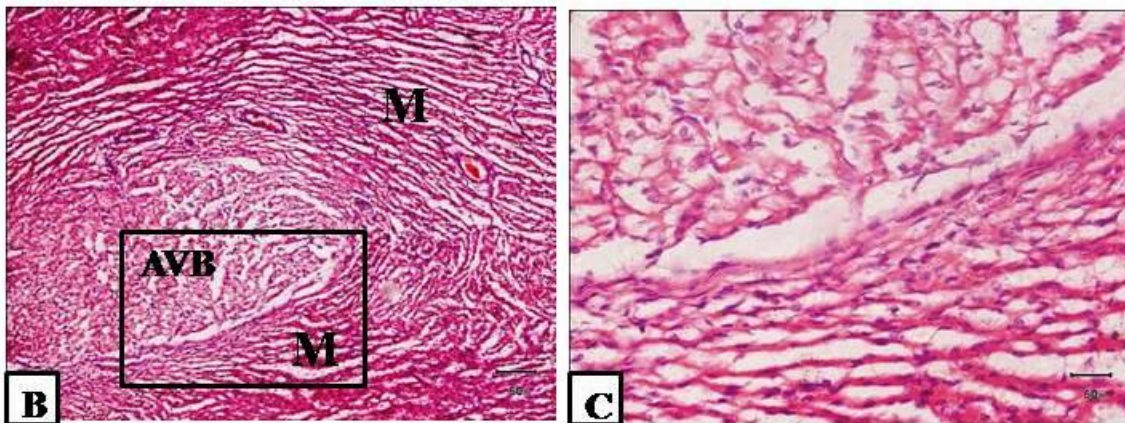
Fig. 23. B: Showing AVB embedded in myocardium of 68 cm CVRL. H&E (X10).
C: Is a magnification of the rectangle in B showing the cytoplasm of AVB fibres was light centrally and dark peripherally (X40).
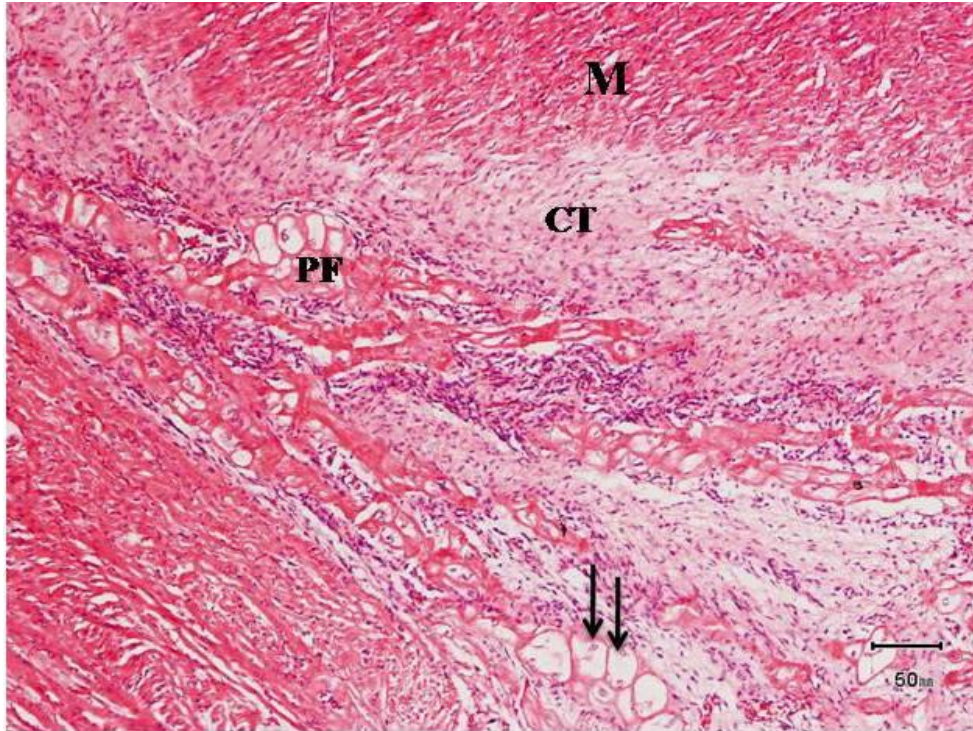
Fig. 24. A photomicrograph showing morphogenesis of Purkinje fibres (PF) and cardiac muscles (M) of camel foetus at 24.5 cm CVRL. Purkinje fibres were embedded in a large amount of connective tissue (CT). Note that some of the fibres were binucleated (arrows) H&E (X10).
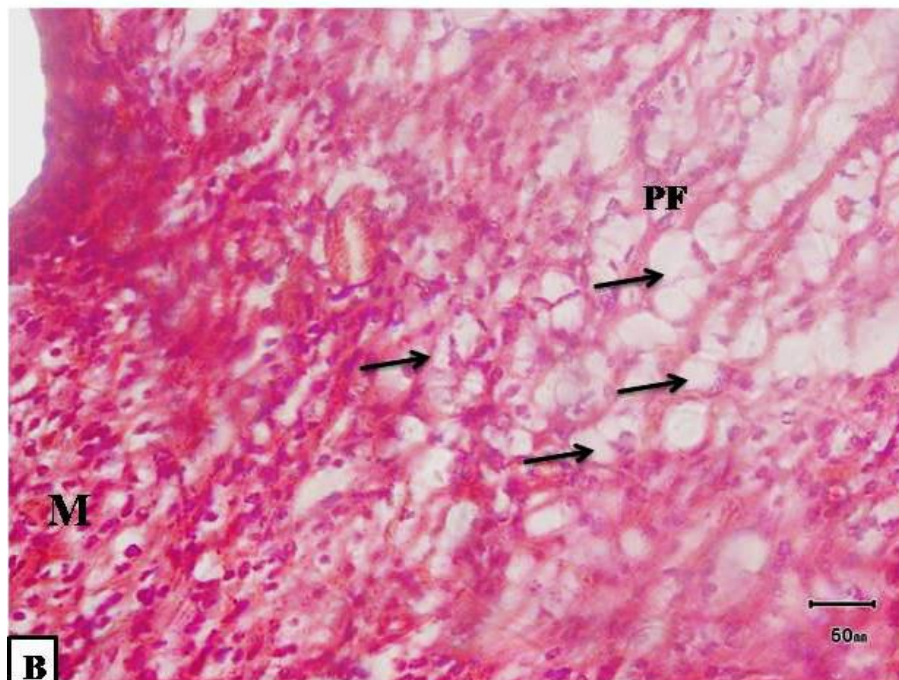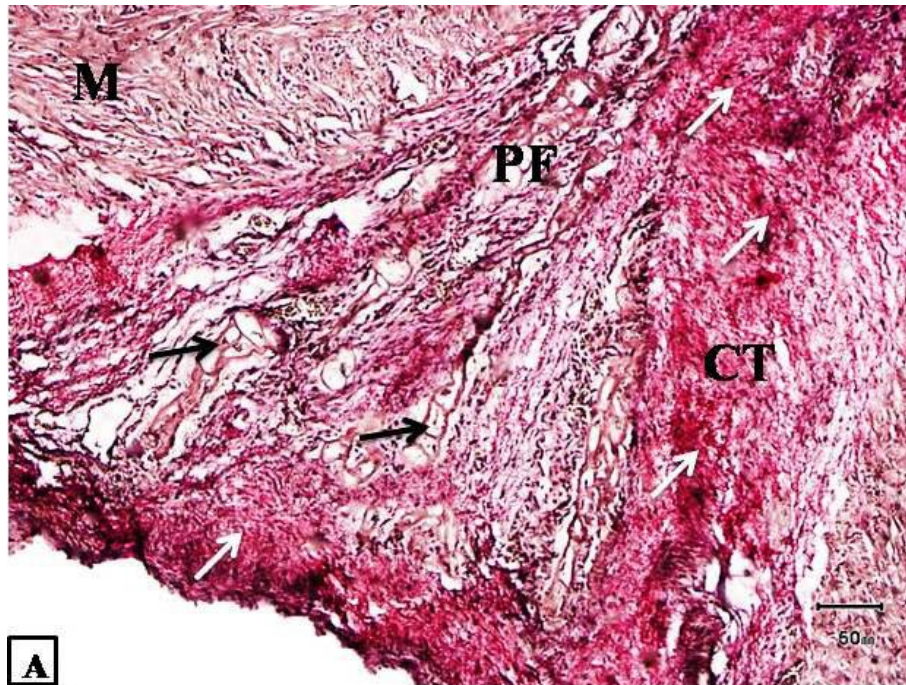
Fig. 25. A: A photomicrograph showing morphogenesis of Purkinje fibres (PF), cardiac muscle (M) of camel foetus at 33 cm CVRL. They are embedded in connective tissue (CT) with large amount of collagen fibres (white arrows). Van Gieson's. (X10).

B: A high magnification of the same section in A showing Purkinje fibres (PF) irregular in shape (black arrows). H&E (X40).
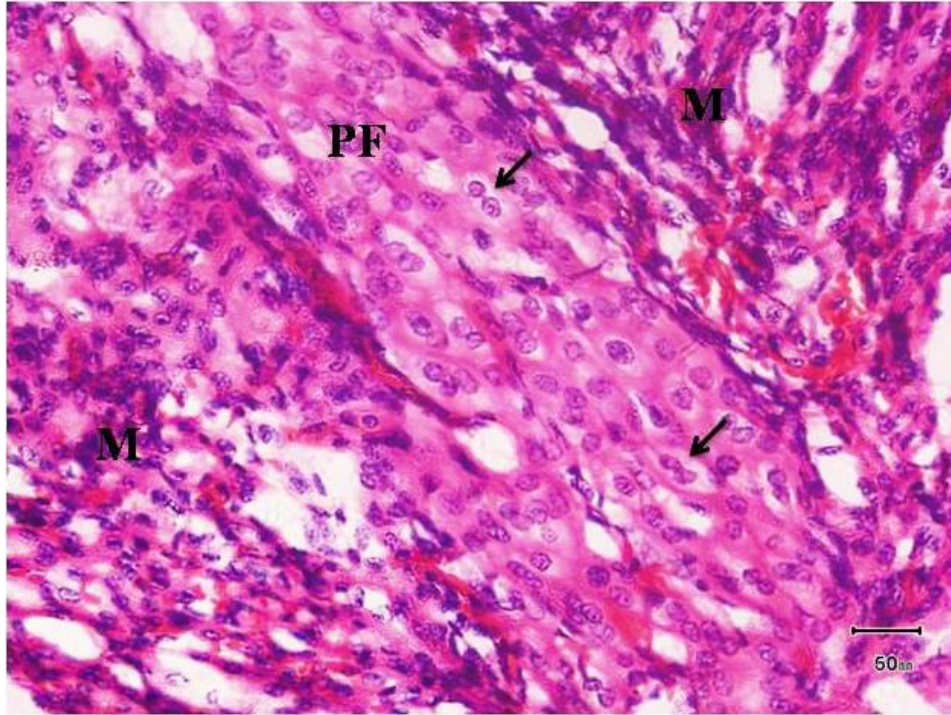
Fig. 26. A photomicrograph showing histogenesis of Purkinje fibres (PF) from cardiac muscles (M) in camel foetus at 41 cm CVRL, PF appeared lighter than cardiac muscle with double nuclei (arrows). H&E (X40).
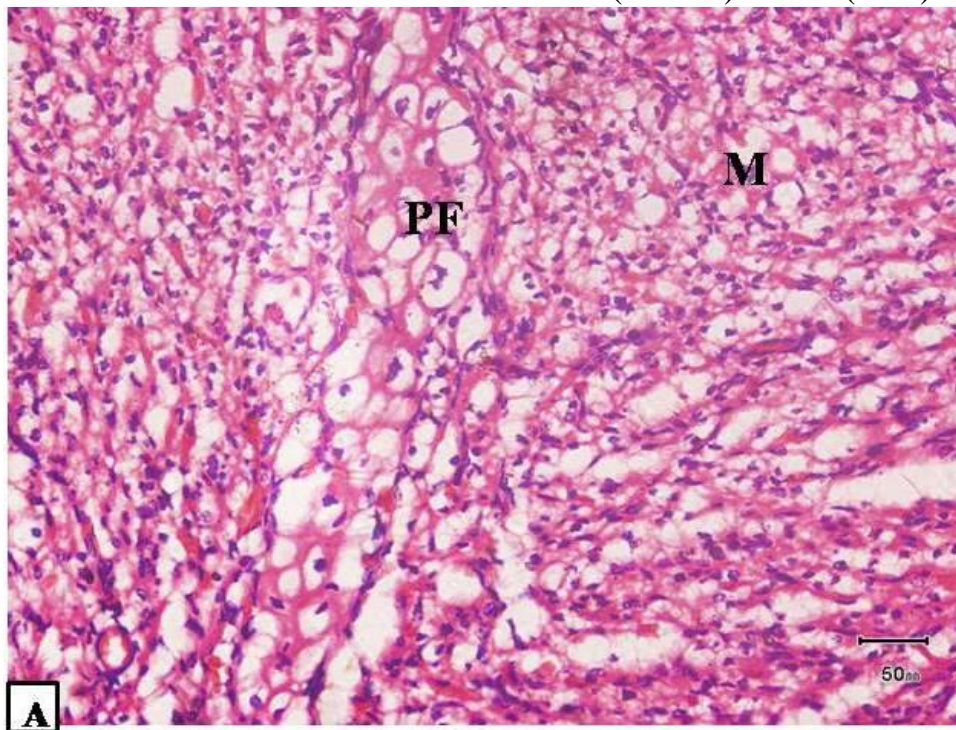

Fig. 27. A: A photomicrograph showing Purkinje fibres (PF) embedded in the ventricular myocardium of camel foetus at 60 cm CVRL. H&E (X40).
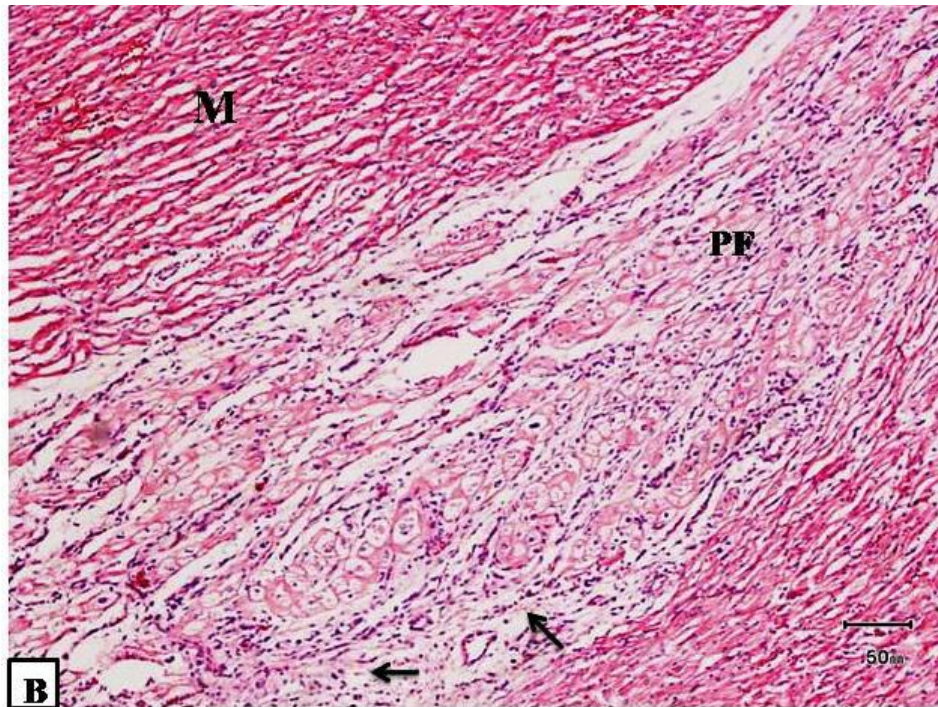
Fig. 27. B: Showing (PF) of camel foetus at 71 cm CVRL as bundles embedded in the connective tissue (arrows) separating cardiac muscle from PF. H&E (X10).
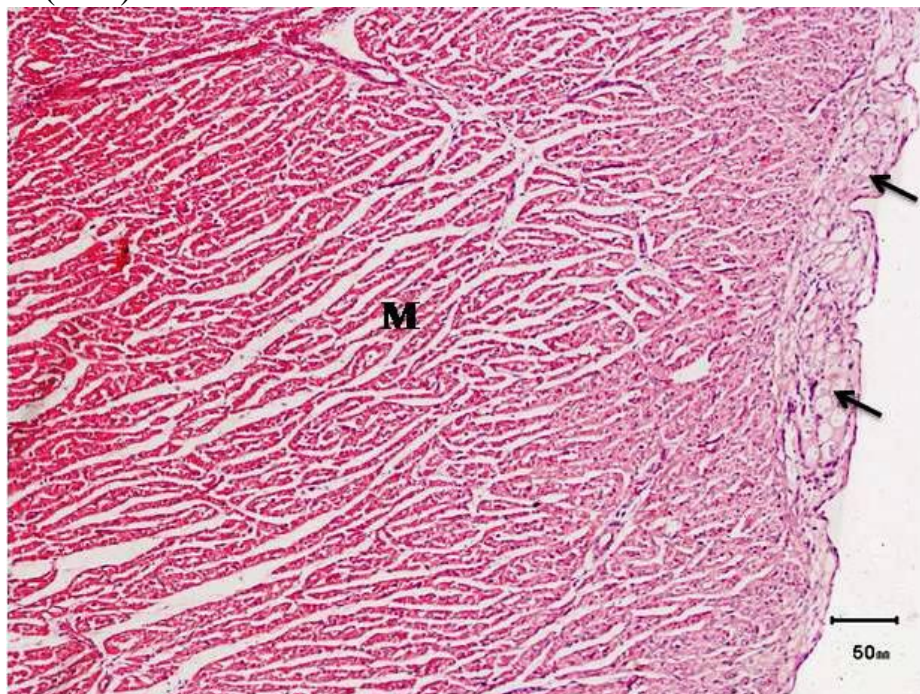

Fig. 28. A photomicrograph showing Purkinje fibres (arrows) situated in the subendocardium, connected to the cardiac muscles (M) and covered by endothelium. Camel foetus at 71 cm CVRL. H&E. (X10).
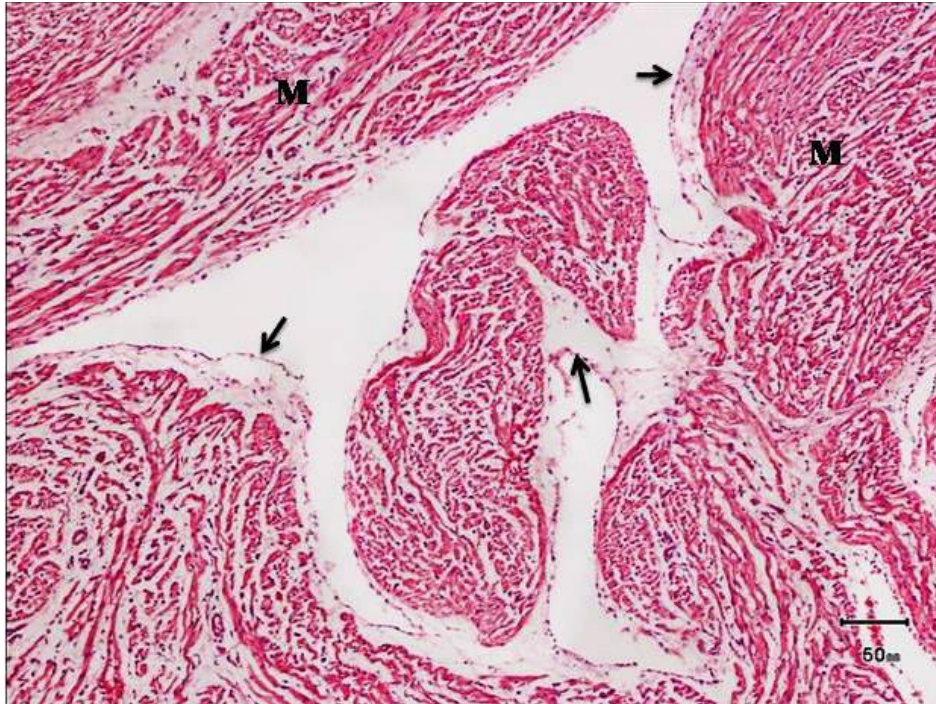
Fig. 29. A photomicrograph showing pectinate muscles (M) in the left atrium of 74 cm CVRL camel foetus lined by simple squamous epithelium (arrows) and thin layer of connective tissue. Note the increase in thickness of pectinate muscles. H&E (X10).
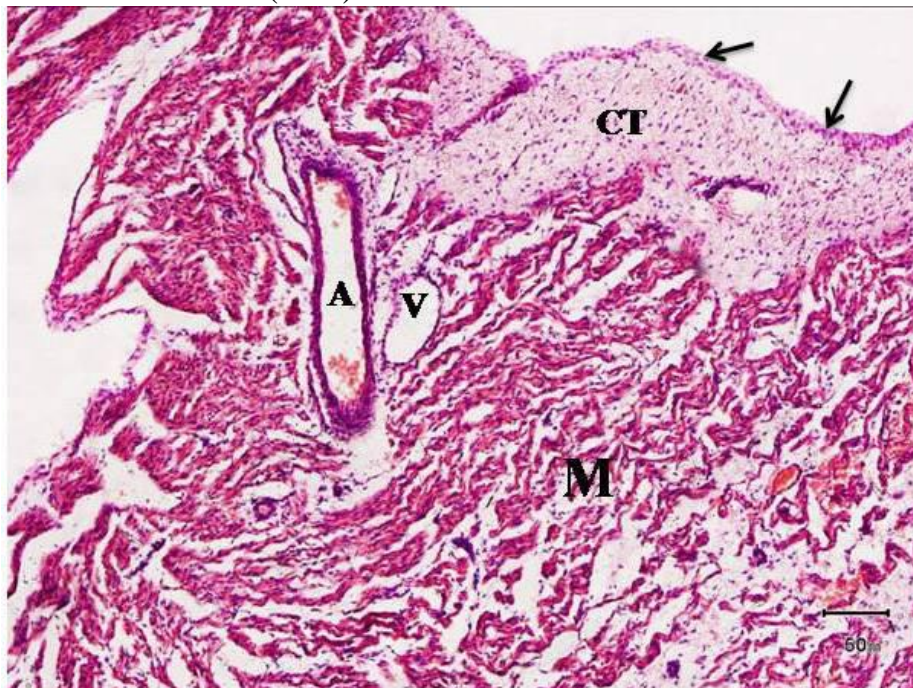

Fig. 30. A photomicrograph showing connective tissue (CT) in the atrial epicardium (arrows) and myocardium (M) of 76 cm CVRL camel foetus. A, arteriole, V, venuole. H&E (X10).

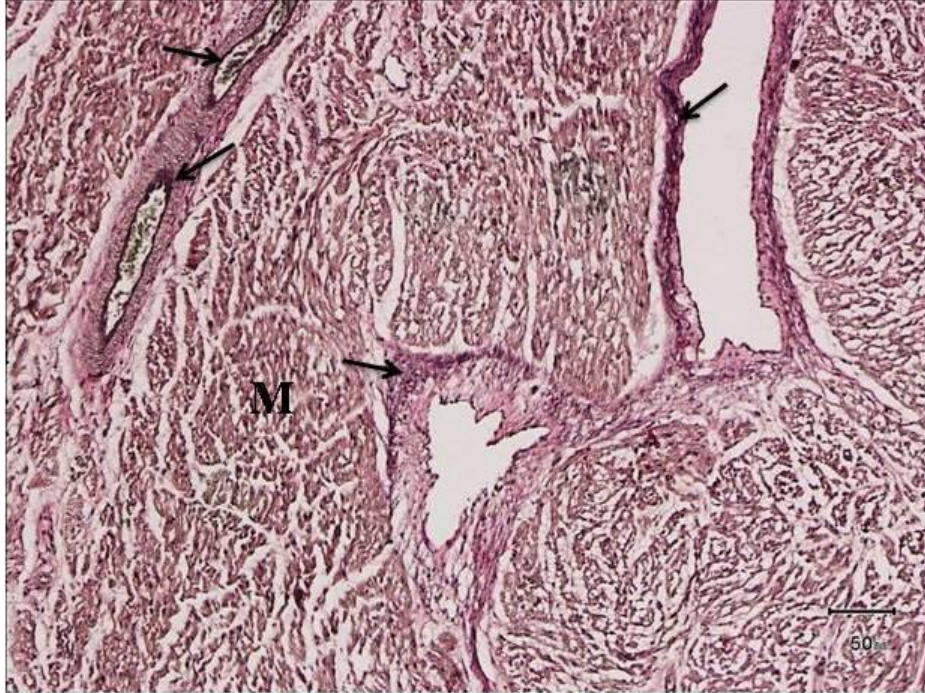**Fig. 31.** A: A photomicrograph showing the atrium of 89 cm CVRL camel foetus. Elastic fibres (arrows) are clear in the endocardium and blood vessels in the atrial myocardium (M). Verhoff's (X10).

Fig. 32. A photomicrograph of atrial myocardium (M) which showed a large amount of connective tissue specially collagenous fibres (arrowheads) under the endothelium (arrows) in 92 cm CVRL. Van Gieson's (X10).
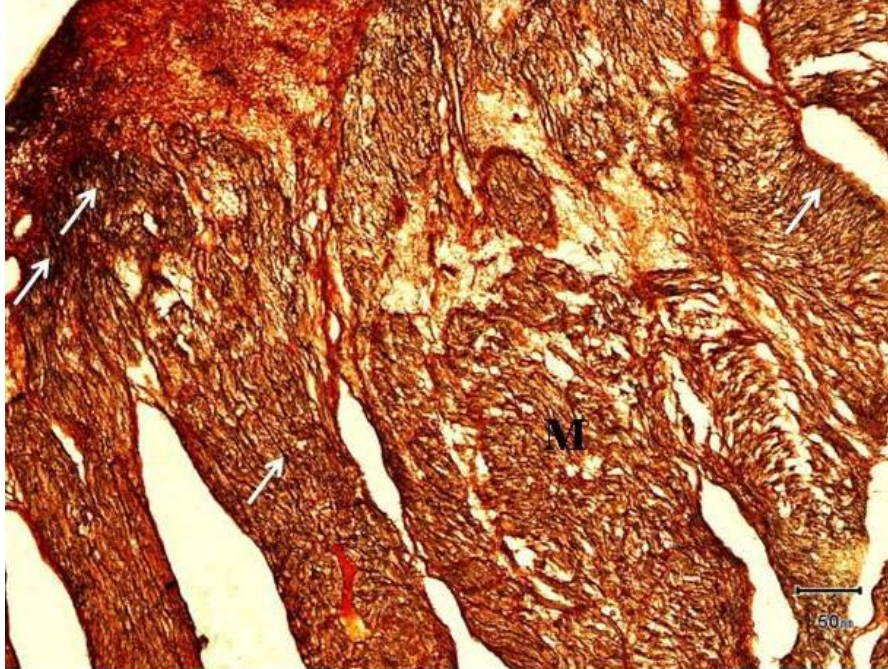
Fig. 33. B: Showing reticular fibres (white arrows) in the atrial wall of 97 cm CVRL camel foetus. Gordon and Sweet (X10).
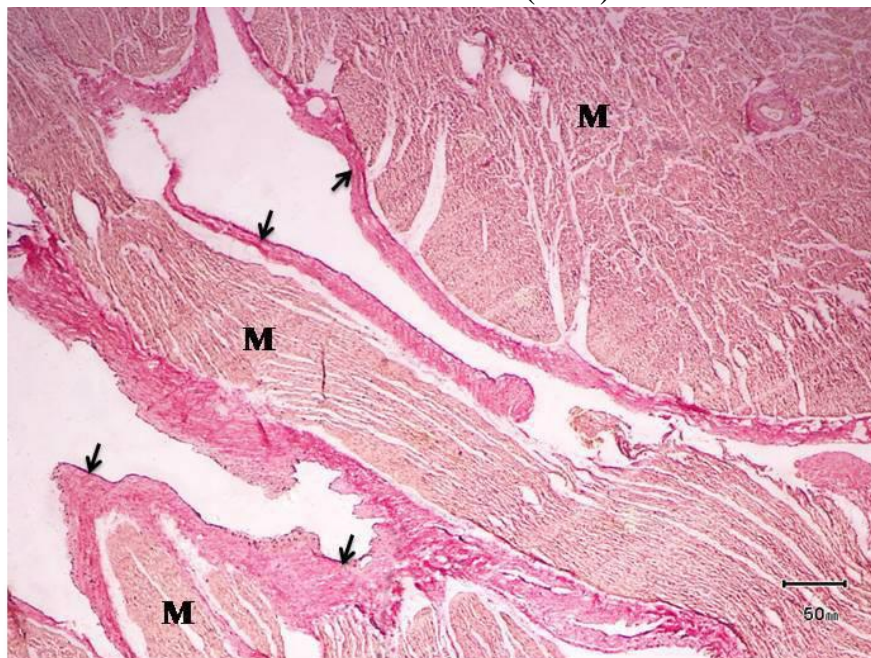
Fig. 34. A photomicrograph showing atrial myocardium (M) of 132 cm CVRL camel foetus, atrial endocardium is lined by simple squamous epithelium (arrows). Large amount of connective tissue especially collagen fibres is present (dark red). Van Gieson's (X4).
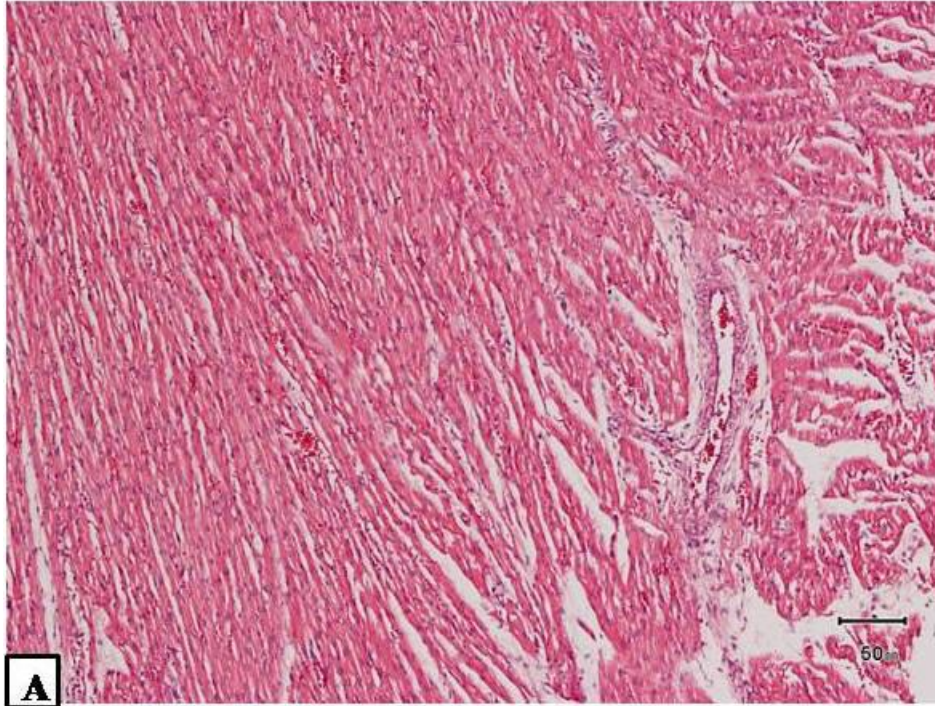
Fig. 35. A: A photomicrograph showing the histological structure of ventricular myocardium in 74 cm. H&E (X10).
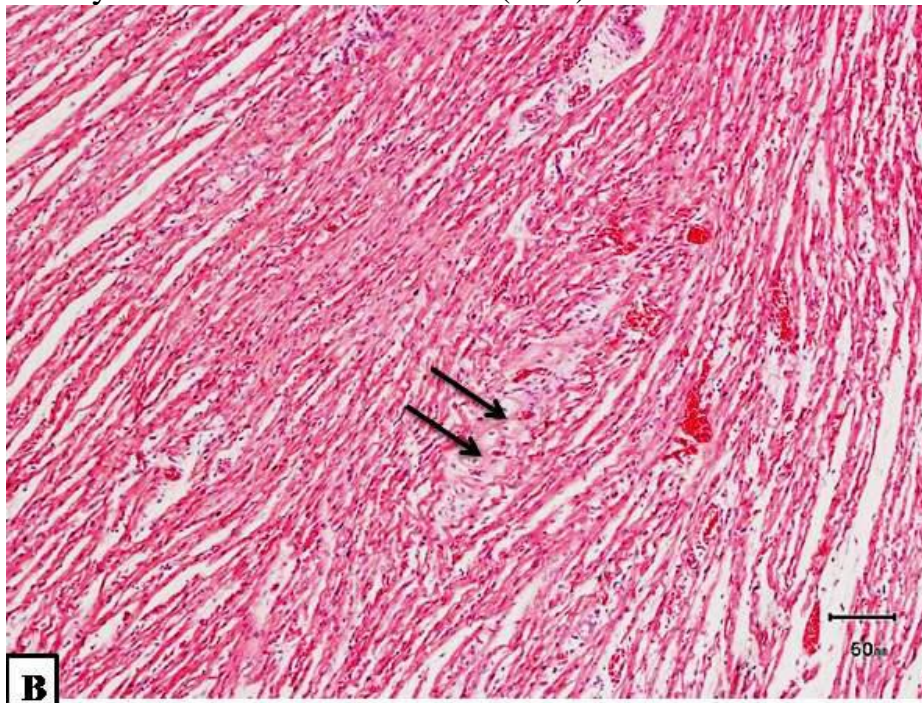
Fig. 35. B: A photomicrograph showing 89 cm CVRL camel foetus cardiac muscle cells. Note the infiltration of PF (arrows) between the ventricular cardiac muscle fibres. H&E (X10).
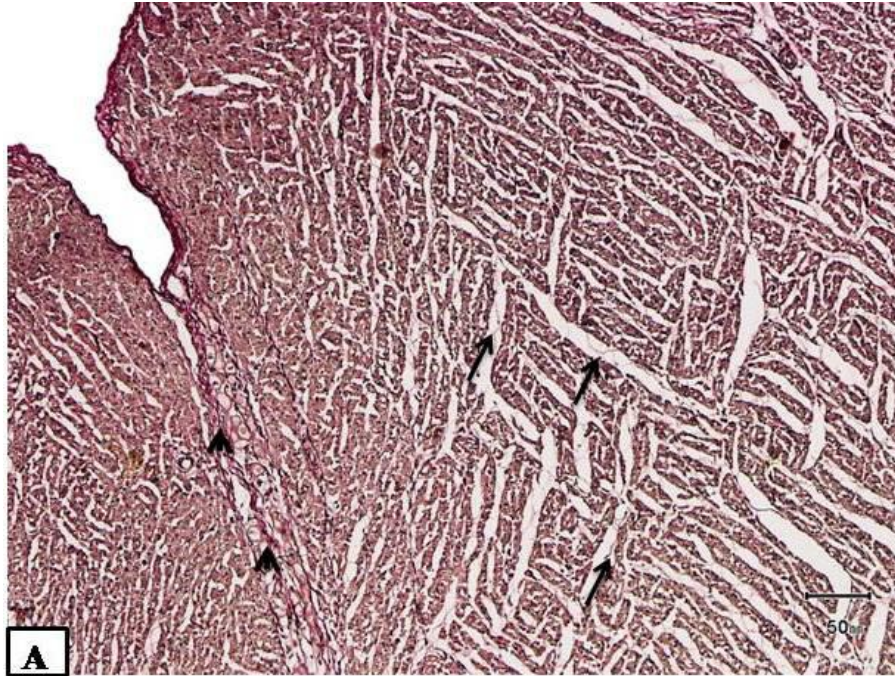
Fig. 36. A: A photomicrograph showing elastic fibres (arrows) in ventricular myocardium of 79.5 cm CVRL camel foetus. Verhoff's (X10).
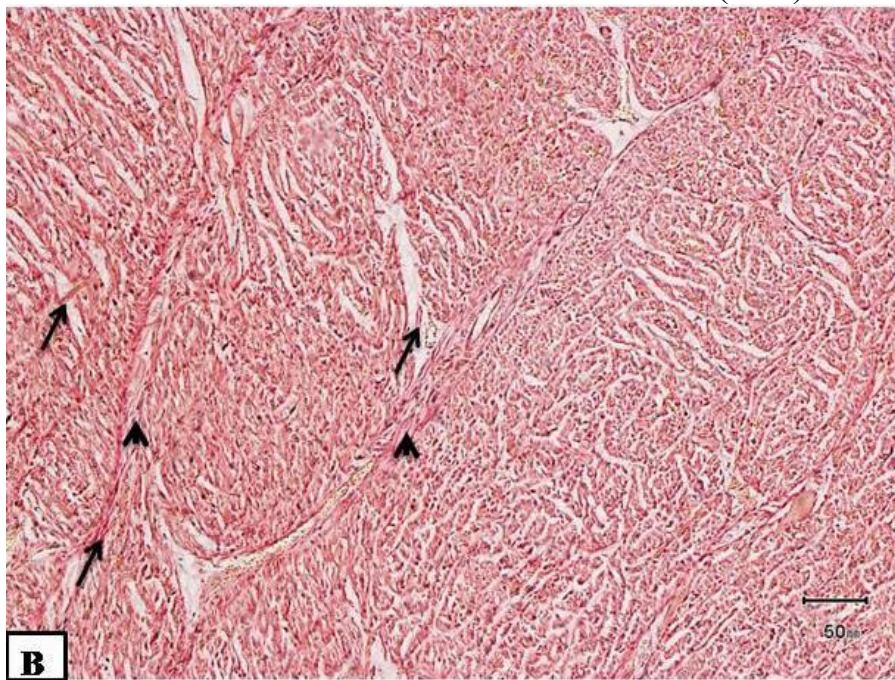
Fig. 36. B: A photomicrograph showing collagenous fibres (arrows) in ventricular myocardium of 88 cm CVRL camel foetus. Infiltration of Purkinje fibres is shown (arrowheads). Van Gieson's (X10).
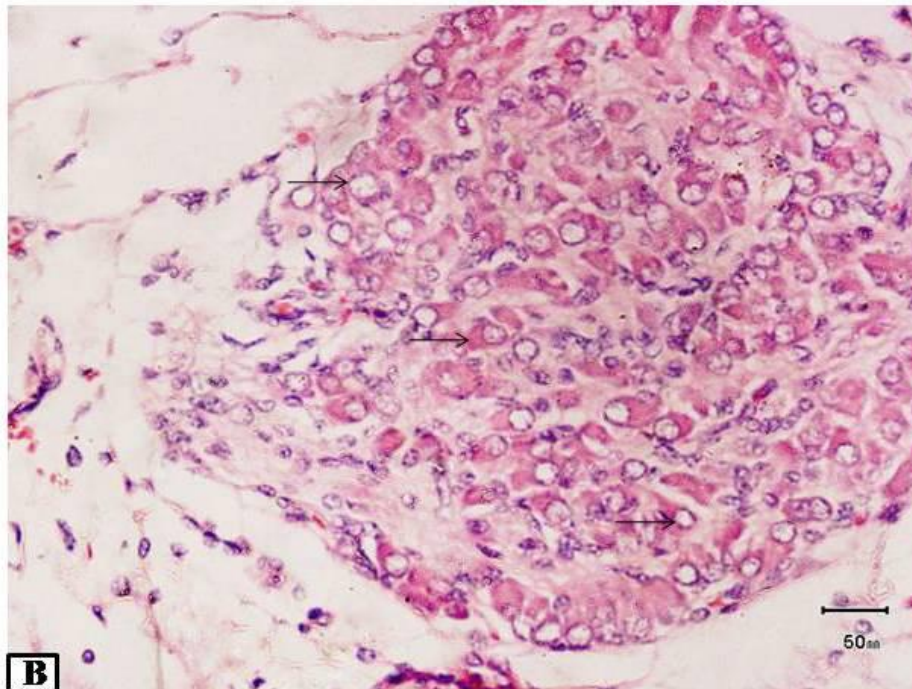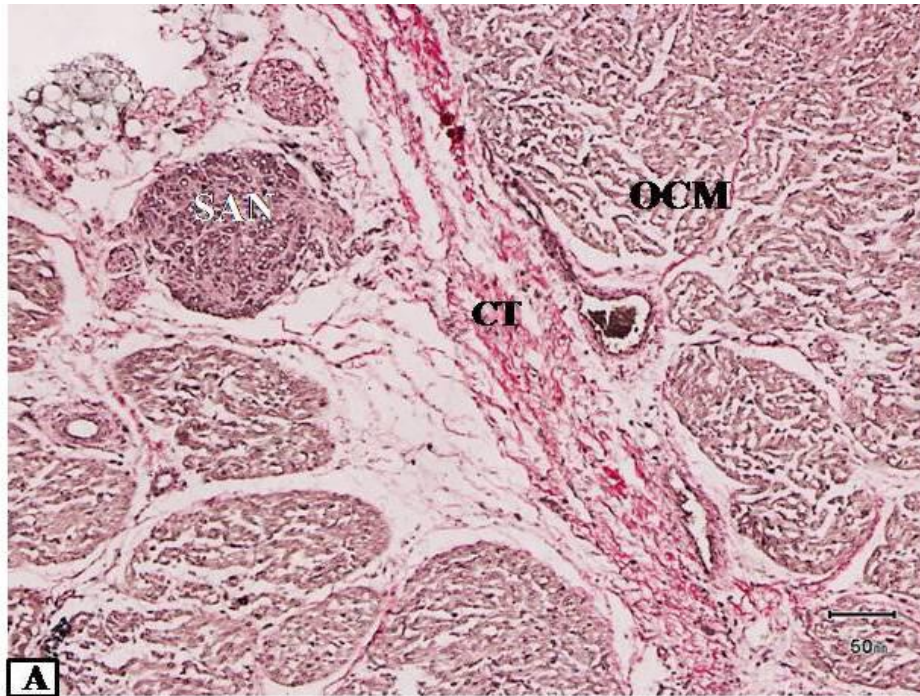
Fig. 37. A: A photomicrograph showing sinoatrial node (SAN) of 74 cm CVRL camel foetus. It is darkly stained, embedded in a fair amount of connective tissue (CT) separating SAN from ordinary cardiac muscle (OCM). Verhoff's (X10).

B: Showing SAN in the same heart. Note that cells have different shapes and sizes, nuclear chromatin was peripherally distributed (arrows). H&E. (X40).
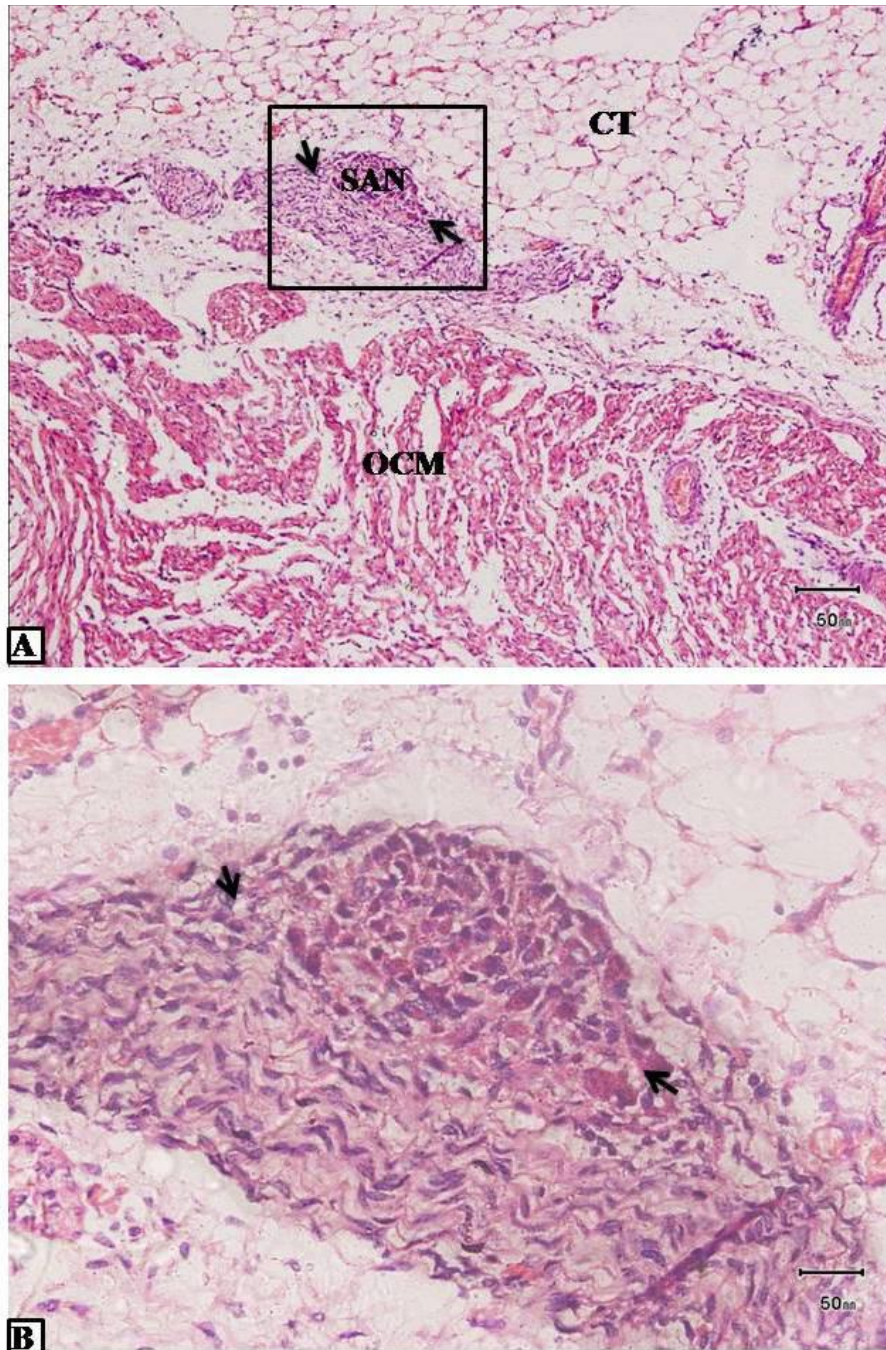
Fig. 38. A: A photomicrograph of the right atrium of camel foetus at 76 cm CVRL showing SAN with elongated ends (arrows) embedded in connective tissue (CT) with adipose tissue. SAN is adjacent to the ordinary cardiac muscle (OCM). H&E. (X10).

B: Is a magnification of the square in A. Note that SAN became elongated in periphery and is embedded in connective tissue. (X40).
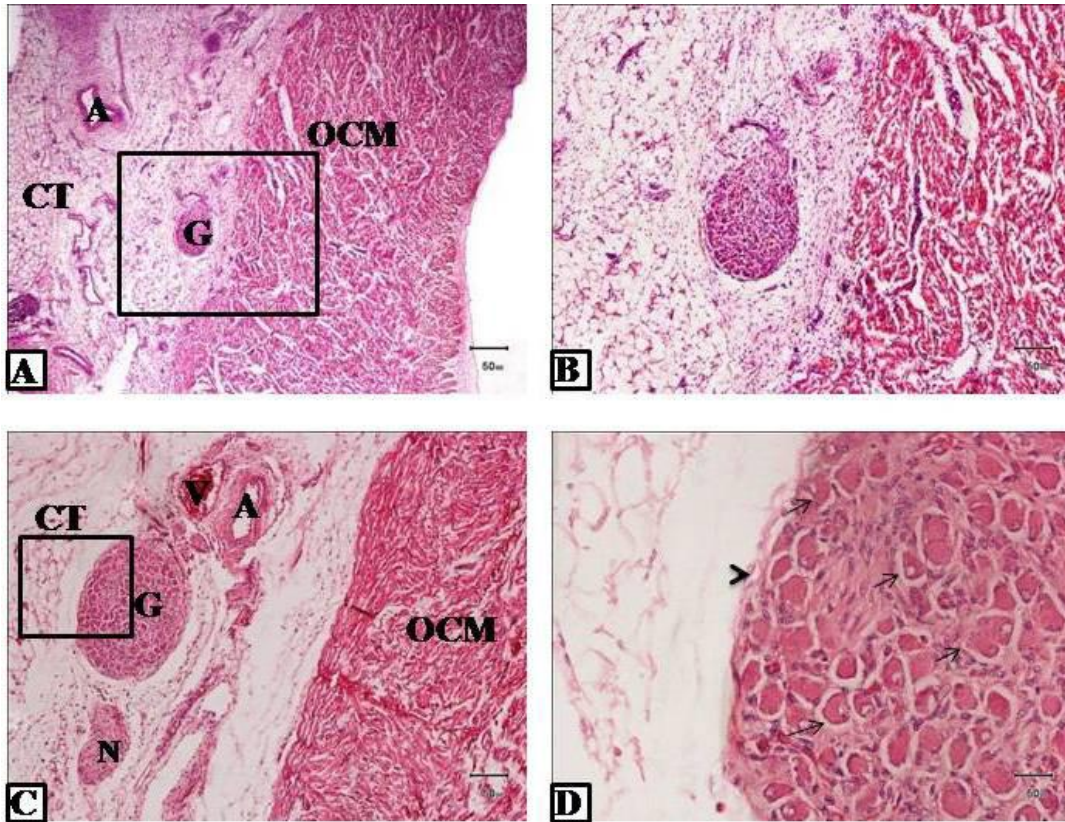
Fig. 39. A: A photomicrograph showing capsulated ganglion (G) of the sinoatrial node (SAN) in the heart of a camel foetus at 76 cm CVRL. Ganglion is embedded in connective tissue (CT) with large amount of adipose cells. H&E (X4). Artery A, ordinary cardiac muscle OCM.

B: Is a magnification of the square in A showing SAN ganglion (X10).

C: Showing SAN ganglion in 79.5 cm CVRL camel foetus. Note A, Artery, V, vein and N, nerve in the connective tissue and ordinary cardiac muscle OCM are shown.

D: Is a magnification of the square in C, showing a thin connective tissue capsule (arrowhead), neurons (arrows) characterized by large nuclei and prominent nucleoli. (X40).
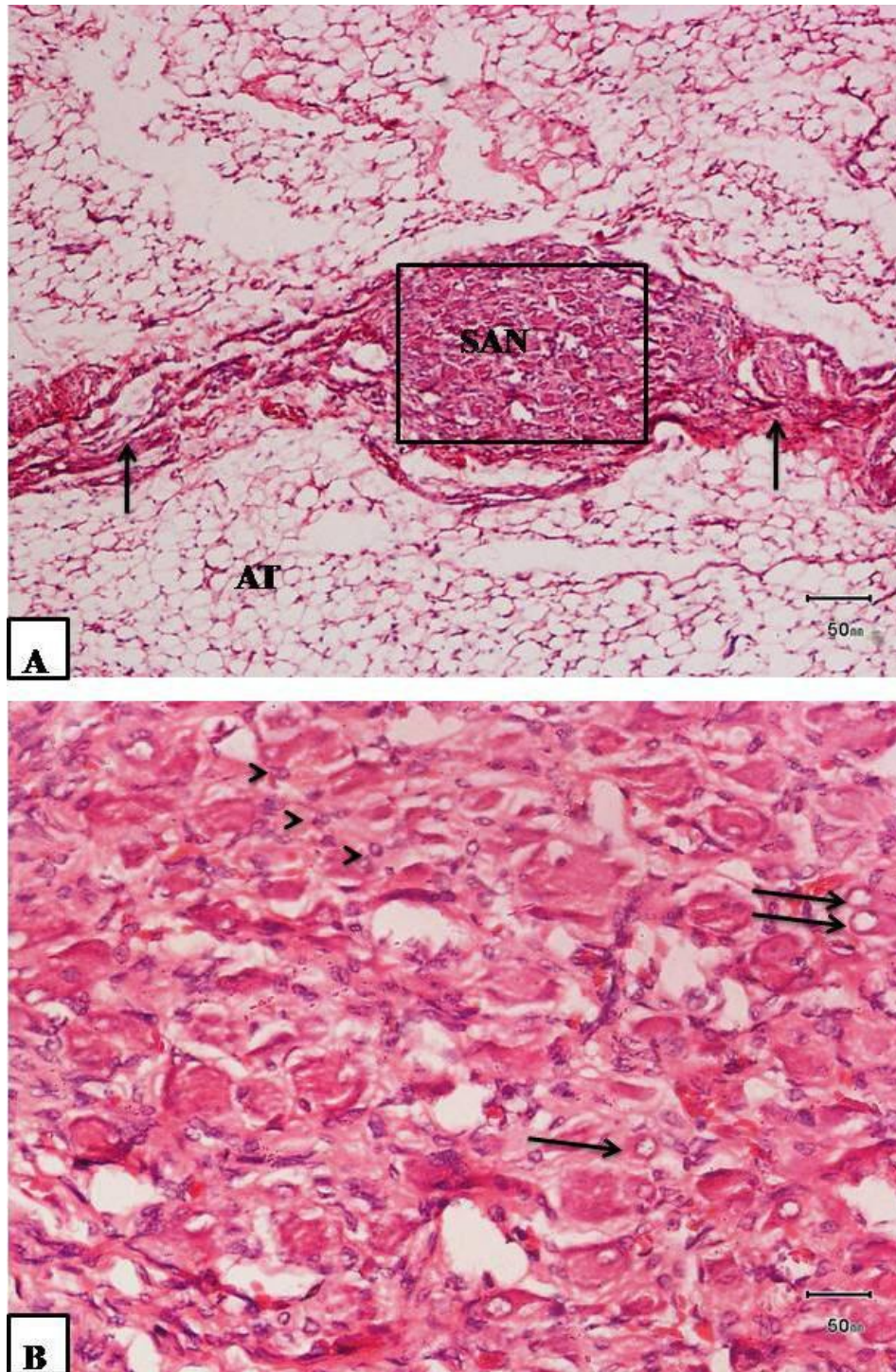
Fig. 40. A: A photomicrograph showing SAN of camel a foetus at 131 cm, SAN with tapering ends (arrows) surrounded by adipose tissue (AT). Van Gieson's (X10).

B: Is a magnification of the rectangle in A, showing SAN cells: Perinuclear clear zone cells (arrows) and Transitional cells (arrowheads). (X40).
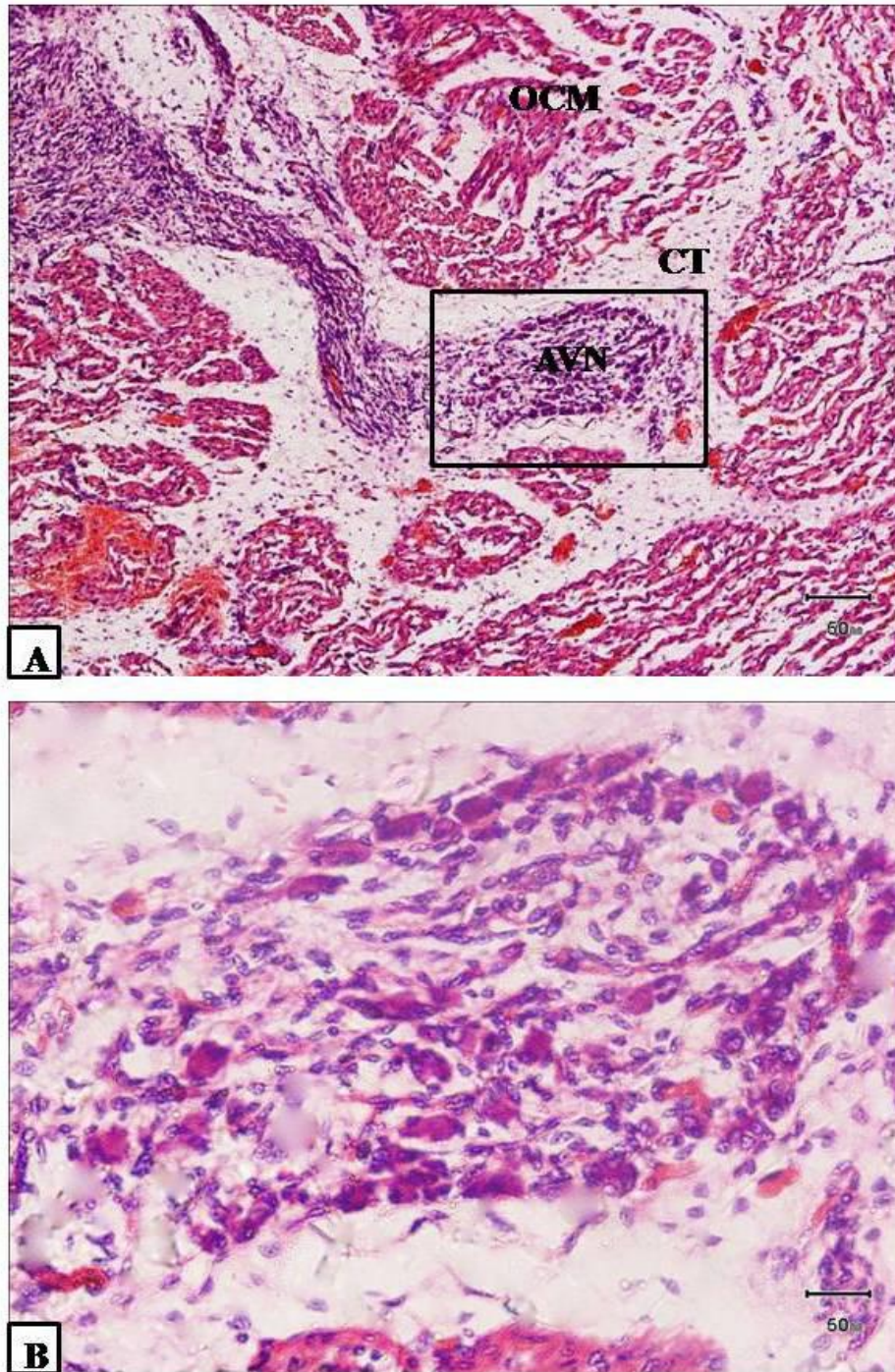
Fig. 41. A: A photomicrograph showing atrioventricular node (AVN) of a camel foetus at 76 cm CVRL. It is located between ordinary cardiac muscles (OCM) surrounded by connective tissue (CT). H&E (X10).
B: Is a magnification of a rectangle in (A) showing AVN cells (X40).
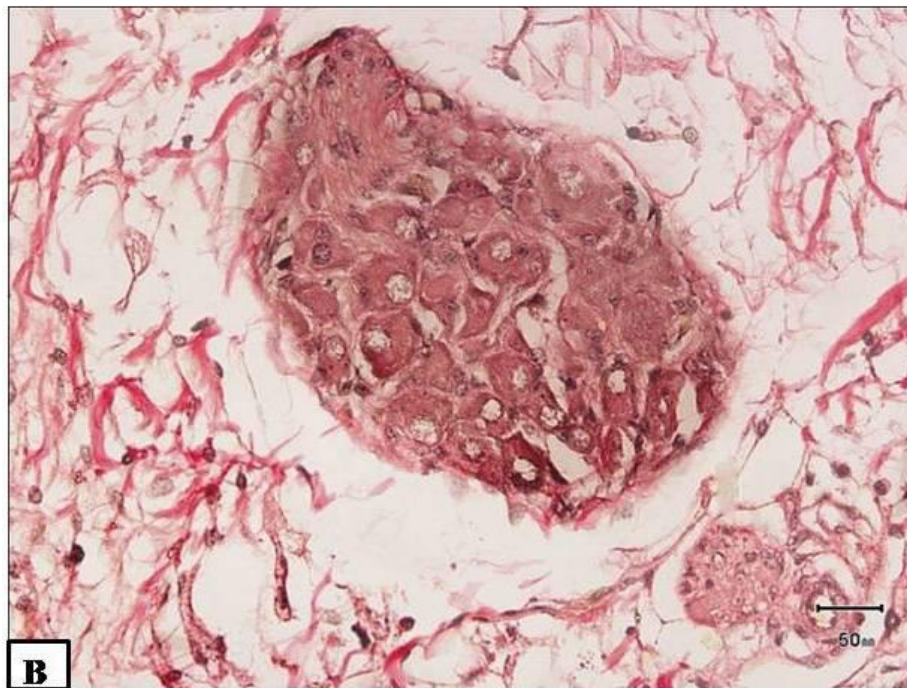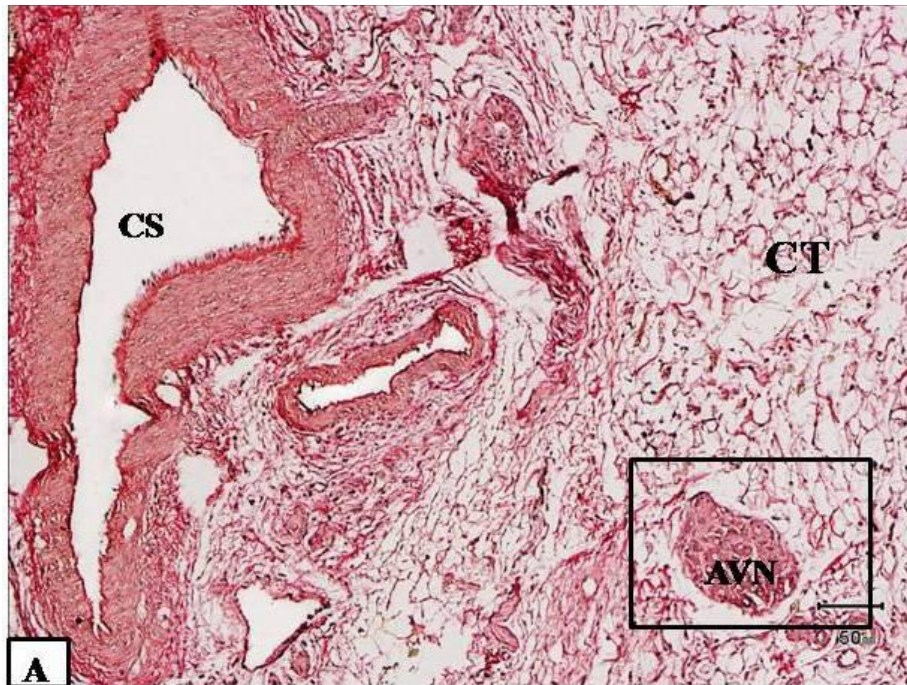
Fig. 42. A: A photomicrograph showing atrioventricular node (AVN) in camel foetus at 89 cm CVRL. It is surrounding by connective tissue (CT) separating the node from coronary sinus (CS). Van Gieson's. (X10).
B: Is a magnification of the rectangle in A showing AVN (X40).
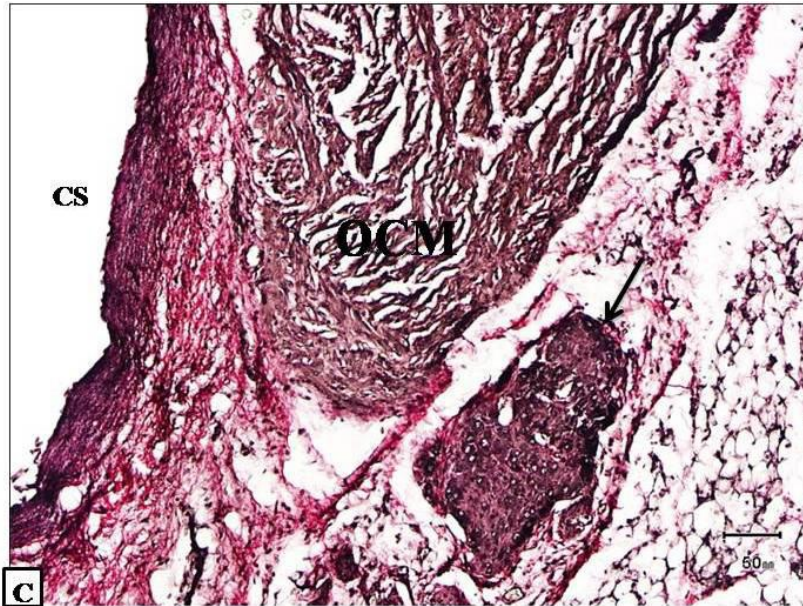
Fig. 42. C: A photomicrograph showing atrioventricular node (arrow) near the ordinary cardiac muscle OCM, and coronary sinus (CS) in camel foetus at 92 cm CVRL. Verhoff's (X10).
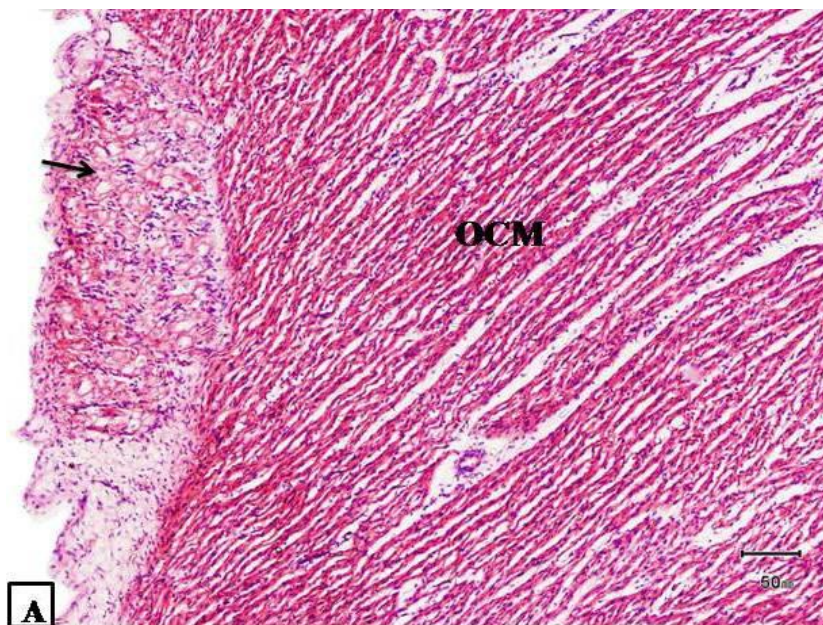
Fig. 43. A: A photomicrograph showing the atrioventricular bundle (AVB) (arrow) at 76 cm CVRL camel foetus. It is located between endocardium and myocardium. H and E (X10).
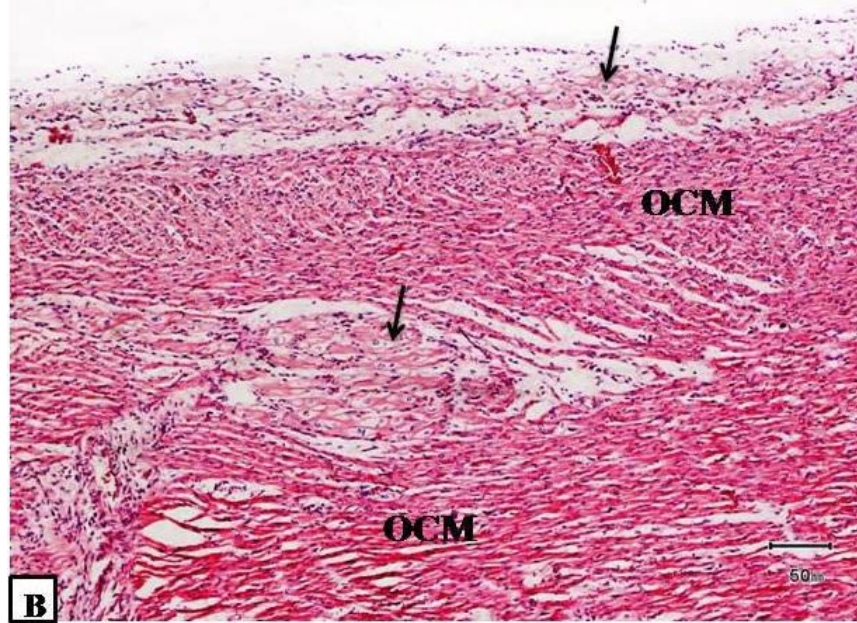
Fig. 43. B: 79.5 cm CVRL camel foetus showing AVB (arrows) between endocardium and myocardium and in between ordinary cardiac muscles (OCM). H&E (X10).
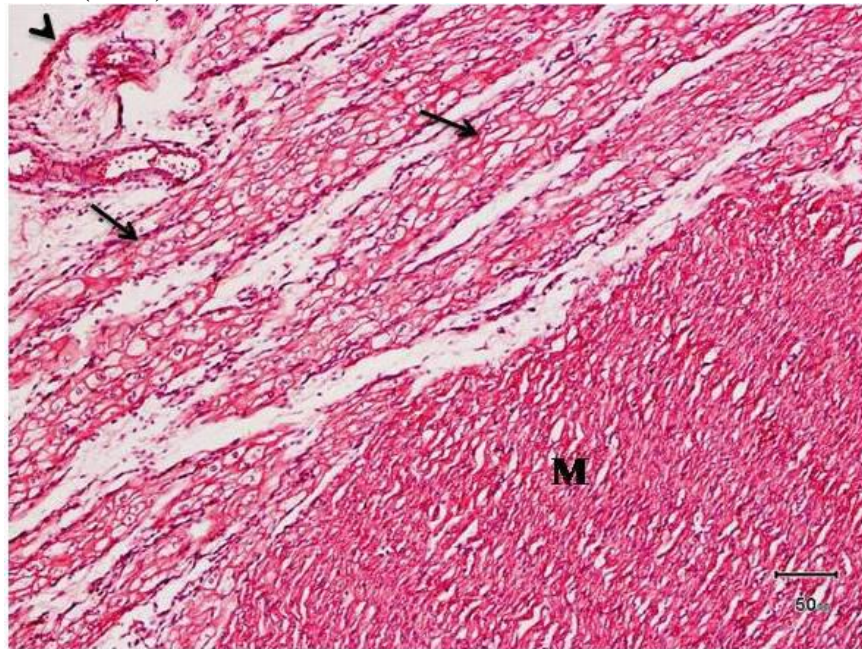
Fig. 44. A photomicrograph of 91 cm CVRL camel foetus showing atrioventricular bundle AVB, (arrows) located between endocardium (arrowhead) and myocardium (M). H&E (X10).
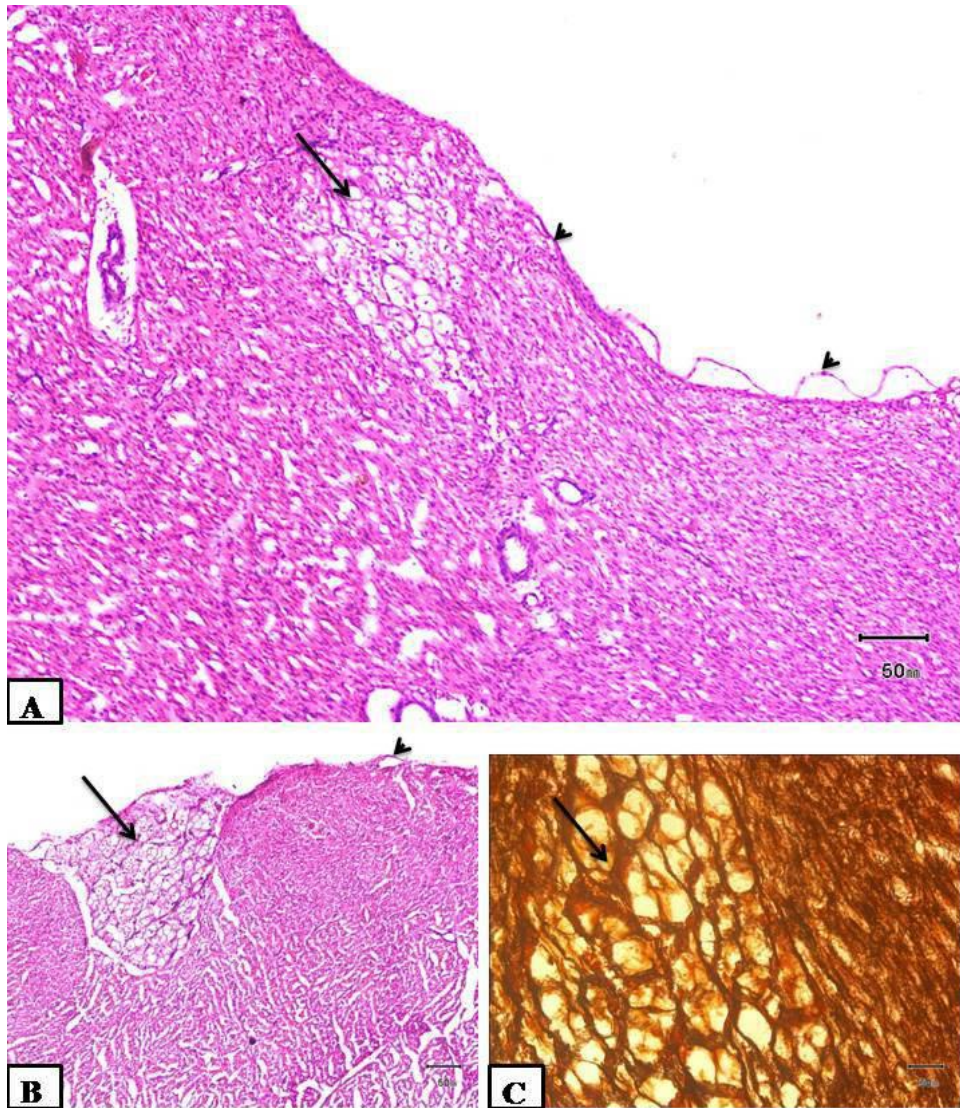
Fig. 45. A and B: Photomicrographs showing atrioventricular bundle (arrow) in camel foetus at 97 cm CVRL. It is located between the myocardial fibres or beneath endocardium (arrowheads). H&E (X10).
C: Showing AVB (arrow) with striation. Gordon and Sweet (X40).
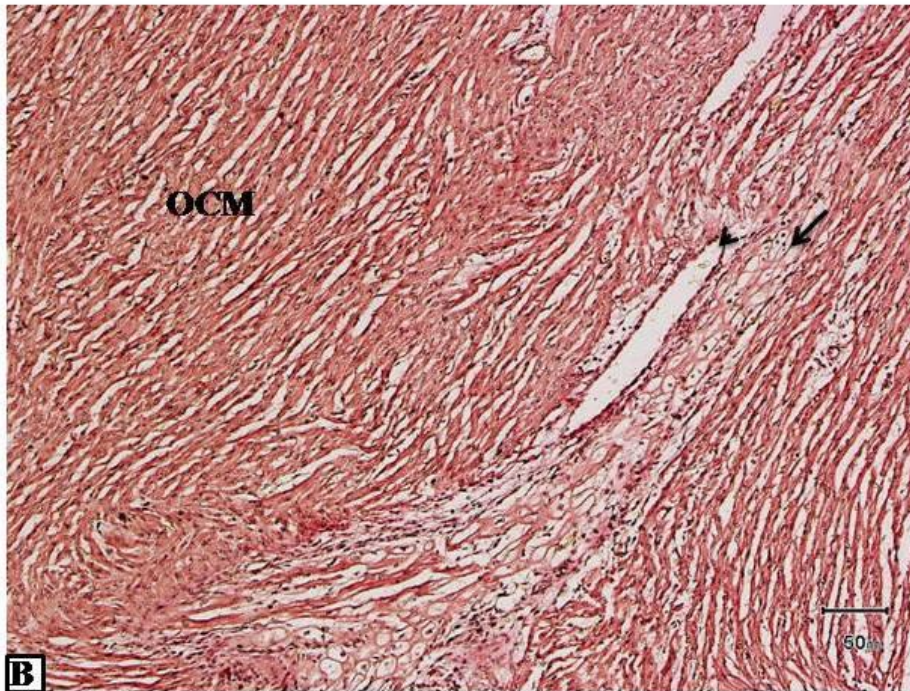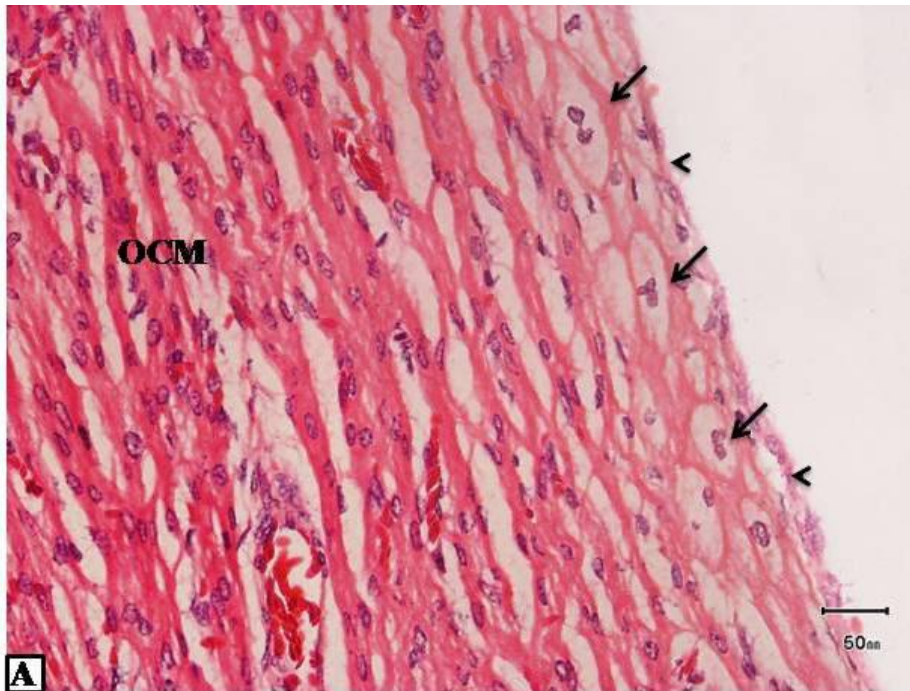
Fig. 46. A: A photomicrograph showing Purkinje fibres (arrows) at 74 cm CVRL, adjacent to endothelium (arrowheads) and ordinary cardiac muscle (OCM). Some of the fibers are double nucleated (arrows). H&E (X40).
B: Showing Purkinje fibres (arrow) of the same age. It is accompanied by a blood vessel (arrowhead) and ordinary cardiac muscle (OCM). Van Gieson's (X10).
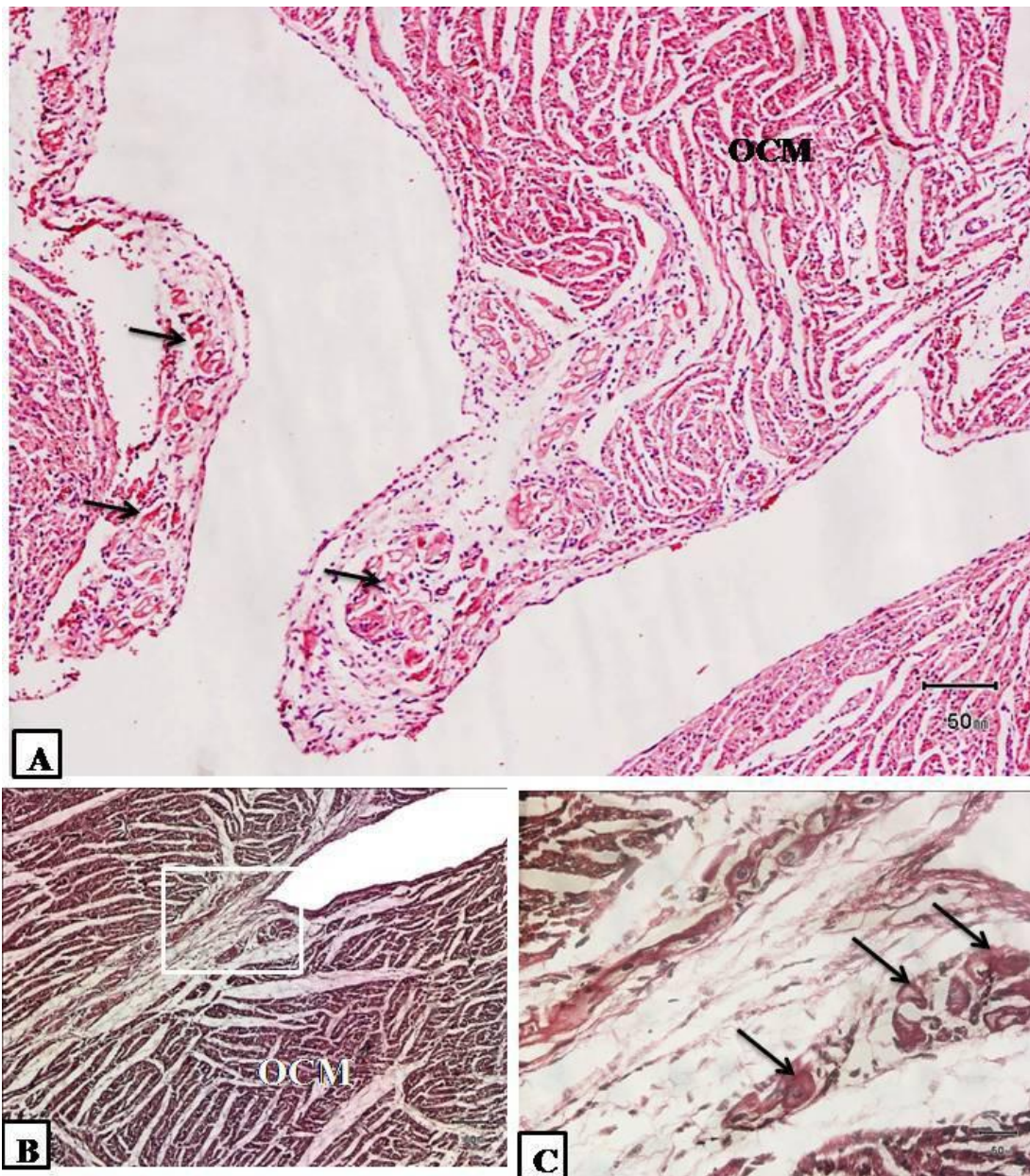
Fig. 47. A, B and C: Photomicrographs showing apical part of left ventricle in heart of camel foetus at 79.5 cm CVRL. Purkinje fibres (arrows) embedded in endocardial connective tissue having dark cytoplasm. H&E (X10)

B: Showing the same section stained with Verhoff's (X10).

C: Is a magnification of the rectangle in B showing PF with dark cytoplasm (X40).
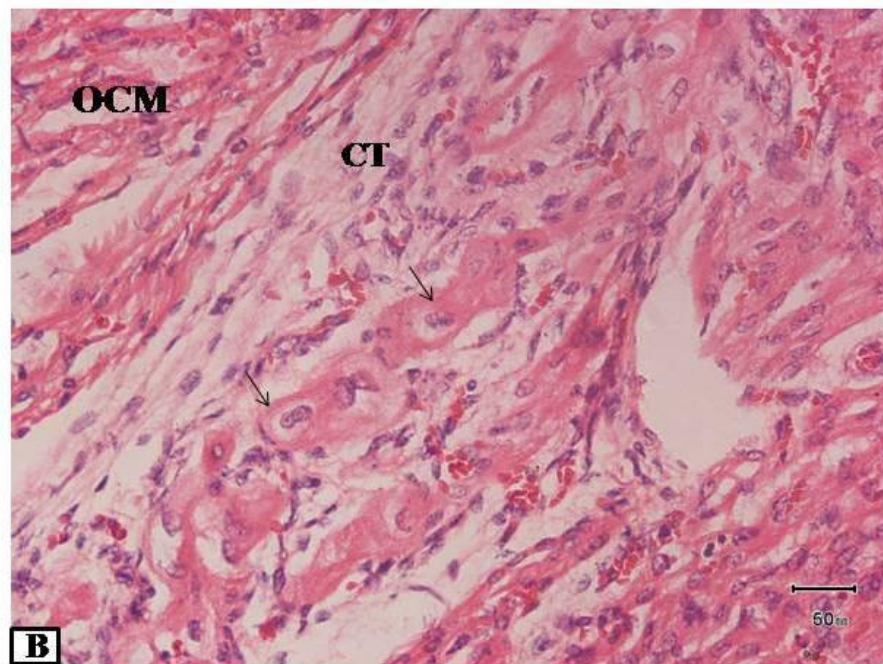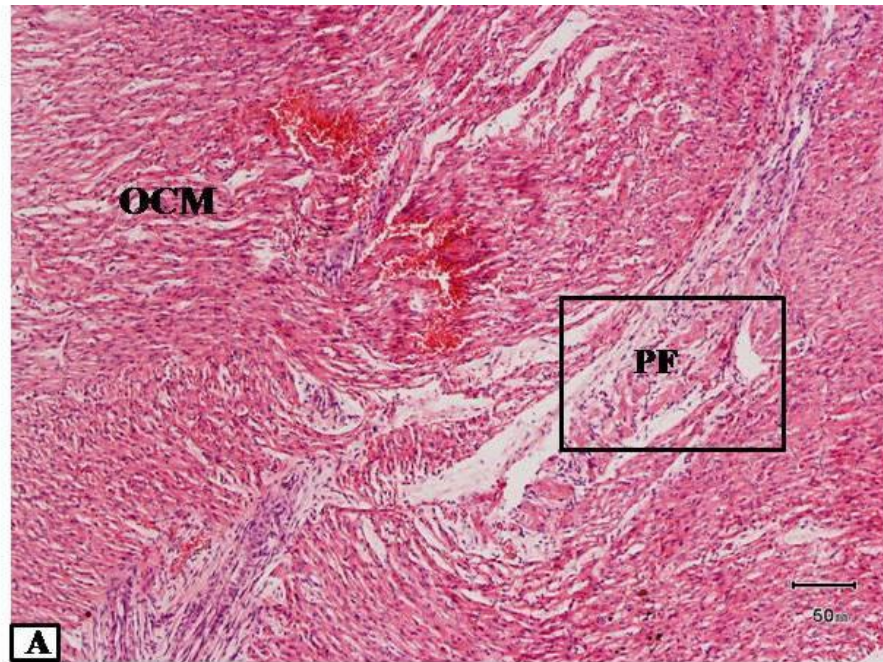
Fig. 48. A and B: Photomicrographs showing PF (arrows) of camel foetus heart at 88 cm CVRL having a dark cytoplasm, separated from ordinary cardiac muscle (OCM) with connective tissue (CT). H&E. A (X10).
B: Is a magnification of the rectangle in A showing some of PF having double nuclei (arrows). (X40).
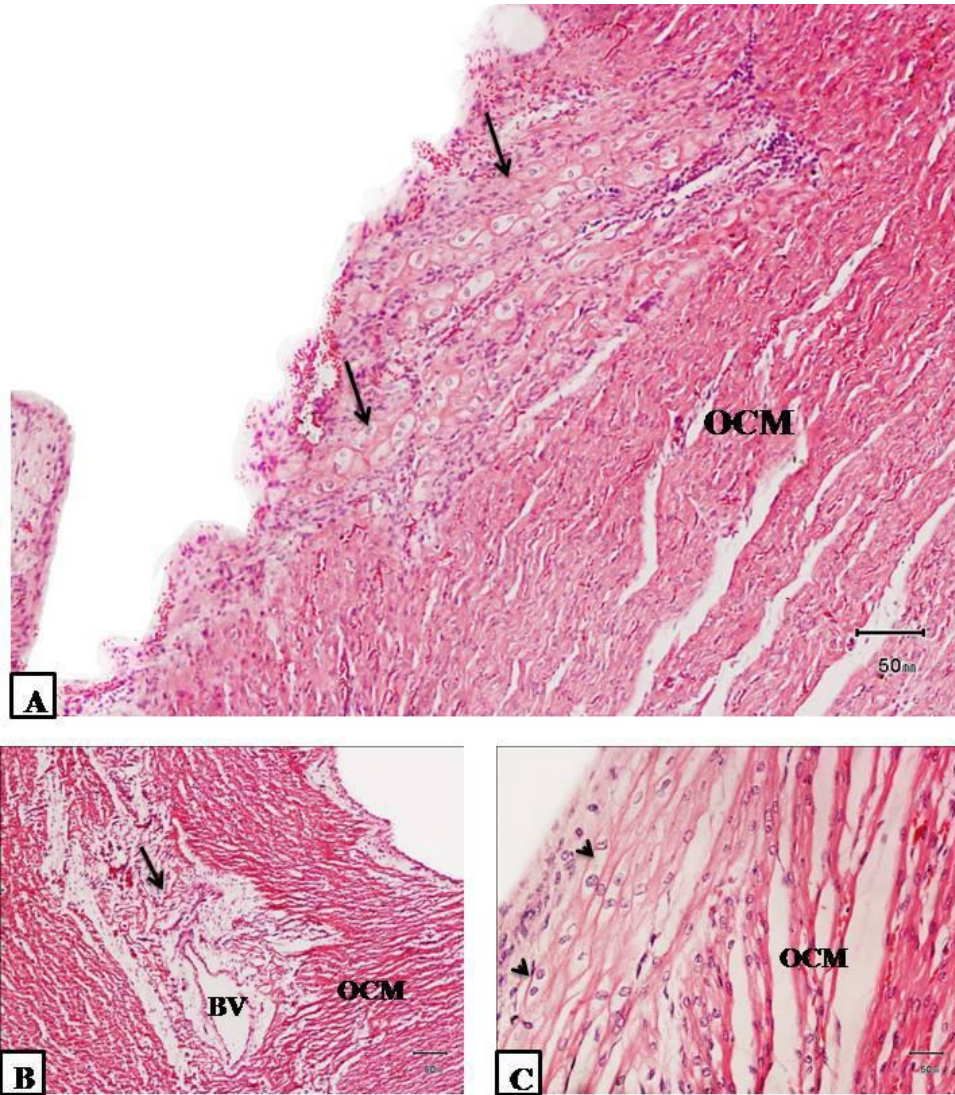
Fig. 49. A: A photomicrograph showing PF (arrows) of camel foetus at 89 cm CVRL. They are appearing as bundles parallel to the ordinary cardiac muscles (OCM).
B: Showing the same age: PF beside blood vessels (BV). H&E (X10).
C: Showing PF (arrowheads) adjacent to the OCM having one or two nuclei. H&E (40).
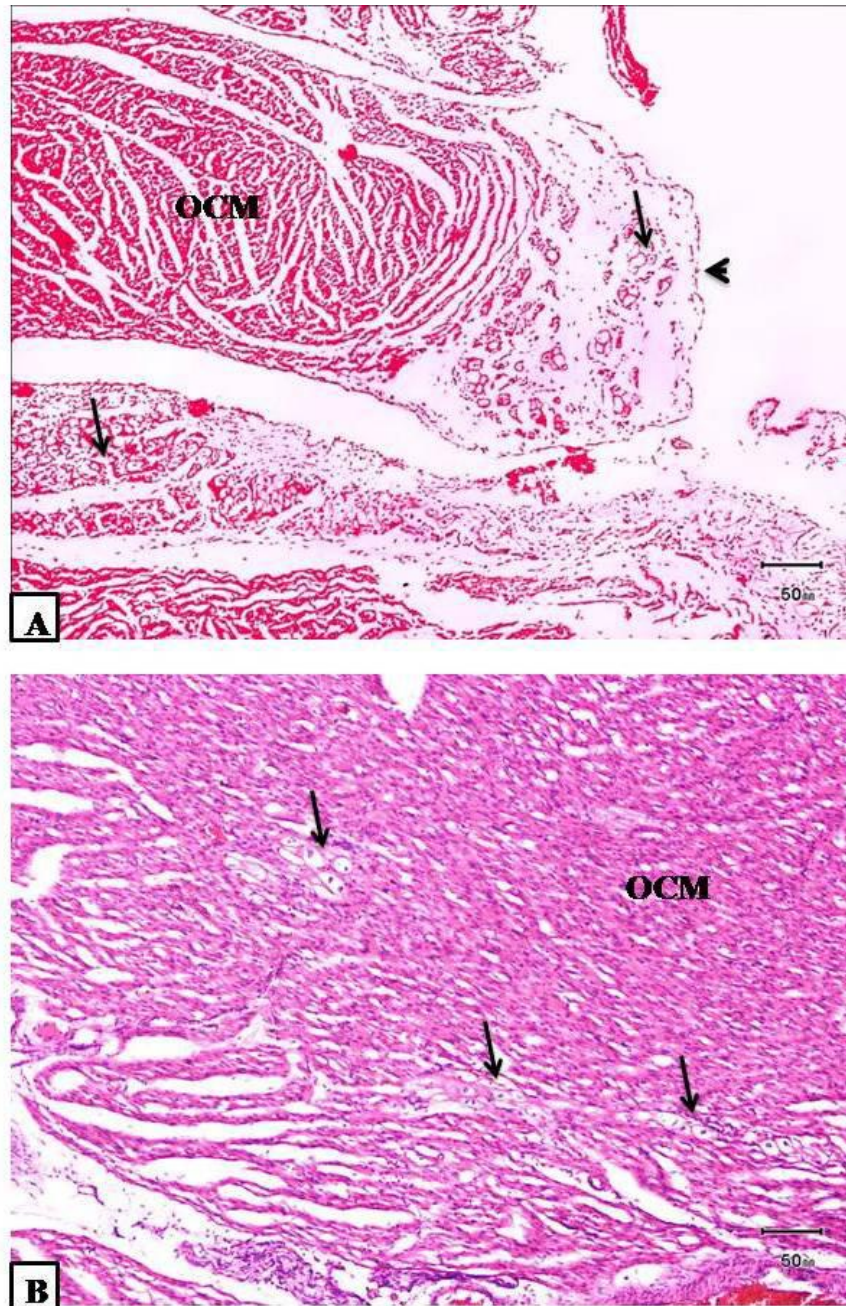
Fig. 50. A: A photomicrograph showing Purkinje fibres (arrows) in camel foetus of 91 cm CVRL. They are embedded in the endocardial connective tissue. Endothelium, (arrowhead).
B: Showing PF (arrows) embedded in the ordinary cardiac muscle (OCM). H&E. (X10).
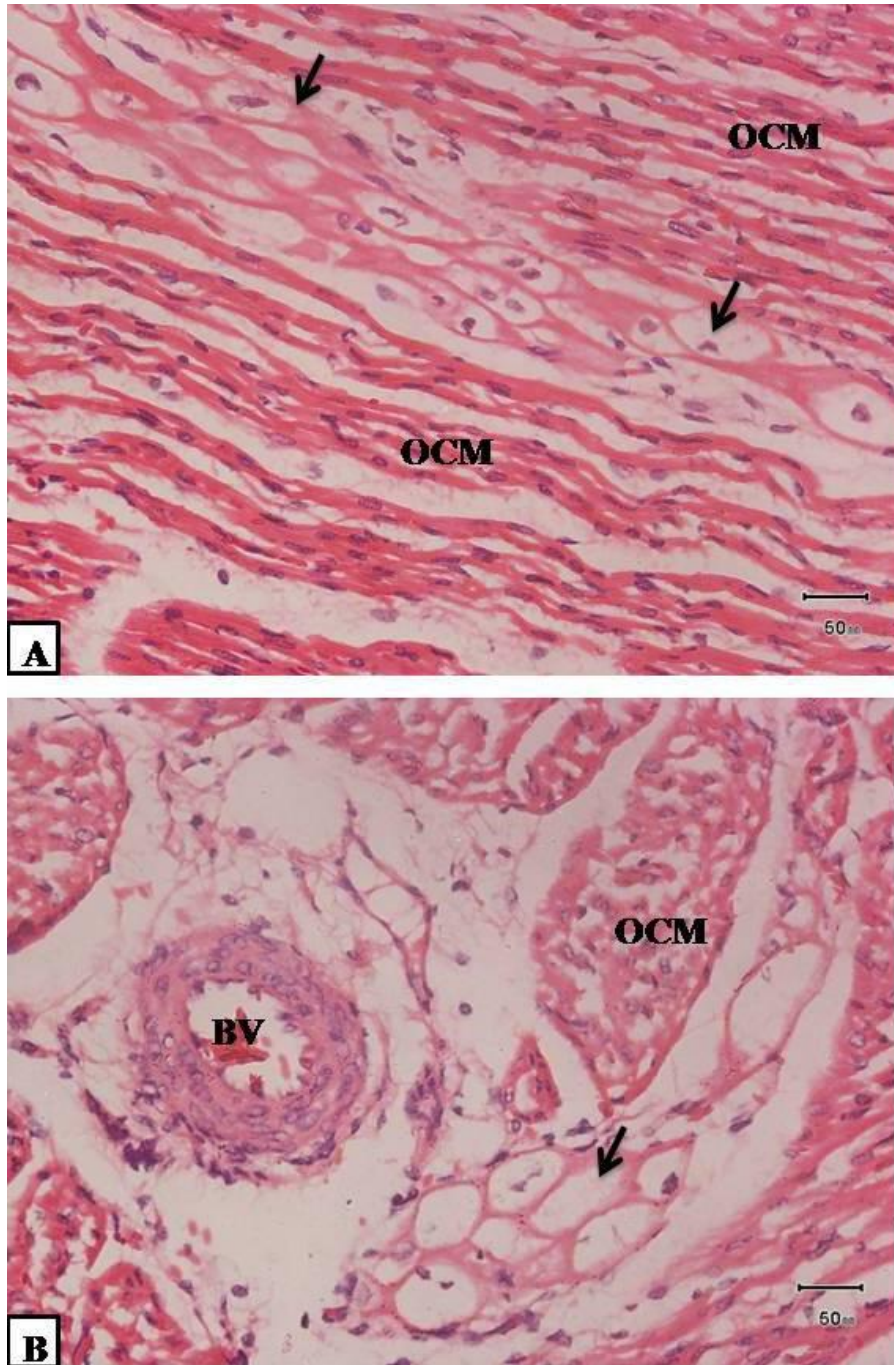
Fig. 51. A: A photomicrograph showing Purkinje Fibres (arrows) in camel foetus of 131 cm CVRL. Purkinje fibers parallel to the ordinary cardiac muscle (OCM).
B: PF (arrow) near the blood vessel in the same heart in A. H&E (X40).

Fig. 52. A and B: Illustrations of the left (A) and right (B) aspects of the heart of dromedary camel showing that the left paraconal interventricular branch and right subsinuosal interventricular branch of coronary arteries covered by myocardial bridges: arrows in A: type I, arrow in B: type II. Left ventricle LV, paraconal interventricular branch PIB, right ventricle RV.
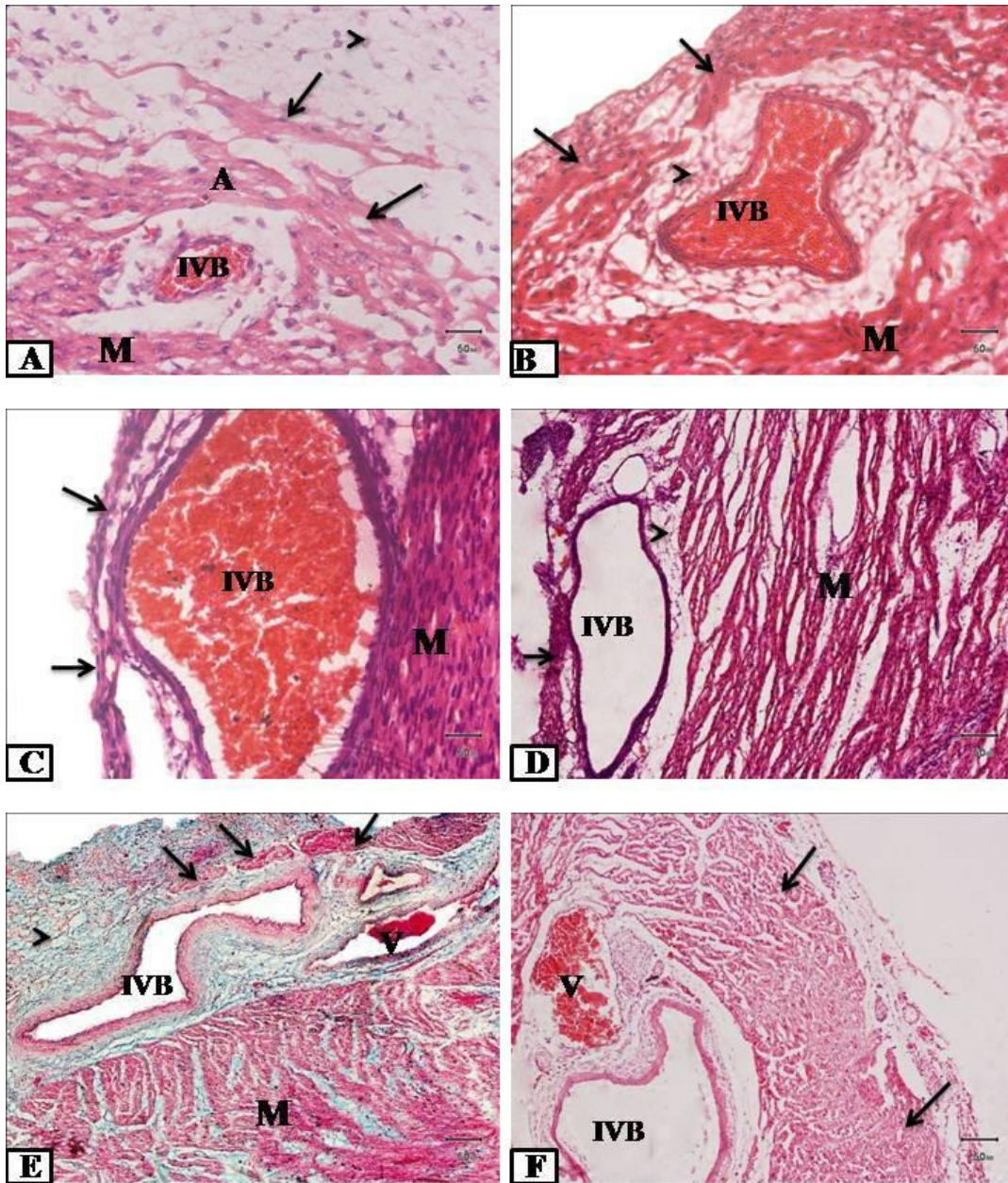
Fig. 53. A, B, C, D, E and F: Photomicrographs showing MBs (arrows) in several forms: as thin layer of myocardium in A: 24.5 cm CVRL, B: 29 cm CVRL, C: 60 cm CVRL and D: 61 cm CVRL, or as interrupted layer of muscle in E: 68 cm CVRL, or as thick layer of myocardium in F: 71 cm CVRL, covering the irregular interventricular branch of coronary artery (IVB) and its branch and vein. Thick layer of epicardial connective tissue (arrowheads). M, myocardium. A, B and C (H&E X40). D and F (H&E X10) E: (Masson's Trichrome X10).
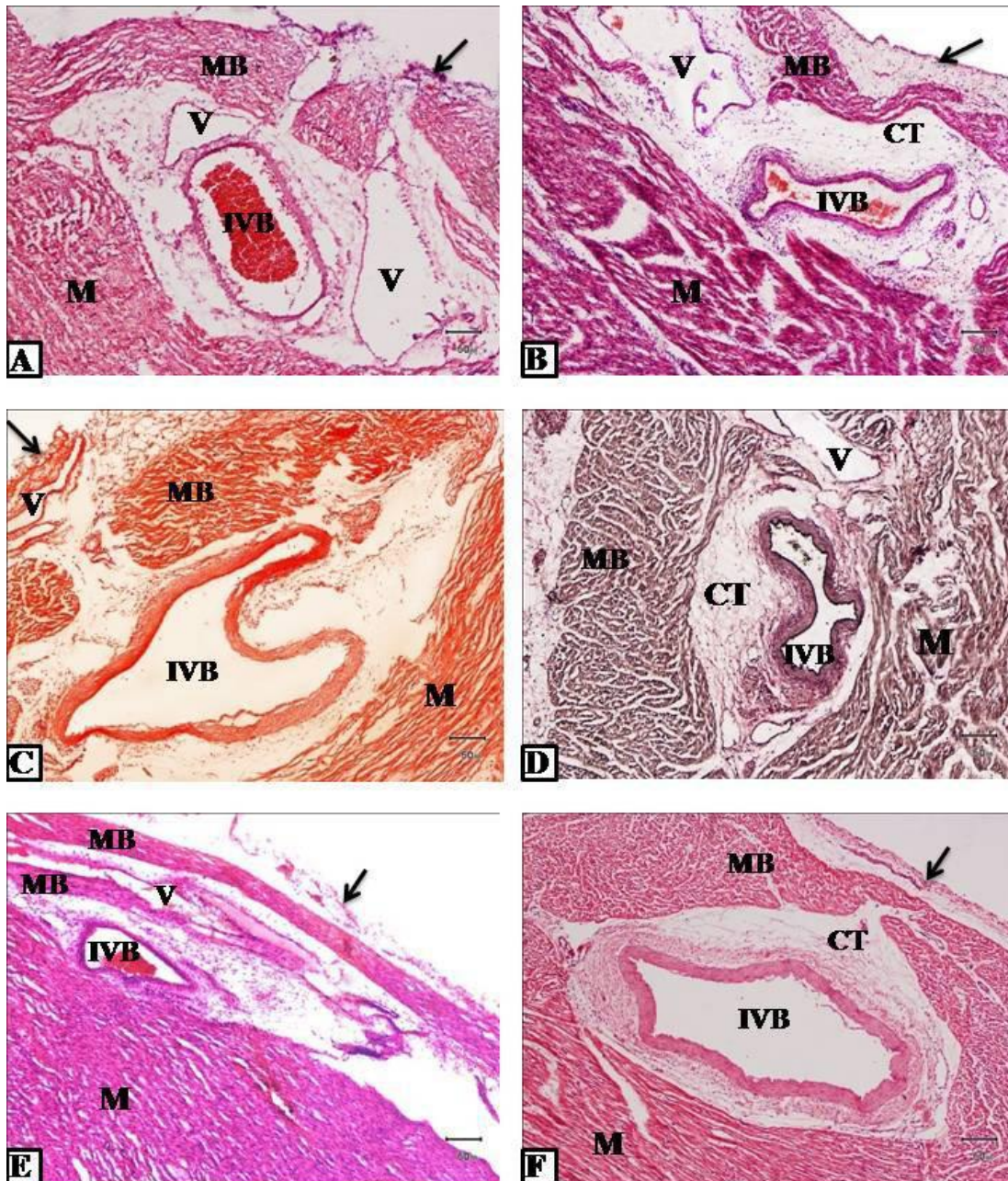
Fig. 54. A, B, C, D, E and F: Photomicrographs showing MBs above interventricular branch of coronary artery (IVB) in camel heart foetuses: interrupted layer of myocardium; A: 74 cm and C: 91 cm CVRL MBs covering (IVB) and the vein (V). D: showing MB as thick continuous layer in 92 cm CVRL. E: 97 cm CVRL appears as two layers covering IVB and V. F: 131 cm CVRL showing MB as thick layer of myocardium (M) peripherally and thin in the middle. Simple squamous epithelium (arrows) of epicardium, connective tissue CT separates MB from IVB. A, B, C and E (H&E, X10). D: Verhoff's (X10). F: Van Gieson's (X10).
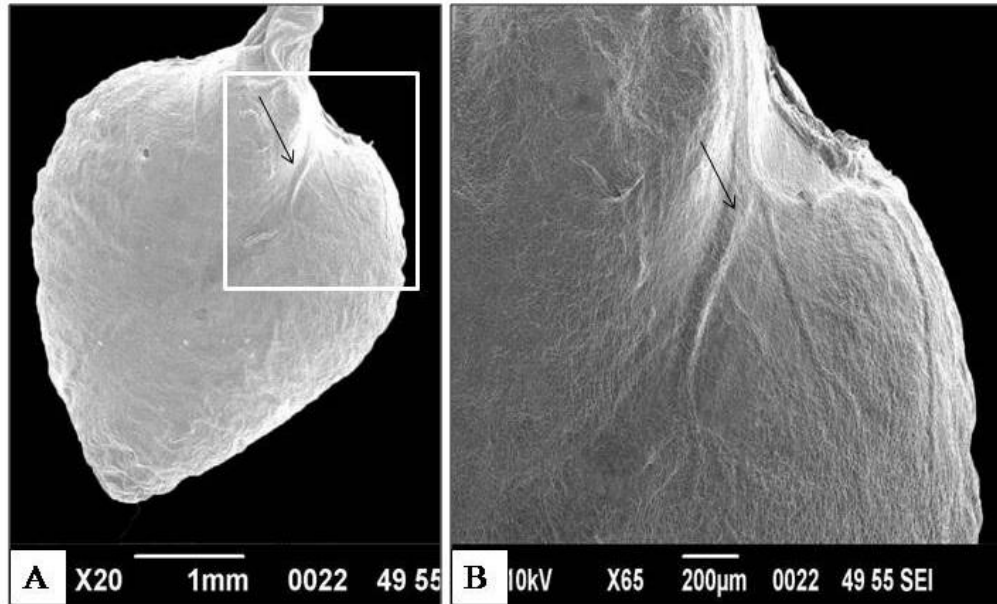
Fig. 55: A: Scanning electron micrographs of the camel heart foetus of 6.8 cm CVRL showing two ventricles as semi-triangular in shape and a shallow left longitudinal groove (arrow).

B: Is a magnification of A showing interventricular branches of coronary artery (arrow) in the upper part of the groove.
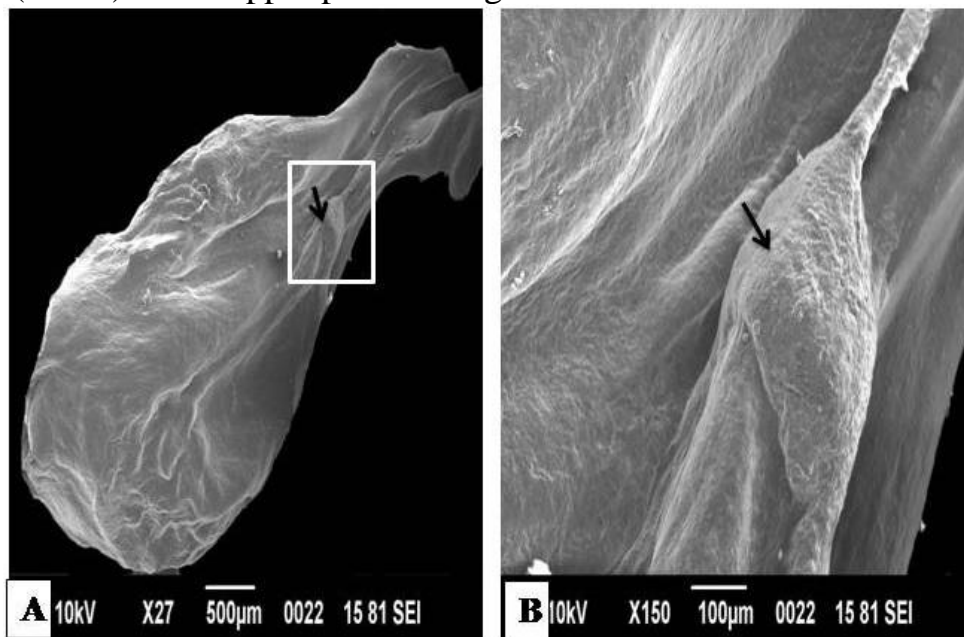
Fig. 56. A: Scanning electron micrographs of the camel heart foetus of 9.2 cm CVRL showing the atrium as a small bud (arrow), the rest of the heart is in the form of two ventricles.

B: Is a magnification of the rectangle in A. The atrium is shown as bud (arrow).

90
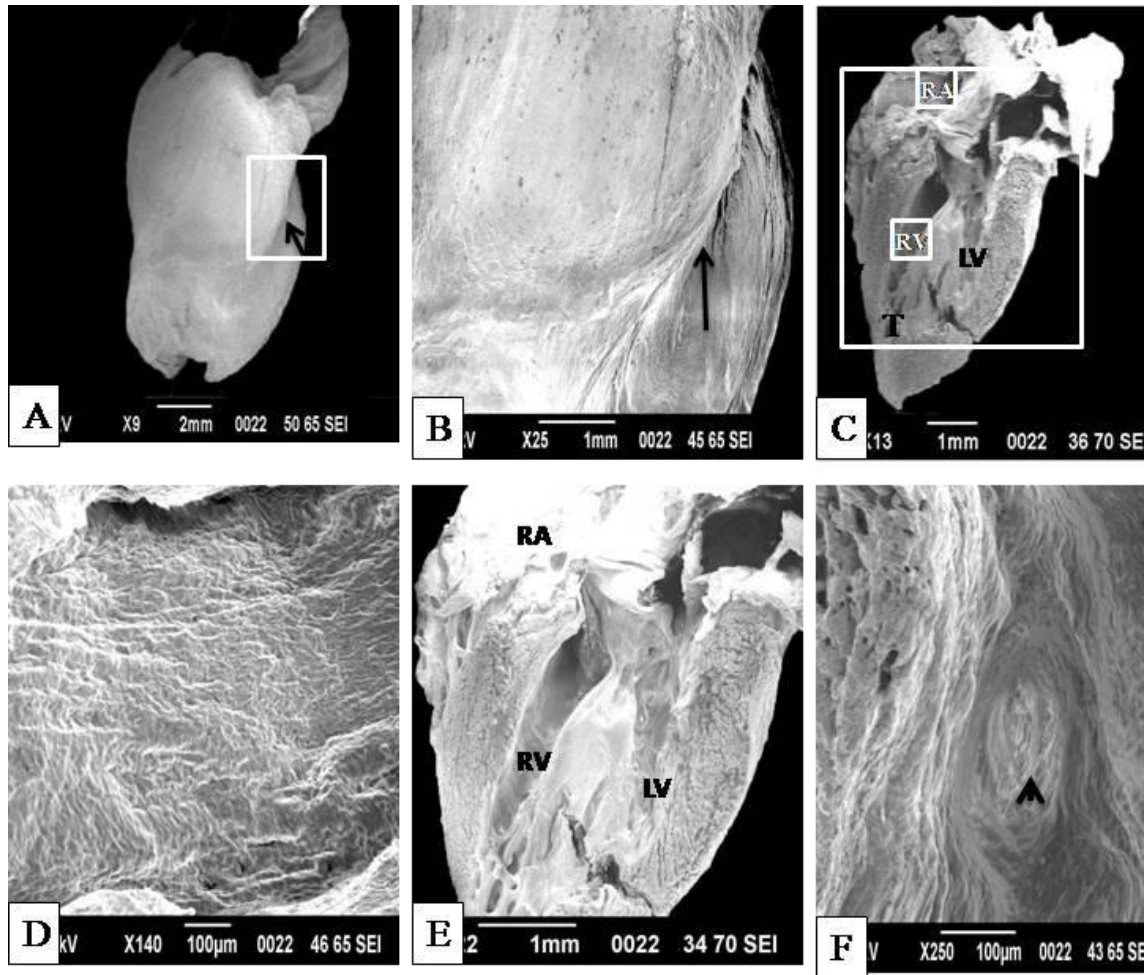
Fig. 57. A, B, C, D, E and F: Scanning electron micrographs of the camel heart foetus of 13 cm CVRL. Arrow in (B) and (A) showing clear left interventricular groove and interventricular branches of coronary artery in the longitudinal groove; (D) is a higher magnification of the upper square in (C) showing wavy appearance of atrial pectinate muscles; E: is a higher magnification of the large rectangle in (C) showing well developed trabeculae carneae (T) in the lower part of right ventricle; (F) is a higher magnification of the lower square in (C) showing ventricular myocardium in the upper part of the ventricular cavity as whirl-shaped (arrowhead).
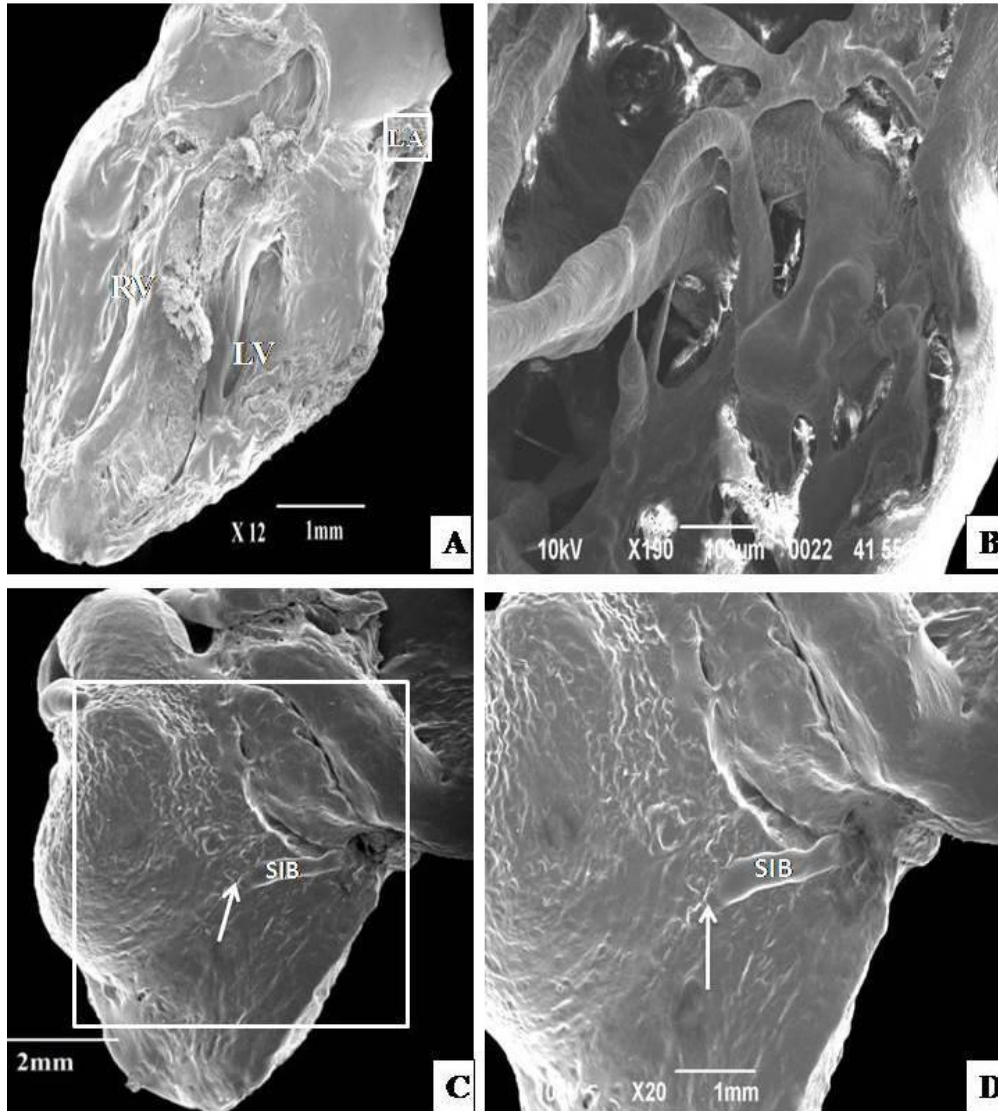
Fig. 58. A: Scanning electron micrograph of the camel heart foetus of 23 cm CVRL. B: A higher magnification of the square in A showing atrial pectinate muscles in the form of cords; C: showing type II myocardial bridge over the subsinuosal interventricular branch of right coronary artery (SIB) dipping in the myocardium (arrow) without reappearing. D: is a magnification of the square in C.
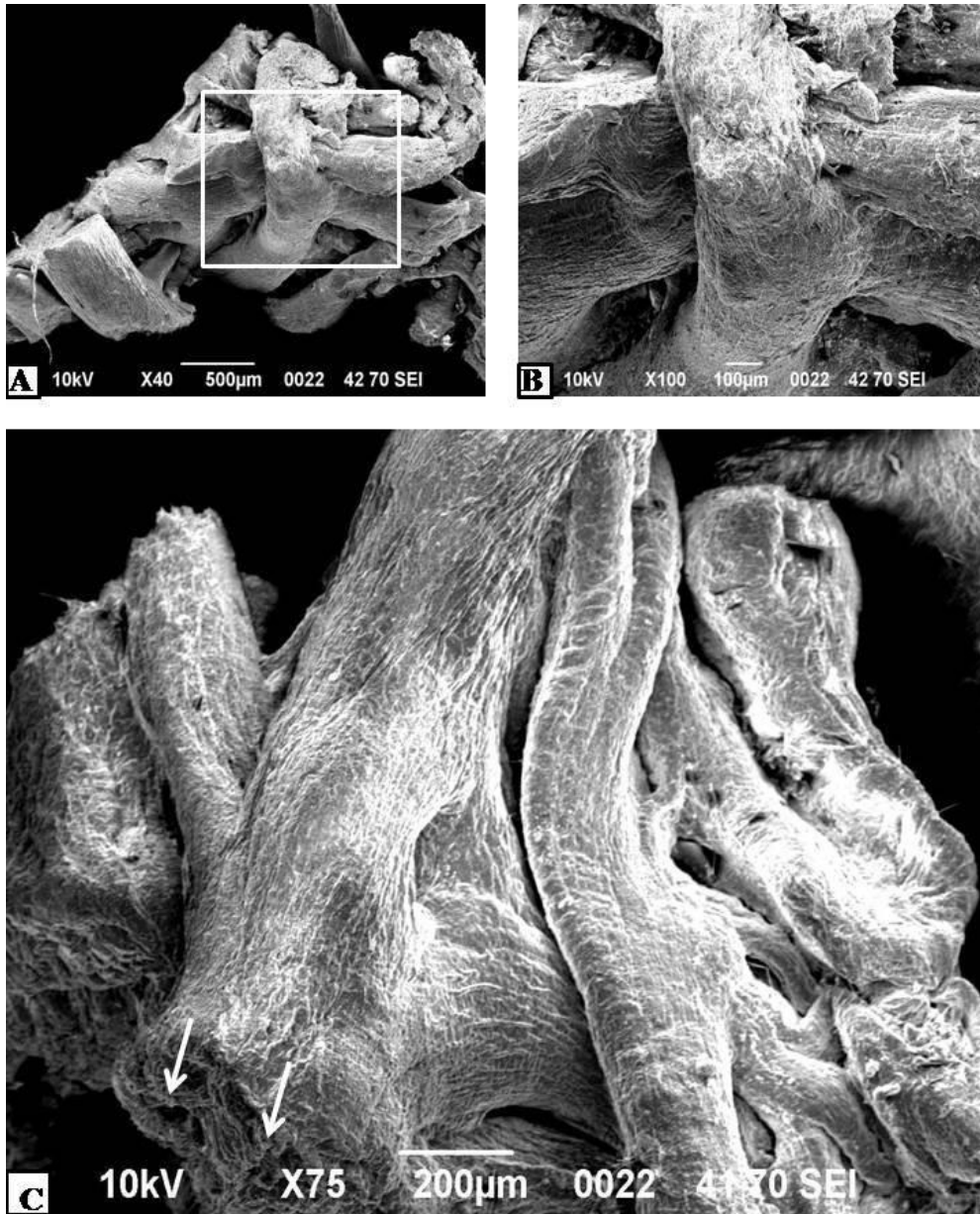
Fig. 59. A, B and C: Scanning electron micrographs showing atrial pectinate muscles of 60 cm CVRL camel foetus as a plexus.

B: Is a magnification of the square in A.

C: Higher magnification of the same age showing some branches of pectinate muscles in cross section (arrows).
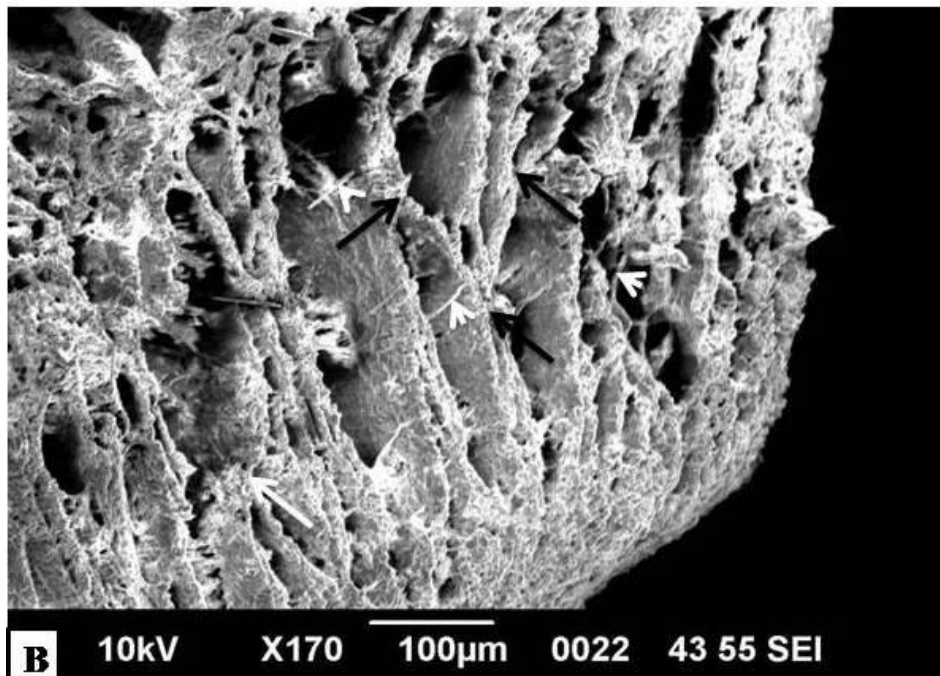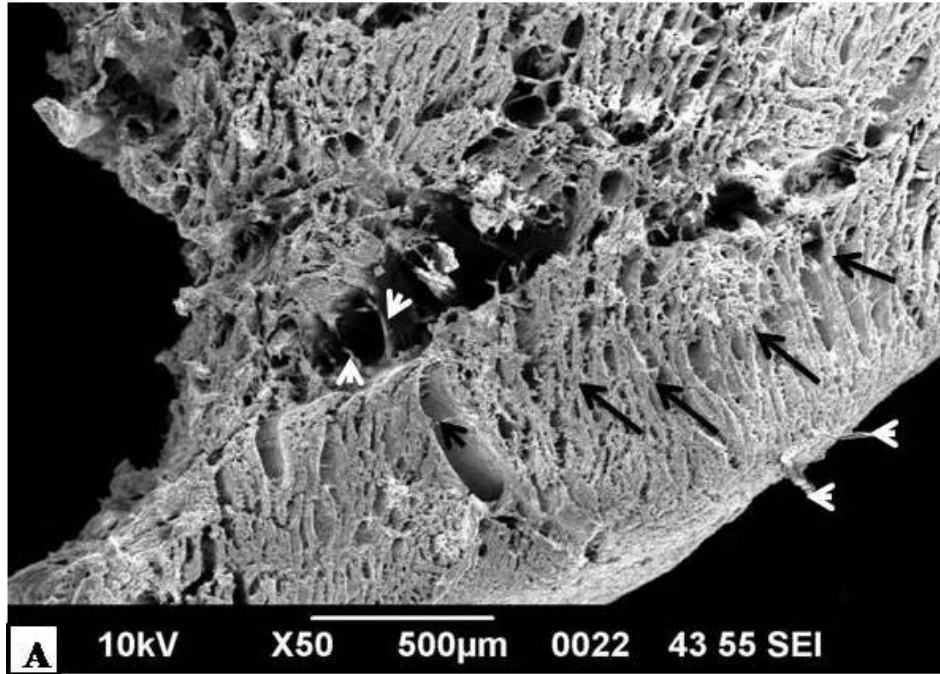
Fig. 60. A and B: Scanning electron micrographs showing branched ventricular myofibrils (arrows) in 60 cm CVRL camel foetus, with connective tissue fibres between them (arrowheads).
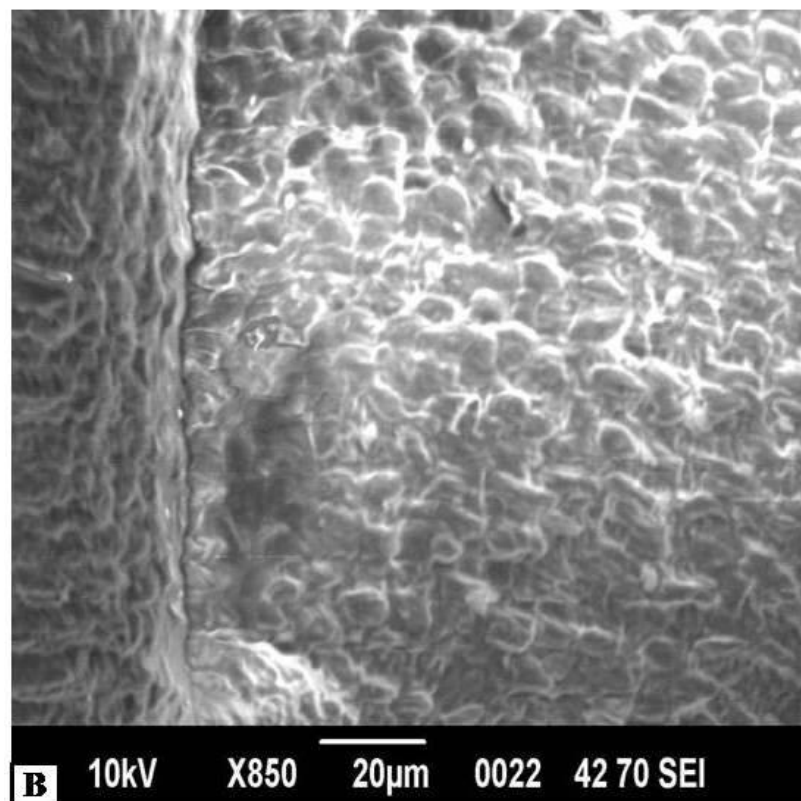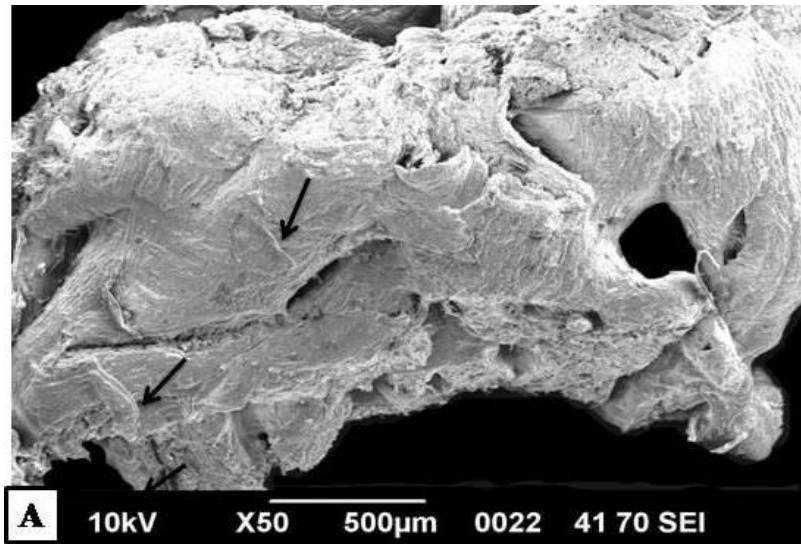
Fig. 61. A: Scanning electron micrograph showing atrial pectinate muscles covered with connective tissue (arrows) in left atrium of 89 cm CVRL camel foetus.
B: Is a higher magnification of the same age showing the epithelium (simple squamous epithelium).
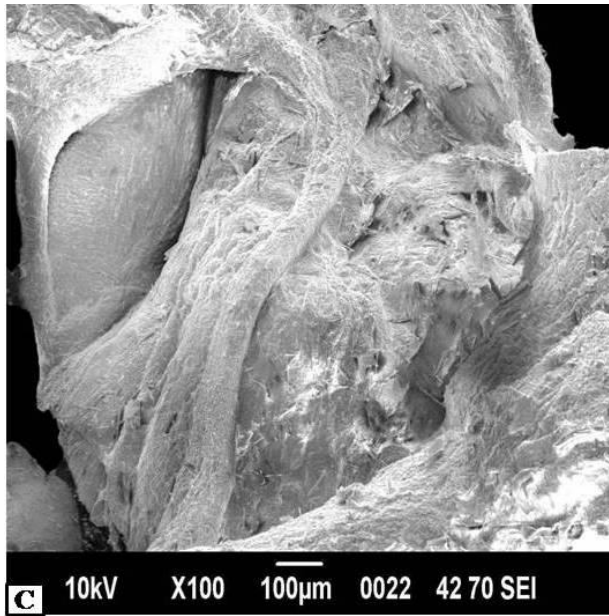
Fig. 61. C: Showing the right atrium covered by pectinate muscles, 101cm CVRL. Note that the connective tissue fibres were not clearly shown.
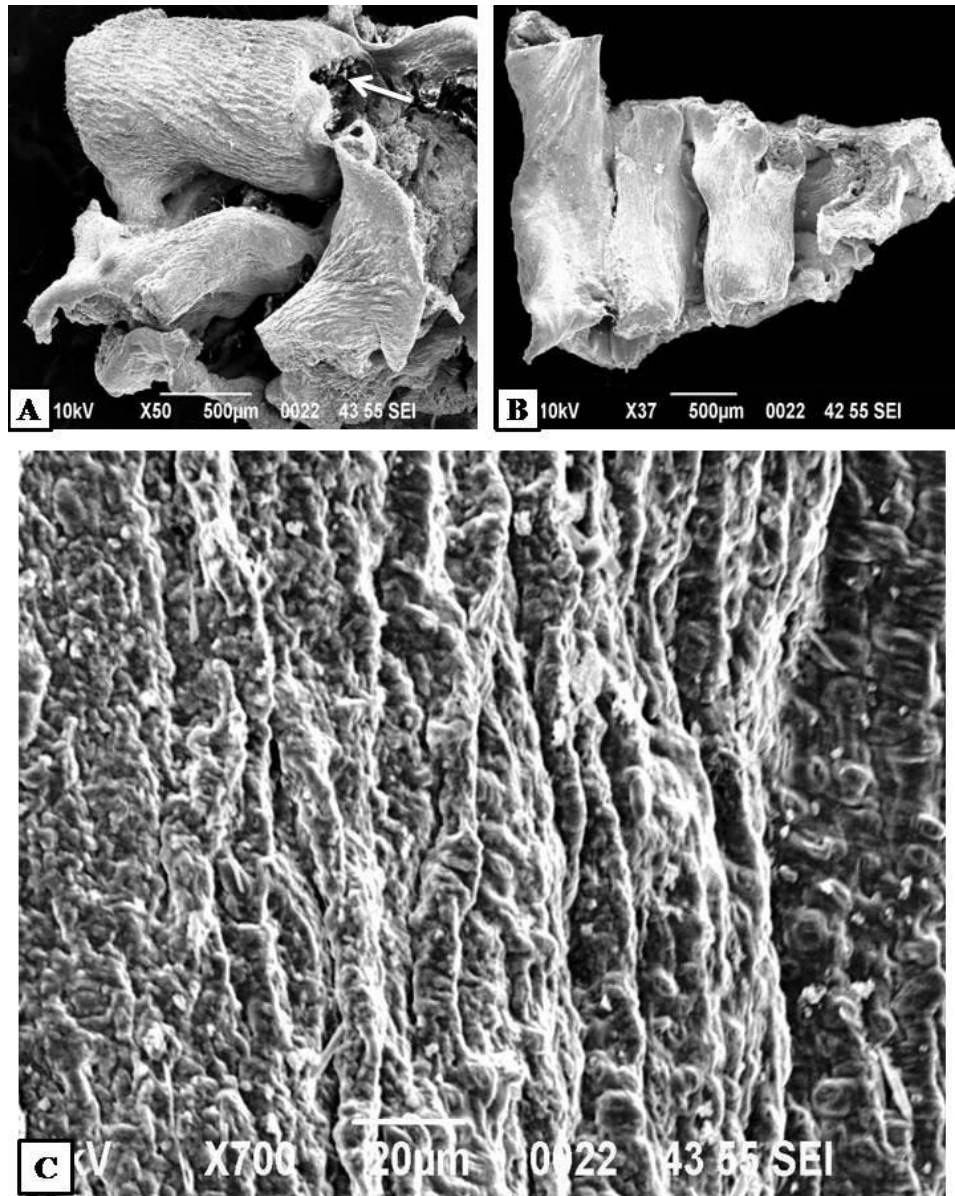
Fig. 62. A and B: Scanning electron micrographs showing cord-like atrial pectinate muscles (arrow) in right atrium of 101 cm CVRL.
C: Is a higher magnification of the same age showing the covering (simple squamous epithelium) in the form of grooves.
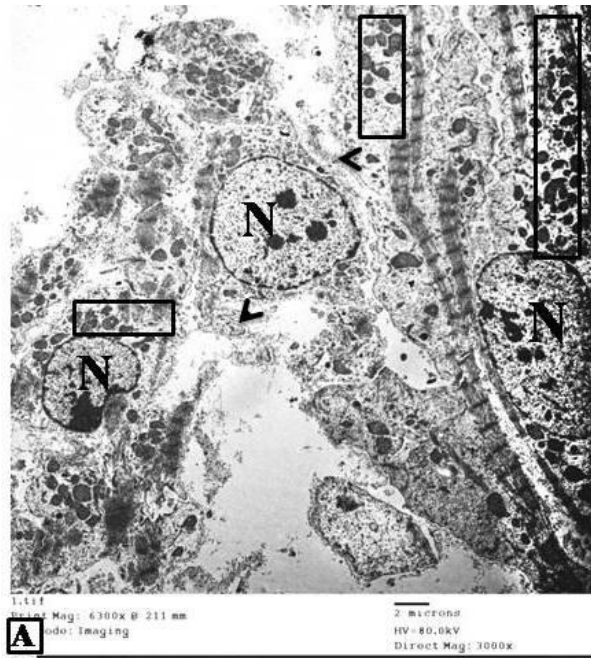
Fig. 63. A: Transmission electron micrograph of the camel foetus heart of 13 cm CVRL showing numerous mitochondria (rectangles) arranged in rows between myofibrils and nuclei (N) with different shapes and sizes, and irregular Z lines, rough endoplasmic reticulum is scattering around nuclei (arrowheads) (X3000).
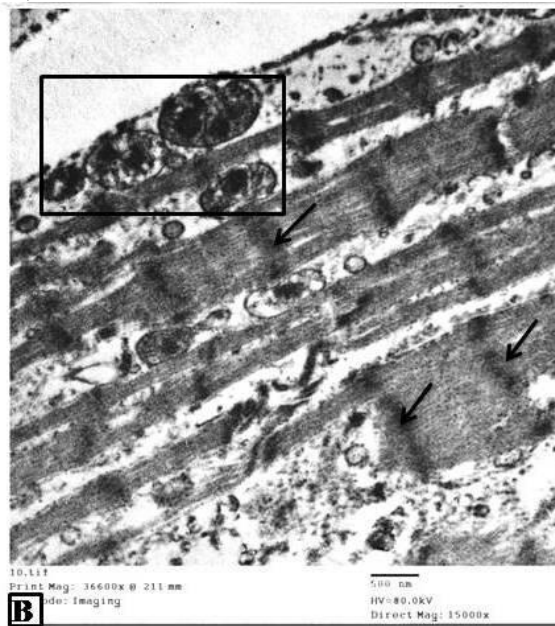
Fig. 63. B: Transmission electron micrograph of the camel foetus heart at 18.5 cm CVRL showing transverse tubular system as pale irregular Z lines (arrows), numerous mitochondria (rectangle) arranged in rows between myofibrils. (X15000).
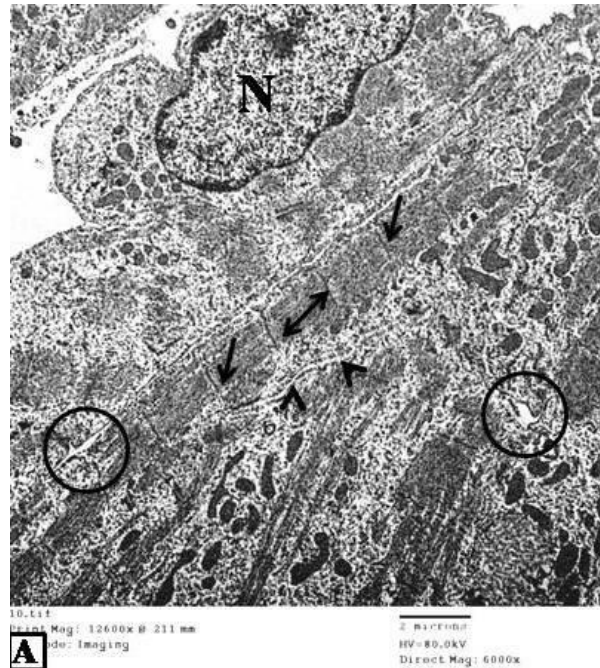
Fig. 64. A: Transmission electron micrograph showing atrial myofibres of 52 cm CVRL camel foetus, myofibril nuclei (N). Cell membrane (arrowheads) with cell junctions (circles). The transverse tubular system appearing as clear Z lines (arrows), and pale I bands (double headed arrow). (X6000).
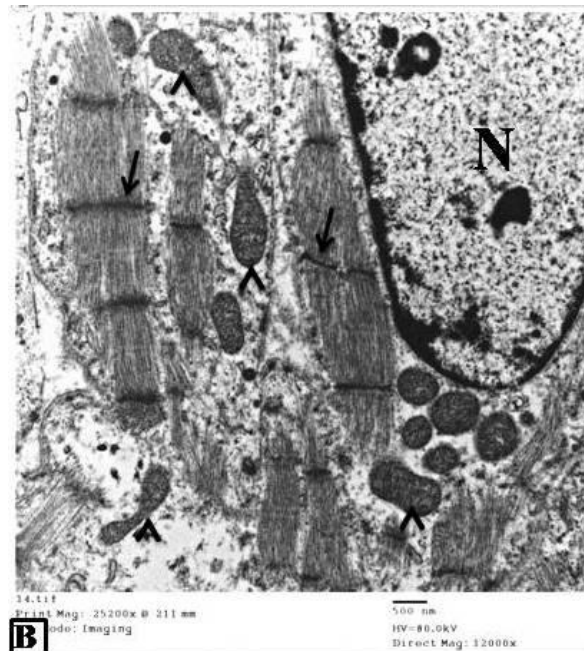
Fig. 64. B: Transmission electron micrograph showing atrial myofibres of 65 cm CVRL, with oval nucleus (N). Mitochondria are numerous with different shapes and sizes (arrowheads), the transverse tubular system appearing as clear Z lines (arrows). (X12000).

99
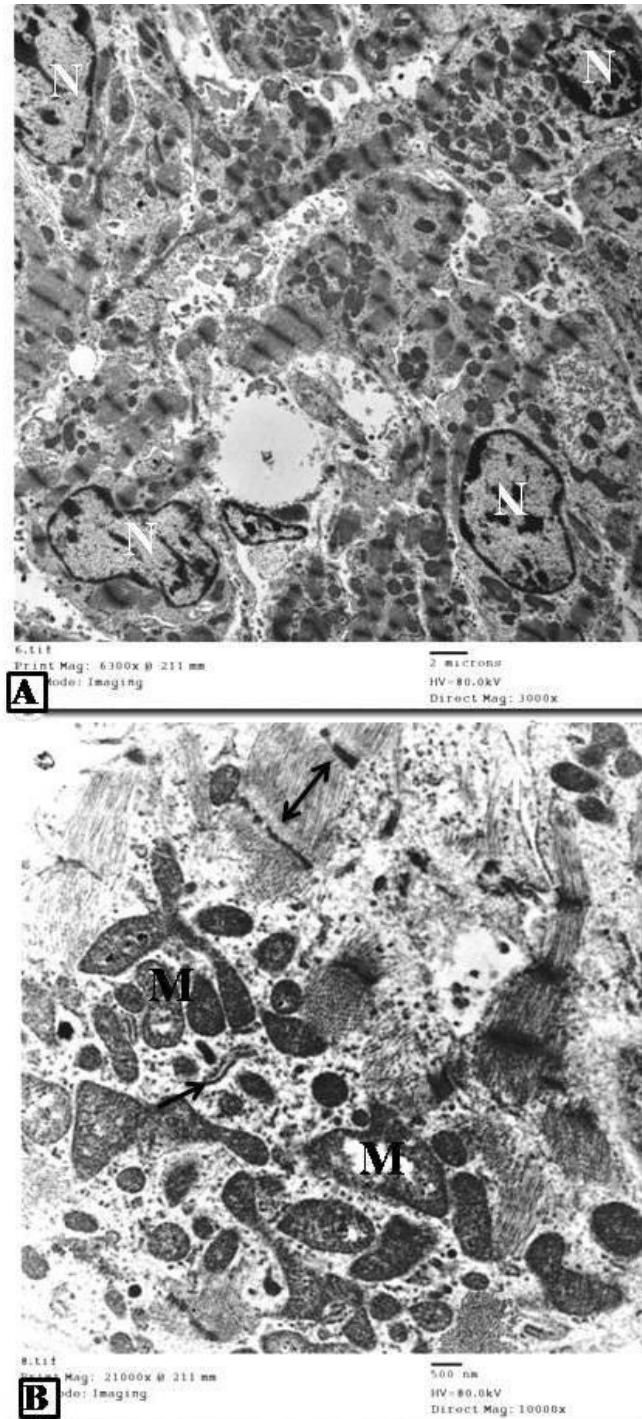
Fig. 65. A and B: Transmission electron micrographs showing ventricular myocardium of 60 cm CVRL; myofibril nuclei were oval or irregular, rough sarcoplasmic reticulum (arrows), mitochondria in different shapes and sizes (M), transverse tubular system appearing as clear Z lines with clear I and A bands (double headed arrow). A: (X3000) and B: (X10000).
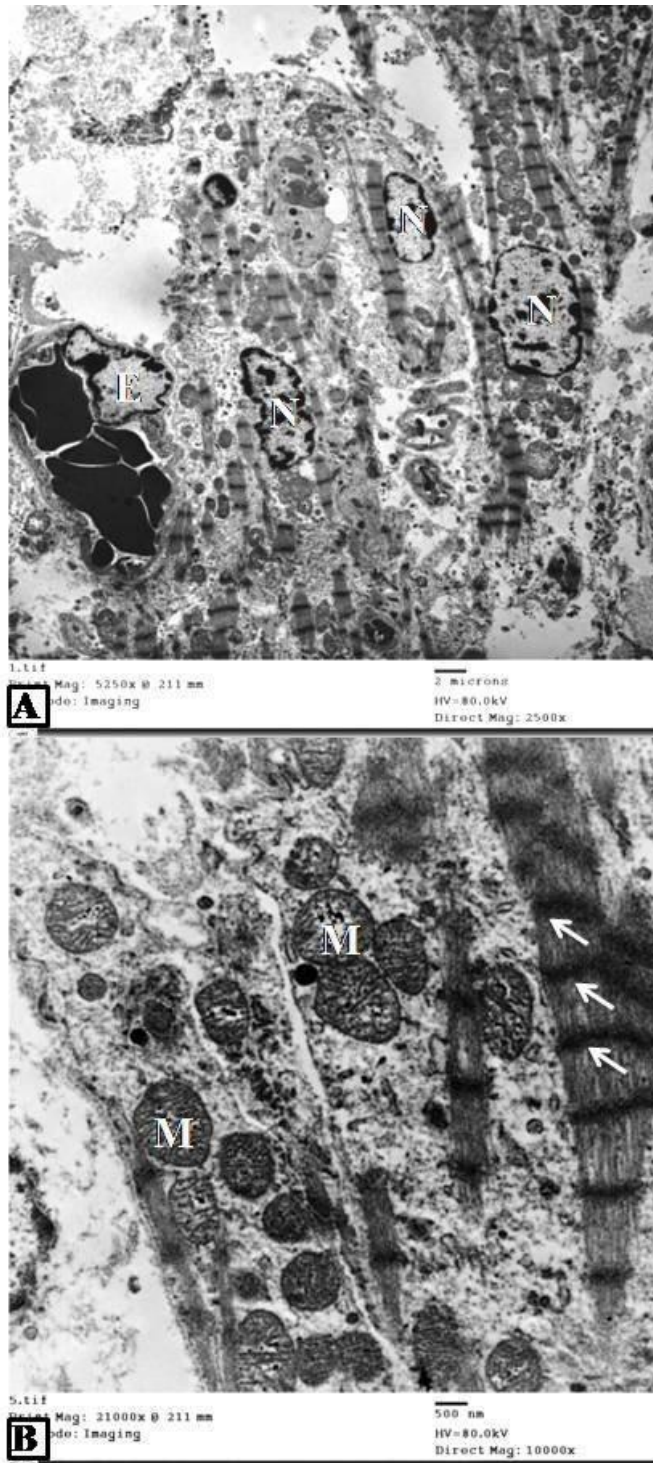
Fig. 66. A and B: Transmission electron micrographs showing myocardial bridges of 65 cm CVRL; myofibril nuclei are oval (N), transverse tubular system appearing as only Z line (arrows), Mitochondria (M) are spherical or oval in shape, E: endothelial nuclei instead refer to the blood capillary. A: (X2500) and B: (X10000).
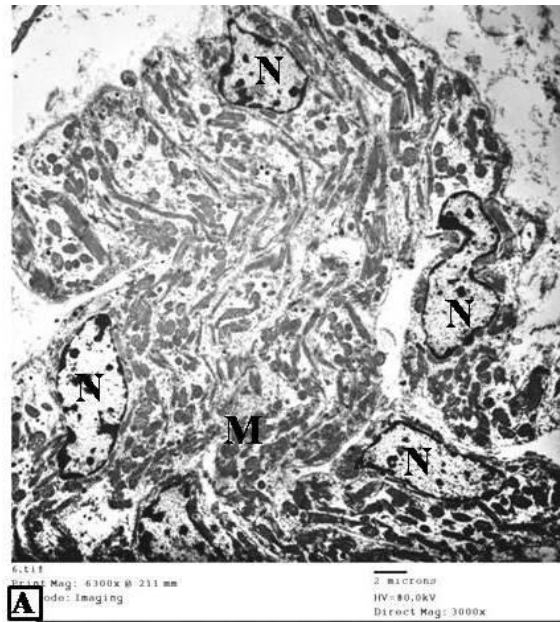
Fig. 67. A: Transmission electron micrograph showing atrial myocardium of 89 cm CVRL. Myofibril nuclei are oval or irregular (N), Mitochondria are scattered around the nuclei and between myofibrils (M). (X3000).
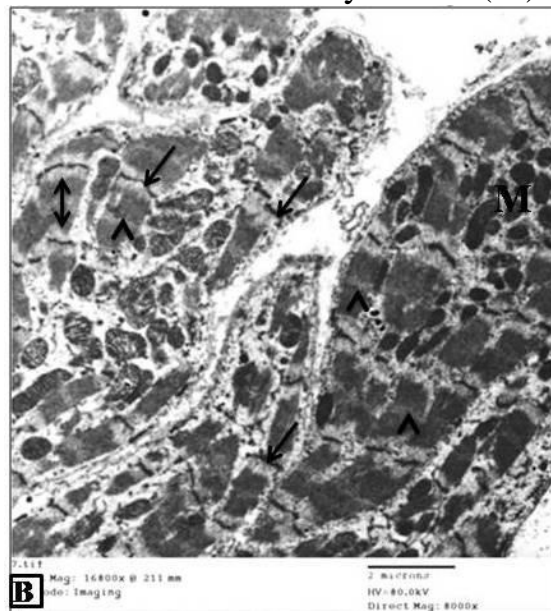
Fig. 67. B: Transmission electron micrograph showing atrial myocardium of 101 cm CVRL. Transverse tubular system appearing as Z lines (arrows) with clear I and A bands (double headed arrow) and pale H zone (arrowheads). (X8000).

Fig. 68. Transmission electron micrograph showing atrial myocardium of 112 cm CVRL. Myofibril nuclei are elongated (EN), clear Z lines (arrows) with clear I and A bands (double headed arrows) and pale H zone (arrowheads) connective tissue nuclei (CN), E, simple squamous epithelium nuclei. (X3000).
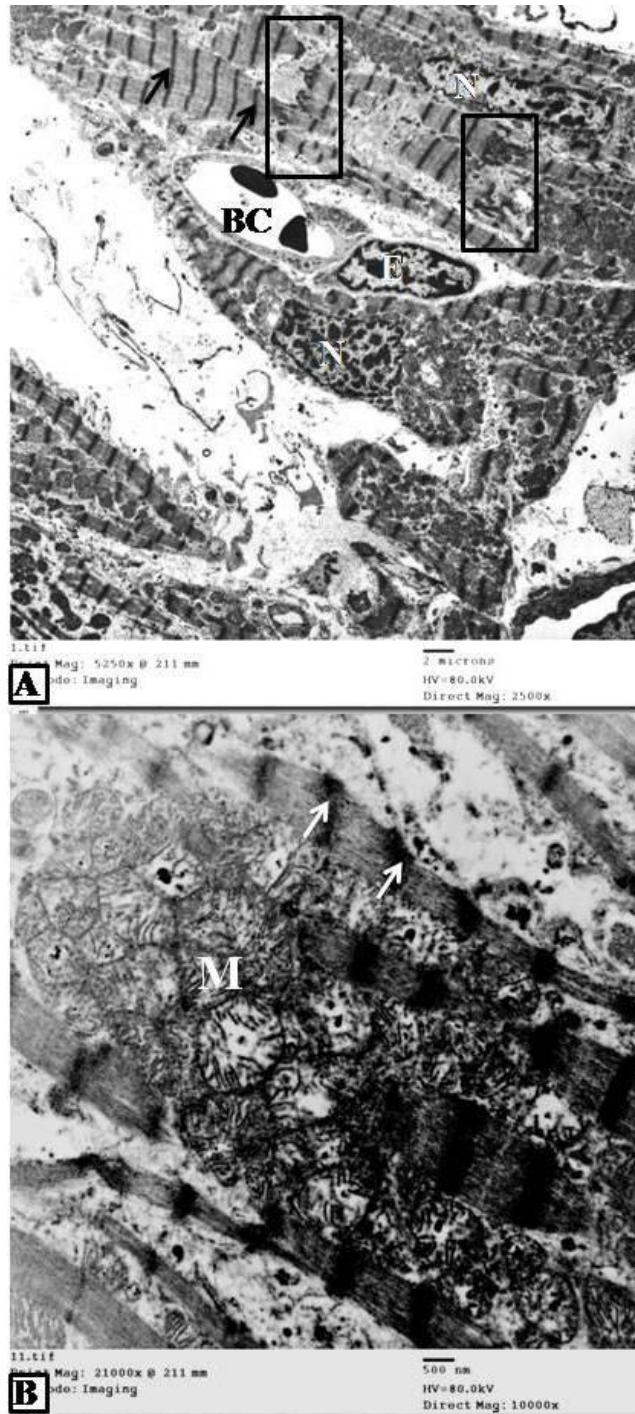
Fig. 69. A and B: Transmission electron micrographs showing myocardial bridges of 89 cm CVRL, myofibril nuclei are elongated or irregular (N), transverse tubular system appearing as Z lines (arrows), intercalated disc (rectangles), crowded and large amount of mitochondria (M) between myofibrils, BC blood capillary, endothelial nuclei, E. A: (X2500), B: (X10000).
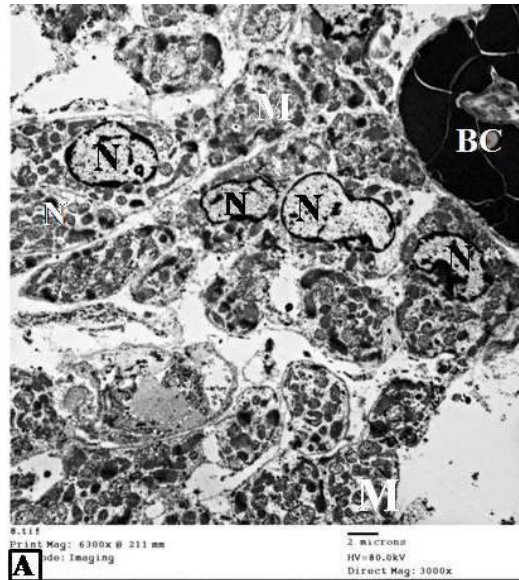
Fig. 70. A: Transmission electron micrograph showing myocardial bridges of 101 cm CVRL. Myofibril nuclei are oval or irregular (N), crowded and large amount of mitochondria (M), blood capillary (BC). (X3000).

Fig. 70. B: Transmission electron micrograph showing myocardial bridges of 112 cm CVRL. Myofibril nuclei are oval or irregular (N), large amount of collagen bundles (arrowheads). Connective tissue cell nuclei are present between the myocardial bundles (C). (X3000).

CHAPTER FOUR

DISCUSSION

4.1. Histology

4.1.1. The Cardiac Muscle and Pericardium

The development of pericardium was studied early in amphibians, birds and mammals (Robinson, 1902). It was associated with the development of the great veins and diaphragm. In mammals the pericardial mesoderm was present in the pericardial portion of the embryonic area. It was completely separated into somatic and splanchnic layers before the head fold appeared. There was a single pericardial cavity which extended from side to side along the anterior boundary of the embryonic area (Robinson, 1902). In our study the pericardium was associated with the diaphragm and thoracic vertebrae. The diaphragmatic part was thick and the vertebral part was thin.

Schlueter and Brand (2012) stated that the epicardium formed an epithelial layer on the surface of the heart. It was derived from a cluster of mesothelial cells which was termed the proepicardium (PE). The PE gave rise not only to the epicardium but also to epicardium-derived cells. These cells populated the myocardial wall and differentiated into smooth muscle cells, fibroblasts, and possibly endothelial cells. Schlueter and Brand (2012) suggested that the PE was made up of distinct cell populations.

In this study the epicardium became thick gradually from first to third trimesters. The epicardium in the first trimester consisted of loose connective tissue and simple squamous epithelium; it became thicker with the increase of the connective tissue. In the third trimester it consisted of a large amount of adipose tissue.

The heart was the first organ to form during embryogenesis and its circulatory function was critical early in development for the viability of the

106

mammalian embryo (Zaffran and Frasch, 2002). In the present study the atria appeared as 3-4 layers of cells arranged as irregular bands. The thickness of the atrial pectinate muscles and thickness of epicardial connective tissue increased depending on the foetal age. However, the ventricles appeared as trabeculation which increased in thickness compared with that at the early and late stages of the first trimester. Morphogenesis of ventricular muscle from connective tissue to myocardium appeared early at the first trimester of gestation. The ventricular trabeculation decreased in the second and third trimesters.

In rabbits the most remarkable development of the heart took place in the period between the 10th and the 13th day of gestation (Balogh and Sótonyi, 2003). Nevertheless, the present study showed histologically important developmental changes as from the first to the second and third trimesters.

Our study agreed with (Savolainen, *et al.*, 2009) who stated that the transition zone between compact and trabeculated tissues was like a spongy layer which was recognized as a network of fine trabeculations.

In developping Zebra fish heart, until maturity, the atrium showed extensive pectinate muscles, and the atrial wall increased to two or three cell layers. The ventricular wall and the compact layer increased to three or four cell layers, while the extent and complexity in trabeculation continued. Further thickening of the heart wall was mainly by increase in cell size (Norman, *et al.*, 2000). On the contrary, our investigation showed that the thickness of the heart wall increased by an increase of the number of cell layers. Aanhaanen *et al.* (2010) who studied the development of the mouse heart found that the atrial part proliferated from the embryonic

atrioventricular canal along with myocytes derived from the developing atrial septum.

4.1.2. The Cardiac Conduction System

4.1.2.1. Sinoatrial Node (SAN)

SAN has been studied in many animals by different histological techniques which revealed a general agreement about its location and appearance of cellular structure (Ghazi and Tadjalli, 1996; Nabipour, 2012; Ghonimi, *et al*., 2015).

In the present study the SAN of camel foetus was found in the subepicardial area at the junction between the cranial vena cava and right atrium. This is in agreement with Ghonimi *et al*. (2015), Ghazi and Tadjalli (1996) in adult camel and Titus (1973) in human. However, Walls (1947) stated that SAN could be found in upper part of the bases of both vena cavae in human foetuses. In the current investigation SAN in the third trimester had an elongated shape with long peripheral tapering ends. Similarly, in equine, Bishop and Cole (1967) found that SAN had a body and long acuminate cranial and caudal crura. However, in the domestic cat it was described as triangular in shape (Ghazi, *et al*., 1998).

In the present investigation two types of cells were recognized. The first type was dark spherical with light nuclei and peripheral chromatin. The second type was small spindle-shaped cells with dark small nuclei. This is in consistency with the findings of Ghazi *et al.* (1998) in the cat. In the present study SAN of camel foetus was embedded in loose connective tissue that contained adipose cells and collagenous fibres. However, Ghonimi *et al*. (2015) claimed that the SAN of camel consisted of stroma and parenchyma and the stroma was made of fibrous connective tissue capsule which sent

thin connective tissue septa. Ghazi *et al.* (1998) also found that, the SAN of cats contained normally a dense collagenous framework.

According to James (1970) the postnatal changes in the development of conduction system were extensive and important. SAN originated in the sinus venosus but subsequently a dense collagenous framework developped. It was added that partitioning of the sinus node by collagen was important not only to the nature of its cellular development but also to its pacemaking function.

The SAN ganglion in the present study was first observed in the third trimester in the subendocardial lamina propria near the cardiac muscles. It was embedded in connective tissue rich in adipose cells, blood vessels and nerves. Earlier, Nonidez (1943) stated that SAN was supplied by axons of neurons of the intramural cardiac ganglia in dog and rhesus monkey. According to Nabipour (2012) the SAN ganglia of human, horse, goat dog and domestic cat were present at the periphery of the node.

The conduction system components were innervated by cardiac ganglia largely derived from the neural crest (Christoffels and Moorman, 2009). A large number of fibroblasts were found within the mature conduction system in the human heart, isolating the ventricular pathways; these fibroblasts were derived from the epicardium, endocardium and neural crest (Christoffels and Moorman, 2009). In this study the cardiac ganglion was observed in the third trimester. This agrees with the latter authors who stated that in the embryo the conduction system was not innervated and interstitial fibroblasts were scattered or absent within the myocardial components of the system. It was the cardiomyocyte, therefore, which was the source and principal cell type of the conduction system.

4.1.2.2. Atrioventricular Node (AVN) and Atrioventricular Bundle (AVB) or Bundle of His

Anatomists who seek to demonstrate the location of the components of cardiac conduction system must be contended with the fact that the components of the system cannot be distinguished from the working myocardial elements by gross dissection (Anderson, *et al.*, 2009). The AVN and AVB originated as separate structures that united together very early in foetal development (James, 1970). The AVB and lower nodal cells were derived from ventricular myocardium (Aanhaanen, *et al*., 2010).

In the current study, unusually, in one section at (17 cm CVRL; 112 days of gestation) AVN appeared as scattered three groups of cells separated from each other by connective tissue rich in fibroblasts.

According to Virágh and Challice (1977) AVN originated from the cells at the distal end of specialized tissue and proliferated into the loose mesenchyme of the dorsal AV cushion. The proliferation took place proximal to the developing interventricular septum with which the specialized inner layer of the AV canal was interconnected.

The AVN was observed early at the first trimester of gestation. AVN was located between the right atrium and right ventricle close to the opening of coronary sinus. At the early and late stage of the second trimester the AVN consisted of spherical cells with oval and central nuclei. In the early stages of the third trimester AVN consisted of a group of darkly stained cells. In the middle and late stages of the third trimester, AVN was embedded in connective tissue and had large amounts of adipose tissue.

In the second trimester AVB appeared as a bundle of lightly stained fibres that were embedded in the myocardium or surrounded by connective tissue and had spherical or oval fibres with spherical central nuclei. In the

early stages of the third trimester AVB appeared as groups of fibres which were covered by connective tissue between the endocardium and myocardium. They had light cytoplasm and pale central nuclei and they were either separated from the myocardium by loose connective tissue or directly attached to it. The fibres had lightly stained nuclei. They also appeared as bundles with lightly stained fibres having spindle-shaped and oval pale nuclei in the endocardium or between the myocardium. AVB fibres at this stage had very clear striations.

Virágh and Challice (1977) studied the histogenesis of the AVN and AVB in mouse embryos. In younger embryos the inner cell layer of the dorsal wall of the AV canal formed a specialized interconnecting tissue between the atrial and ventricular muscles. In this study of the camel foetus, AVN was also observed close to the right atrioventricular opening and it was surrounded by an accumulation of fibroblasts and separated from the surrounding ordinary cardiac muscles by a loose connective tissue which contained reticular fibres.

The primordia of AVN and AVB of 11- and 12-days mouse embryo, (Virágh and Challice, 1977) were interconnected with the ventricular trabeculae and were in contact with the myocardium of the interventricular septum. In the 12-days embryos blood capillaries and connective tissue cells began to isolate the primordium of the conducting system from the force producing myocardium.

Arguello *et al*. (1988) studied the development of the AVN and AVB of embryonic chick hearts by using electrophysiological and morphological techniques. The dorsal wall of the AV canal and the interatrial septum were explored to determine if they contribute to the formation of the AVN and AVB. The earliest identification of the AVN and upper AVB group of cells

111

was achieved at 5-6 days of development. The earlier AVN and AVB responses had similar characteristics to those of the adult heart. It was concluded that the AVN and upper AVB cells were derived from the low interatrial septum. The possibility that AV canal cells contribute to this event was discarded.

Nabipour (2004) studied the histology of AVB in the guinea pig. The cells of the AVB appeared to be organized into fascicles separated by fine fibrous septa. The majority of the cells of AVB were ovoid in shape with light cytoplasm and central nuclei. He also descried intercalated discs at the AVN intercellular junctions. This study agreed with the previous study regarding the shape and organization of AVB but disagreed with it regarding the presence of intercalated discs at the AVN intercellular junctions. In the current study no ganglia were seen associated with the AVB. This was in agreement with the findings of Nabipour (2004) in the guinea pig who stated that the innervation of AVB was poor and no ganglia were present within or around the AVB and its branches.

Nabipour and Shahabodini (2007) studied the histological structure of the AVN and AVB in 4 months-old ovine foetuses of five animals using routine histological techniques and specific staining methods. They reported that the AVN was caudally located and adjacent to the root of the aorta. It was almost spherical in shape and consisted of spiral cells. The node was mainly composed of perinuclear clear zone cells (P cells). In contrast, in the early stages of the third trimester in this study the AVN consisted of a group of darkly stained cells with oval and central nuclei. These cells were surrounded by connective tissue that consisted of a large amount of fibroblasts.

The AVB was a direct continuation of the AVN and passed through the fibrous ring toward the apex of the interventricular septum where the right branch of the bundle was detached. The cells of the AVB were wider, shorter and lighter than normal myocardial cells. Some of the bundle cells had been changed to Purkinje cells, whereas some others remained unchanged (Nabipour and Shahabodini, 2007). In this study the AVB appeared in the second trimester as a bundle of lightly stained fibres that were embedded in the myocardium, or as fibres lightly stained centrally and darkly stained peripherally with clear peripheral striations. In the third trimester the bundles consisted of lightly stained fibres with spindle-shaped and oval pale nuclei which were located in the subendocardial lamina propria and between the myocardial fibres, or separated from the myocardium by loose connective tissue or directly attached to it.

4.1.2.3. Purkinje Fibres (PF)

It is well known that Purkinje fibres are found in the subendocardium. They are larger than cardiac muscle cells, but have light glycogen content, fewer myofibrils and no T-tubules (Eliška, 2006). They are specialized conducting fibres which extend from the interventricular septum, to the papillary muscles and up the lateral walls of the ventricles. Nevertheless, studies on the development of Purkinje fibres of the camel foetus appeared to be lacking.

Parto *et al.* (2013) stated that Purkinje fibers or Purkinje cardiomyocytes were part of the cardiac conduction system and classified as specific heart muscle tissue responsible for the heart impulses. According to this author most of the Purkinje fibres in ostrich heart composed of a clear structure with less sarcoplasm. The myofibrils tended to be confined to a

thin ring around the periphery of the cells with one or more large nuclei centrally located within the fibre.

In this study the differentiation of Purkinje fibres from myocytes was very clear at the early stages of gestation in camel foetus. PF appeared as darkly stained striated fibres and double nuclei appeared in many fibres. PF were embedded in connective tissue or attached to the ordinary cardiac muscle.

In the third trimester of gestation the PF had light cytoplasm and most of them were double nucleated.

4.2. Myocardial Bridges (MBs)

Thej *et al.* (2012) defined myocardial bridging in humans as a congenital coronary anomaly with a variety of clinical manifestations. Verhagen *et al*. (2013) stated that MB is a band of myocardium covering a coronary artery segment, typically located in the left anterior descending (LAD) coronary artery. Bridged segments of the coronary artery are isolated from the influence of perivascular adipose tissue and the coronary artery segments covered with MB have a lower calcium score than segments without MB (Verhagen, *et al*., 2013).

Review of the literature revealed that the vast majority of research on myocardial bridges had been carried out on humans. The most common site of myocardial bridge is over the anterior interventricular branch of the left coronary artery (Migliore, *et al*., 2013). Other reported locations include: the diagonal branch of the left coronary artery, the left marginal branch, inferior interventricular branch of the left coronary artery, right coronary artery, right marginal artery, and inferior interventricular branch of the right coronary artery (Lima, *et al.*, 2002; Loukas, *et al*., 2006; Bharambe and Arole, 2008). However, Migliore *et al*. (2013) reported that all myocardial bridges were

located in the mid segment of the left anterior descending coronary artery with a mean length of 17±9 mm.

Marwa-Babiker and Taha (2015) stated that in the adult camel the myocardial bridges were covered by a large amount of adipose tissue. This adipose tissue infiltrated the cardiac muscles of the bridge. In the present study the MB had connective tissue separating the bridge from interventricular branch of coronary artery especially in the third trimester of gestation. Sometimes the MB was attached to the coronary branch and there was no adipose tissue infiltrating the MB or no connective tissue separating the MB from myocardium or interventricular branch of coronary artery. The cross section of the interventricular branch of coronary artery under the MB in the second and third trimester was often irregular in shape and sometimes oval, consisting of many layers of smooth muscle fibres in tunica media and collagenous and elastic fibres in tunica adventitia.

4.3. Histometry

In the adult camel the thickness of MB ranges between 7-15 mm. (Erden, *et al*., 2006). According to the present study the thickness of MBs of the third trimester 172.28±25.90 µm was significantly thicker than that of the second trimester 49.92±12.55 µm and the thickness of the wall of the interventricular branch of coronary artery of the third trimester 48.72±25.09 µm was significantly thicker than that of the second trimester 28.38±12.16 µm. This indicated that the development rate of the wall of myocardial bridge and interventricular branch of coronary artery increased with advancing age.

4.4. Ultrastructure

The ultrastructure of foetal heart was early studied by many authors in many animals; rabbit (Muir, 1957); chicken (Manasek, 1968); rat (Melax and Leeson, 1969) and (Chacko, 1976) and human (McNutt, 1970).

In sheep, the ultrastructure of ventricular myocardium has been studied using both TEM and SEM (Myklebust, *et al*., 1975). The development of the sheep foetal heart at 90 days of gestation and 36 days post-natal was also investigated (Sheldon, *et al*., 1976; Brook, *et al*., 1983). Furthermore, the pattern of myofibril development was studied during the whole foetal period (Kim, *et al*., 1992). Sarcomeres were studied in the rat by TEM to reveal the structure of myocyte (Xavier-Vidal, *et al*., 1997).

Cardiac atrial and ventricular myocytes and their intercalated discs in the mammalian heart were cylindrical in shape, bifurcate, and connected end-to-end at the intercalated discs. The intercalated discs in the myocardium showed a stair-like profile (Shimada, *et al*., 2004). In this study in the first trimester of camel foetus, intercalated discs were not observed, but only Z lines with irregular striations were detected. The intercalated discs however, first appeared in the third trimester in the form of a zigzag.

Scanning electron microscopy of dog hearts showed extensive communications between mitochondria, sarcoplasmic reticulum, and nuclear envelope (Sybers and Ashraf, 1975). In the present study, mitochondria were also numerous with different shapes and sizes and were located around the nuclei and between the fibrils.

Cardiac myocytes were similar to skeletal muscle; their contractile proteins were organized into sarcomeres with contractile units a protein matrix known as Z line which was primarily composed of the protein a-actinin (Barnett, 2009). This is also true for the present study in which the

transverse tubular system appeared early as a pale, irregular Z lines. In early development of sheep foetus, cardiac myocytes contained large amounts of glycogen, scattered mitochondria and peripheral myofibrils. Transverse tubules were absent and sarcoplasmic reticulum and intercalated discs were poorly developed (Smolich, 1995). In the early developmental stages of the myocytes of camel foetus in this investigation only irregular Z lines were observed.

During late foetal and early postnatal development of sheep, myofibrils extended into the myocyte interior and attained the mature appearance. The glycogen particles were reduced in size. In addition, transverse tubules developped and the morphological appearance of the sarcoplasmic reticulum and intercalated disc became increasingly complex (Smolich, 1995). Xavier-Vidal *et al*. (1997) reported in the rat myocytes well fixed with well-developped sarcomeres disposed in an irregular form in the myocyte cytoplasm. In this study at the late stages of the third trimester transverse tubular system was well developped, intercalated discs and large amount of collagen were shown.

Literature pertinent to the present study of scanning electron microscopy of camel foetal heart is virtually lacking.

Measurements of the length and width were done. The heart during the first third of first trimester had approximately similar dimensions. However, the length increased more than the width during the late stages of the first trimester. In this study the longitudinal groove started gradually as a shallow groove but the coronary groove was not observed till the last stage of first trimester of gestation. This indicated that the longitudinal grooves developped before the coronary groove.

The atrial pectinate muscles showed a wavy appearance at the early stages of first trimester and gradually developped and appeared as large branching and anastomosing cords at late stages of first trimester of gestation.

Myocardial bridges were grossly investigated the third trimester of gestation in camel foetus (Marwa-Babiker and Taha, 2013), also with light microscopy in adult camel (Marwa-Babiker and Taha, 2015). Two types of myocardial bridges were recognized; in type I the interventricular branch of coronary artery dipped once or twice in the myocardium and reappear on the longitudinal groove. However, in type II the artery dipped in myocardium without reappearing. In this study type II myocardial bridges were observed in the late stages of first trimester. Moreover, the interventricular branch of coronary artery dipped in myocardium at the proximal third of longitudinal groove without reappearing.

In Sprague-Dawley rat's embryos most of organelles development and formation of the striated system occurred in the second trimester (Chacko, 1976). Similarly in our study organelles development started clearly in the second trimester and continued in the third trimester. Transverse tubular system started clearly from first trimester as irregular Z lines. In the second trimester the transverse tubular system had clear Z lines, with clear I and A bands. In the third trimester of gestation the transverse tubular system showed clear Z lines with clear I and A bands and pale H zones.

The present prenatal morphological and histometric studies on MBs in camel were done for the first time. Myocardial bridges were investigated in this study by TEM in the second and third trimesters. They had a less developping transverse tubular system than the ordinary cardiac muscle in the same stages. The atrial and ventricular myocardium consisted of long

cylindrical muscle cells which were often bifurcated and connected with contiguous cells. These cells had rich sarcoplasmic reticulum and well-developed myofibrils in the mammalian heart (Shimada, *et al.*, 1986). Atrial pectinate muscles were investigated in the present study with the scanning electron microscopy and were measured using an electron microscope with processing software. They appeared as plexiform connected cords covered by simple squamous epithelium. Pectinate muscle thickness measured about 130.7-488.2 μm in X75 in the second trimester. However, the measurement values in the third trimester of gestation were about 72.05-243.03 μm (X75) and 132.06-756.9 μm (X50).

4.5. Morphometry

The present study is the first report regarding ultrastructural morphomerty of the prenatal camel heart.

Ultrastructural quantitative morphometry has been studied earlier in different mammalian species. According to Barth *et al*. (1992) the myocardial content of mitochondria was a very specific and constant value for any particular species, the smallest animals having the highest content; it ranged between 22.0-37.0% in dog, pig, cat, rabbit, guinea-pig, rat and mouse. However, myofibrillar volume density showed no species variability being about 60.0% in all species.

In humans (Schaper, *et al*., 1985) the myocytes were composed of 23% mitochondria 59% myofibrils, and 18% cytoplasm.

No significant difference (P>0.05) was detected between myofibrils length in the first, second and third trimester; whereas the myofibrils of the first trimester were significantly (P<0.01) wider than those of second and third trimesters. There was also no significant difference (P>0.05) between the length and width of mitochondria in second and third trimesters.

However, the length of mitochondria in the first trimester was significantly longer than that in the second and third trimester.

The sarcomere of the myofibril of the third trimester was significantly thicker than that of the first and second trimester.

In this study the nuclei of the connective tissue cells of the myocardium in the first trimester were significantly longer than those of the second and third trimesters. On the other hand, the width of these nuclei in the three gestational stages revealed no significant difference. The nuclei of the connective tissue cells of the myocardial bridges in the third trimester were significantly longer than those of myocardium in the ordinary cardiac muscles of the first, second and third trimesters. The width of connective tissue nuclei of the myocardial bridges had no significant difference from that of myocardium in the three gestational stages.

CONCLUSION

The development of the heart of camel foetus was not fully completed during the first trimester of gestation. Significant histological and developmental changes of the foetal heart were observed throughout the three gestational ages. The cardiac conduction system showed very important histological developmental changes throughout the three gestational ages. The myocardium showed significant developmental changes especially in the transverse tubular system. Two histologically different types of MBs were observed during the second and third trimesters. No significant differences were detected in ultrastructural morphometric measurements of myofibrils, connective tissue nuclei, mitochondria of myofibrils and sarcomere thickness of myocardium and MBs during the three trimesters.

RECOMMENDATIONS

1- Further morphological studies including SEM and TEM are recommended to reveal the developmental changes of the cardiac conduction system.

2- Atrial natriuretic hormone (ANH) is secreted by the atrial myocytes and is involved in homeostatic control of body water, sodium, potassium and adipose tissue. Future immunohistochemical localization of this hormone will be of vital importance.

3- Molecular biology of the genes governing the development of myocardial bridges (MBs) needs to be investigated.

REFERENCES

Aanhaanen, W.T.J., Mommersteeg, M.T.M. and Norden, J. (2010). Developmental origin, growth, and three-dimensional architecture of the atrioventricular conduction axis of the mouse heart. *Circulation Research*, **107**: 728-736.

Alegria, J.R., Herrmann, J., Holmes, R.D., Lerman, A. and Rihal, S.C. (2005). Myocardial bridging. *European Heart Journal*, **26**: 1159-1168.

Anderson, R.H., Yanni, J., Boyett, M.R., Chandler, N.J. and Dobrzynski, H. (2009). The anatomy of the cardiac conduction system. *Clinical Anatomy*, **22** (1): 99-113.

Anversa, P., Olivetti, G. and Loud, A.V. (1980). Morphometric study of early postnatal development in the left and right ventricular myocardium of the rat: I. hypertrophy, hyperplasia, and binucleation of myocytes. *Circulation Research,* **46** (4): 496-502.

Arguello, C., Alanis, J. and Valenzuela, B. (1988). The early development of the atrioventricular node and bundle of His in the embryonic chick heart. An electrophysiological and morphological study. *Development*, **102**: 623-637

Aytan, P., Ulusal, G., Yenigiin, E.C., Yildirim, O., Pirpir, A. and Yildirim, S. (2006). Muscular bridges causing non-ST-segment elevation myocardial infarction. *Anadolu Kardiyol Derg*, **6**: 374-375.

Balogh, E. and Sótonyi, P. (2003). Histological Studies on Embryonic Development of the Rabbit Heart. Acta Veterinaria Hungarica, **51** (1): 1-13.

Bancroft, D.G. and Stevens, A. (1990). *Theory and Practice of Histological Techniques.* 3rd ed. Bath press, Avan. Churchill Livingston. Edinburgh. London and New York.

Bancroft, D.G. and Stevens, A. (2008). *Theory and Practice of Histological Techniques.* 6th ed. Bath press, Avan. Churchill Livingston. Edinburgh. London and New York.

Barnett, V.A. (2009) *Hand book of cardiac Anatomy and Physiology and Devices (cardiac myoctes).* Edited by P. A. Laizzo Humana press Inc. Totowa NJ: 113.

Barth, E. Stämmler, G., Speiser, B. and Schaper, J. (1992). Ultrastructural quantitation of mitochondria and myofilaments in cardiac muscle from 10 different animal species including man. *Journal of Molecular and Cellular Cardiology,* **24** (7): 669-681.

Bharambe, V.K. and Arole, V. (2008). The study of myocardial bridges. *Journal of Anatomical Society of India*, **57** (1): 14-21.

Bishop, S.P. and Cole, C.R. (1967). Morphology of the specialized conducting tissue in the atria of the equine heart. *Anatomical Record,* **158** (4): 401-415.

Brook, W.H., Connell, S., Cannata, J., Maloney, J.E. and Walker, A.M. (1983). Ultrastructure of the myocardium during development from early fetal life to adult life in sheep. *Journal of Anatomy,* **137** (4): 729-741.

Canale, E., Smolich, J.J. and Campbell, G.R. (1987). Differentiation and innervation of the atrioventricular bundle and ventricular Purkinje system in sheep heart. *Development*, **100** (4): 641-651.

Chacko, K.J. (1976). Observations on the ultrastructure of developing myocardium of rat embryos. *Journal of Morphology*, **150** (3): 681-709.

Chen, J.S. and Lin, C.L. (2003). Myocardial bridging. *Tzu Chi Medical Journal*, **15** (6): 357-362.

Chen, M.L., Chen, C.H., Chao, I.M. and Lo, H.S. (2004). Dipyridamole Thallium-201 Myocardial Single Photon Emission Computed Tomography in Myocardial Bridging a Case Report. *Acta cardiologica sinica*, **20**: 37-41.

Christoffels, V.M. and Moorman, A.F.M. (2009). Development of the Cardiac Conduction System. *Circulation: Arrhythmia and Electrophysiology*, **2**: 195-207.

Darius, B. (2014). Myocardial Bridge. Bibliography: 1. Braunwald's Heart Disease; 2. Harrison's Principles of Internal Medicine; 3. European Society of Cardiology-Clinical Practice Guidelines. Heart Update.com Aleea Sanatatii, 300129, Timisoara, Romania.

Demirsoy, E., Arbath, H., Ünal, M., Yağan, N., Yilmaz, O., Tükenmez, F., Şener, D. and Sönmez, B. (2006). Coronary rupture to the right ventricle during PTCA for myocardial bridge. *Anadolu Kardiyol Derg*, **6**: 377-379.

Duan, D., Yu, S. and Cui, Y. (2012). Morphological study of the sinus node and its artery in yak. *The Anatomical Record*, **295** (12): 2045-2056.

Eliška, O. (2006). Purkinje fibers of the heart conduction system the history and present relevance of the Purkinje discoveries. *ČASOPIS LÉKAŘŮ ČESKÝCH*, **145** (4): 329-335.

Elwishy, A.B., Hemeida, N.A., Omer, M.A., Mobarak, A.M. and ElSayed, M.A.I. (1981). Functional changes in the pregnant camel with special reference to fetal growth. *British Veterinary Journal*, **137**: 527-537.

Erden, H., Turan, E. and Kara, M.E. (2006). The course of the interventricular coronary arteries and myocardial bridges in one-humped camel. *The Journal of the Faculty of veterinary medicine. Istanbul University*, **32** (3): 1-6.

Fernández, P.M. (2002). *Manual de biologíadeldesarrollo. Manual Moderno. p. 243. ISBN 968-426-976-5.*

Ghazi, S. R. and Tadjalli, M. (1993). The anatomy of the atrioventricular bundle in the heart of camels (*Camelus dromedarius*). *Veterinary Research Communications*, **17** (6): 411-416.

Ghazi, S.R. and Tadjalli, M. (1996). Anatomy of the sinus node of camels *(Camelus dromedarius). Anatomia Histologia Embryologia*, **25** (1): 37-41.

Ghazi, S.R., Tadjalli, M. and Baniabbas, A. (1998). Anatomy of the sinus node of domestic cats (*Felis catus*). *Journal of Applied Animal Research*, **14**: 57-64.

Ghonimi, W. Balah, A. Bareedy, M.H. Salem, H.F., Soliman, S.M, Elbaz, A., Helal, A. and Abuel-Atta, A.A. (2015). Sinu-atrial node of mature dromedary camel heart (*Camelus dromedarius*) with special emphasis on the atrial Purkinje like cardiomyocytes. *Cell Biology*, **3** (2): 25-33.

Iuchi, A., Ishikawa, Y., Akishima-Fukasawa, Y., Fukuzawa, R., Akasaka, Y. and Ishii, T. (2013). Association of variance in

anatomical elements of myocardial bridge with coronary atherosclerosis. *Atherosclerosis*, **227**: 153-157.

James, T.N. (1970). Cardiac conduction system: Fetal and postnatal development. *American Journal of Cardiology*, **25** (2): 213-226.

Johnston, I.A., Fitcht, N., Zummo, G., Wood, R.E., Harrison, P. and Tota, B. (1983). Morphometric and ultrastructural features of the ventricular myocardium of the haemoglobin-less icefish (*Chaenocephalus aceratus*). *Comparative Biochemestry and Physiology*, **76A**: 475-480.

Kanan, C.V. (1971). Observation on the pattern and distribution of the coronary vessel of the camel (*Camelus dromedarius*). *Acta Morphol Neerl Scand,* **8**: 321-332.

Kim, H.D., Kim, D.J., Lee, I.J., Rah, B.J., Sawa, Y. and Schaper, J. (1992). Human fetal heart development after mid-term: morphometry and ultrastructural study. *Journal of Molecular and Cellular Cardiology*, **24** (9): 949-965.

Kosinski, A. and Grzybiak, M. (2001). Myocardial bridging in the human heart: myocardial aspects. *Folia Morphologica*, **60** (1): 65-68.

Kosinski, A., Grzybiak, M., Shwarek, M. and Hreezeeha, J. (2004). Distribution of muscular bridges in the adult human heart. *Folia Morphologica (warsz)*, **63** (4): 491-498.

Lima, V.J., Cavalcati, J.S. and Tashiro, T. (2002). Myocardial bridges and their relationship to the anterior intervenetricular branch of the left coronary artery. *Arquivos Brasileiros de Cardiologia*, **79** (3): 219-222.

Loukas, M., Curry, B., Bowers, M., Louis, R.G., Bratczak, A., Kiedrowski, M., Kamionek, M., Fudalej, M. and Wagner, T.

(2006). The relationship of myocardial bridges to coronary artery dominance in the adult human heart. *Journal of Anatomy*, **209** (1): 43-50.

Manasek, F.J. (1968). Embryonic development of the heart. I. A light and electron microscopic study of myocardial development in the early chick embryo. *Journal of Morphology*, **125** (3): 329-365.

Marwa-Babiker, A.M. and Taha, A.A.M. (2013). Myocardial bridges of the heart of the dromedary camel (*Camelus dromedarius*). *University of Khartoum Journal of Veterinary Medicine and Animal Production*, **4** (1): 90-105.

Marwa-Babiker A.M., Ismail, H.I. and Taha, A.A.M. (2013). Biochemical analysis on the Camel heart *(Camelus dromedarius). Proceedings of the conference of sustainability of camel populations and production, King Faisal University, Al-Ahsa, Saudi Arabia.*

Marwa-Babiker, A.M. and Taha A.A.M. (2015). Histology of the myocardial bridges and the related arteries of the adult dromedary camel (*Camelus dromedarius*). *Sudan Journal of Science and Technology*, **16** (2): 1-8.

Marwa-Babiker, A.M. and Taha A.A.M. (2015). Studies on the course and congenital anomaly of the coronary arteries in the dromedary camel (*Camelus dromedarius*). *Ruminant Science*, **4** (1): 1-5.

McNutt, N.S. (1970). Ultrastructure of intercellular junctions in adult and developing cardiac muscle. *The American Journal of Cardiology*, **25** (2): 169-183.

Melax, H. and Leeson, T.S. (1969). Fine structure of developing and adult intercalated discs in rat heart. *Cardiovascular Research*, **3** (3): 261-267.

Migliore, F., Maffei, E., Marra, M.P., Bilato, C., Napodano, M., Corbetti, F., Zorzi, A., Andres, A.L., Sarais, C., Cacciavillani, L., Favaretto, E., Martini, C., Seitun, S., Cademartiri, F., Corrado, D., Iliceto, S. and Tarantini, G. (2013). Artery myocardial bridging and apical ballooning syndrome. *Cardiol Img. The American College of Cardiology Foundation*, **6**: 32-41.

Miquerol, L., Moreno-Rascon, N., Beyer, S., Dupays, L., Meilhac, S.M., Buckingham, M.E., Franco, D. and Kelly, R.G. (2010). Biphasic development of the mammalian ventricular conduction system. *Circulation Research*, **107** (1): 153-161.

Moorman, A., Webb, S., Brown, N.A., Lamers, W. and Anderson, R.H. (2003). Development of the heart: (1) formation of the cardiac chambers and arterial trunks. *Heart (British Cardiac Society),* **89** (7): 806-814.

Moorman, A.F.M. and Christoffels, V.M. (2003). Cardiac chamber formation: development, genes and evolution. *Physiological Review,* **83**: 1223-1267.

Muir, A.R. (1957). An electron microscope study of the embryology of the intercalated disc in the heart of the rabbit. *The Journal of Biophysical and Biochemical Cytology*, **3** (2): 193-202.

Myklebust, R., Dalen, H. and Saetersdal, T.S. (1975). A comparative study in the transmission electron microscope and scanning electron microscope of intracellular structures in sheep heart muscle cells. *Journal of Microscopy,* **105** (1): 57-65.

Nabipour, A. (2012). Comparative histological structure of the sinus node in mammals. *Turkish Journal of Veterinary and Animal Science*, **36** (5): 463-469.

Nabipour, A. (2004). Histology of the atrioventricular bundle in the heart of Guinea pig (*Cavia percellus*). *Iranian Journal of Veterinary Research, University of Shiraz*, **5** (2) 7-13.

Nabipour, A. and Shahabodini, M.R. (2007). Histological study of the atrioventricular node and bundle in the heart of ovine fetus. *Iranian Journal of Veterinary Research, University of Shiraz,* 1**8** (1): 64-70.

Nawal, S.O., Osman, D.I., and Abdalla, A.B. (2002). The morphology of the heart of the dromedary. *The Sudan Journal of Veterinary Science and Animal Husbandry,* **41** (1&2): 1-13.

Nonidez, J. (1943). The structure and innervation of the conductive system of the heart of the dog and rhesus monkey, as seen with a silver impregnation technique. *American Heart Journal*, **26** (5): 577-597.

Norman, H.U., Sedmera, D., Yost, H.J. and Clark, E.B. (2000). Structure and function of the developing zebrafish heart. *The Anatomical Record*, **260**: 148-157.

Olivetti, G., Anversa, P. and Loud, A.V. (1980). Morphometric study of early postnatal development in the left and right ventricular myocardium of the rat II. Tissue composition, capillary growth, and sarcoplasmic alterations. *Circulation Research*, **46** (4): 503-512.

O'Rahilly, R. and Müller, F. (1987). *Developmental stages in human embryos*. ed. 637 (Institution of Washington, Washington).

Parto, P., Tadjalli, M., Ghazi, R. and Salamat, M.A. (2013). Distribution and structure of Purkinje fibers in the heart of ostrich (*Struthio camelus)* with the special references on the ultrastructure. *International Journal of Zoology,* **10:** 1155-1161.

Polliack, A., Lampen, N., Clarkson, B.D., Deharven, E., Bentwich, Z, Siegal, F.P. and Kunkel, H.G. (1973). Identification of human B and

T lymphocytes by scanning electron microscopy. *The Journal of Expermental Medicine,* **138**: 607-624.

Qureshi, A.S., Shah, M., Rehan, S., Pasha, R.H. and Ullah, H.A. (2013). Histomorphometrical investigations on the heart, kidneys and adrenal glands in normal teddy goats (*Capra hircus*) using image analysis system. *Journal of the Pakistan Medical Association,* **33** (2): 155-159.

Redkar, A., Montgomery, M. and Litvin, J. (2001). Fate map of early avian cardiac progenitor cells. *Development*, **128**: 2269-2279.

Robinson, A. (1902). The early stages of the development of the pericardium. *Journal of Anatomy and Physiology*, **37** (1): 1-17.

Sánchez-Quintana, D. and Yen, Ho. S. (2003). Anatomy of cardiac nodes and atrioventricular specialized conduction system. *Revista Española de Cardiología,* **56** (11): 1085-1092.

Savolainen, S.M., Foley, J.F. and Elmore, S.A. (2009). Histology atlas of the developing mouse heart with emphasis on E11.5 to E18.5. *Toxicologic Pathology*, **37** (4): 395-414.

Schaper, J., Meiser, E. and Stammler, G. (1985). Ultrastructural morphometric analysis of myocardium from dogs, rats, hamsters, mice, and from human hearts. *Circulation Research,* **56**: 377-391.

Schlueter, J. and Brand, T. (2012). Epicardial progenitor cells in cardiac development and regeneration. *Journal of Cardiovascular Translational Research,* **5**: 641-653.

Sheldon, C.A., Friedman, W.F. and Sybers, H.D. (1976). Scanning electron microscopy of fetal and neonatal lamb cardiac cells. *Journal of Molecular and Cellular Cardiology,* **8** (11): 853-862.

Sheridan, D.J., Cullen, M.J. and Tynan, M.J. (1977). Postnatal ultrastructural changes in the cat myocardium: a morphometric study. *Cardiovascular Research*, **11** (6): 536-540.

Shimada, T., Kawazato, H., Yasuda, A., Ono, N. and Sueda, K. (2004). Cytoarchitecture and intercalated disks of the working myocardium and the conduction system in the mammalian heart. The *Anatomical Record. Part A Discoveries in Molecular Cellular and Evolutionary Biology*, **280** (2): 940-951.

Shimada, T., Noguchi, T., Asami, I. and Campbell, G.R. (1986). Functional morphology of the conduction system and the myocardium in the sheep heart as revealed by scanning and transmission electron microscopic analysis. *Archivum histologicum japonicum,* **49** (3): 283-295.

Shinjo, S.K., Oba-Shinjo, S.M. and Barbato de Prates, N.E.V. (2004). Bovine myocardial bridge morphology and association with coronary atherosclerosis. *Brazilian Journal of morphological Sciences,* **21** (2): 95-98.

Singh, H., Singh, C., Kumar, A., Aggarwal, N. and Banerji, A. (2005). Acute myocardial infarction secondary to myocardial bridge treated with drug-eluting stent. *Indian Heart Journal.* **57**: 734-737.

Smolich, J.J. (1995). Ultrastructural and functional features of the developing mammalian heart: a brief overview. *Reproduction, Fertility and Development*, **7** (3): 451-61.

Smuts, M.S. and Benzuidenhout, A.J. (1987). *Heart and Arteries in: Anatomy of the Dromedary.* Clavendon press oxford. 142-147.

Stalsberg, H. and de Haan, R.L. (1969). The precardiac areas and formation of the tubular heart in the chick embryo. *Developmental Biology,* **19** (2): 128-159.

Sybers, H.D. and Ashraf, M. (1975). Scanning electron microscopy of the heart. *Recent Advances in Studies on Cardiac Structure and Metabolism*, **6**: 305-311.

Taha, A.A.M. and Abdel-Magied, E.M. (1996). The coronary arteries of the dromedary camel *(Camelus dromedarius)*. *Anatomia Histologia Embryologia,* **25**: 295-299.

Thej, M.J., Kalyani, R. and Kiran, J. (2012). Atherosclerosis and myocardial bridging: Not a benign combination. An autopsy case report. *Journal of Cardiovascular Disease Research,* **3** (2): 176-178.

Thienpont, D., Rochette, F. and Vanparijs, O.F.J. (1986). *Diagnosing Helminthiasis by Corprological Examination*. 2[ed] Ed. Bress, Belgium.

Titus, J.L. (1973). Normal anatomy of the human cardiac conduction system. *Anesthesia and Analgesia*, **52** (4): 508-514.

van den Hoff, M.J.B., Kruithof, B.P.T. and Moorman, A.F.M. (2004). Making more heart muscle. *Bio Essays,* **26**: 248-261.

Verhagen, S.N. Rutten, A. Meijs, M.F. Isgum, I. Cramer, M.J., van der Graaf, Y. Visseren, F.L.J. (2013). Relationship between myocardial bridges and reduced coronary atherosclerosis in patients with angina pectoris. *International Journal of Cardiology*, **167**: 883-888.

Virágh, S. and Challice, C.E. (1977**).** The development of the conduction system in the mouse embryo heart: II. Histogenesis of the atrioventricular node and bundle. *Developmental Biology*, **56** (2): 397-411.

Walls, E.W. (1947). The development of the specialized conducting tissue of the human heart. *Journal of Anatomy*, **81**: 93-110.

Xavier-Vidal, R., Cunha, R.C. and Madi, K. (1997). Quantitative study using semithin section of the rat fetal myocardium. *Revista chilena de anatomía,* **15**2 : 209-216.

Zaffran, S. and Frasch, M. (2002). Early signals in cardiac development. *Circulation Research*, **91** (6): 457-469.

APPENDIX

Between-Subjects Factors

		Value Label	N
stage	1	Stage 1	15
factors	2	Stage 2	60
	3	Stage 3	39
	1	13 cm CVRL	7
	2	18.5 cm CVRL	8
	3	52 Left atrium	5
	4	60 CVRL Ventricular myocardium	9
	5	60 Left Atrium	10
	6	60 Right atrium	10
	7	65 Left atrium	8
	8	65 Right atrium	9
	9	65 myocardial bridges	9
	10	89 Left atrium	4
	11	89 Right atrium	4
	12	89 Myocardial bridge	3
	13	101 Right atrium	7
	14	101 Myocardial bridges	9
	15	112 Left atrium	6
	16	112 Myocardial bridges	6

135

Descriptive Statistics

	stage	factors	Mean	Std. Deviation	N
Myofibril nuclei3000x Length		13 cm CVRL	8.40143	2.006111	7
		18.5 cm CVRL	5.18750	1.291740	8
	Stage 1	Total	6.68733	2.305117	15
	Stage 2				
	Stage 3	52 Left atrium	7.21400	2.647995	5
	Total	60 CVRL Ventricular myocardium	7.16778	1.473582	9
			6.42200	2.743035	10
		60 Left Atrium	8.06400	3.033660	10
		60 Right atrium	5.46125	1.616888	8
		65 Left atrium	5.21667	2.539483	9
		65 Right atrium	6.71000	1.521710	9
		65 myocardial bridges	6.60783	2.395688	60
		Total			
		89 Left atrium	7.71500	1.931951	4
		89 Right atrium	3.86000	.431741	4
		89 Myocardial bridge	9.54000	2.393763	3
		101 Right atrium	5.17429	1.823110	7
		101 Myocardial bridges	4.10778	1.509278	9
		112 Left atrium	9.74000	3.067448	6
		112 Myocardial bridges	7.14167	2.308744	6
		Total	6.39487	2.926379	39
		13 cm CVRL	8.40143	2.006111	7
		18.5 cm CVRL	5.18750	1.291740	8
		52 Left atrium	7.21400	2.647995	5
		60 CVRL Ventricular myocardium	7.16778	1.473582	9
			6.42200	2.743035	10
		60 Left Atrium	8.06400	3.033660	10
		60 Right atrium	5.46125	1.616888	8
		65 Left atrium	5.21667	2.539483	9
		65 Right atrium	6.71000	1.521710	9
		65 myocardial bridges	7.71500	1.931951	4
		89 Left atrium	3.86000	.431741	4
		89 Right atrium	9.54000	2.393763	3
		89 Myocardial bridge	5.17429	1.823110	7
		101 Right atrium	4.10778	1.509278	9
		101 Myocardial bridges	9.74000	3.067448	6
		112 Left atrium	7.14167	2.308744	6
		112 Myocardial bridges	6.54544	2.558778	114
		Total			

136

Descriptive Statistics

	stage	factors	Mean	Std. Deviation	N
Myofibril nuclei3000x Width	Stage 1 Stage 2 Stage 3 Total	13 cm CVRL	4.37429	1.694027	7
		18.5 cm CVRL	2.16250	.378144	8
		Total	3.19467	1.614284	15
		52 Left atrium	3.17800	.973535	5
		60 CVRL Ventricular myocardium	4.15556	1.400519	9
			2.77600	1.118374	10
		60 Left Atrium	3.12100	.653630	10
		60 Right atrium	2.90925	1.116901	8
		65 Left atrium	3.62333	1.382398	9
		65 Right atrium	3.67889	1.059498	9
		65 myocardial bridges	3.35423	1.168743	60
		Total			
		89 Left atrium	3.75250	.774871	4
		89 Right atrium	1.72950	1.135464	4
		89 Myocardial bridge	3.11333	1.086662	3
		101 Right atrium	3.19857	1.123068	7
		101 Myocardial bridges	2.47444	.786100	9
		112 Left atrium	1.30150	.333175	6
		112 Myocardial bridges	2.61000	.787934	6
		Total	2.54864	1.100241	39
		13 cm CVRL	4.37429	1.694027	7
		18.5 cm CVRL	2.16250	.378144	8
		52 Left atrium	3.17800	.973535	5
		60 CVRL Ventricular myocardium	4.15556	1.400519	9
			2.77600	1.118374	10
		60 Left Atrium	3.12100	.653630	10
		60 Right atrium	2.90925	1.116901	8
		65 Left atrium	3.62333	1.382398	9
		65 Right atrium	3.67889	1.059498	9
		65 myocardial bridges	3.75250	.774871	4
		89 Left atrium	1.72950	1.135464	4
		89 Right atrium	3.11333	1.086662	3
		89 Myocardial bridge	3.19857	1.123068	7
		101 Right atrium	2.47444	.786100	9
		101 Myocardial bridges	1.30150	.333175	6
		112 Left atrium	2.61000	.787934	6
		112 Myocardial bridges	3.05764	1.257679	114
		Total			

Between-Subjects Factors

		Value Label	N
stage factors	1	Stage 1	7
	2	Stage 2	3
	3	Stage 3	20
	1	13 cm CVRL	4
	2	18.5 cm CVRL	3
	3	52 Left atrium	3
	11	89 Right atrium	4
	12	89 Myocardial bridge	3
	13	101 Right atrium	4
	14	101 Myocardial bridges	5
	16	112 Myocardial bridges	4

Descriptive Statistics

	stage	factors	Mean	Std. Deviation	N
Connective t. Nuclei 3000 Length	Stage 1 Stage 2 Stage 3 Total	13 cm CVRL	7.88750	.093229	4
		18.5 cm CVRL	4.03000	1.221106	3
		Total	6.23429	2.180114	7
		52 Left atrium	5.95000	.518845	3
		Total	5.95000	.518845	3
		89 Right atrium	2.47000	.225241	4
		89 Myocardial bridge	3.33667	.300222	3
		101 Right atrium	5.09750	1.528820	4
		101 Myocardial bridges	6.88800	1.293781	5
		112 Myocardial bridges	6.60000	1.664191	4
		Total	5.05600	2.106257	20
		13 cm CVRL	7.88750	.093229	4
		18.5 cm CVRL	4.03000	1.221106	3
		52 Left atrium	5.95000	.518845	3
		89 Right atrium	2.47000	.225241	4
		89 Myocardial bridge	3.33667	.300222	3
		101 Right atrium	5.09750	1.528820	4
		101 Myocardial bridges	6.88800	1.293781	5
		112 Myocardial bridges	6.60000	1.664191	4
		Total	5.42033	2.046695	30
Connective t. Nuclei 3000 Width	Stage 1 Stage 2	13 cm CVRL	3.08250	.170367	4
		18.5 cm CVRL	2.52000	.917878	3
		Total	2.84143	.621086	7
		52 Left atrium	2.50000	.842852	3
		Total	2.50000	.842852	3

138

Descriptive Statistics

stage	factors	Mean	Std. Deviation	N
Stage 3 Total	89 Right atrium	1.69750	.012583	4
	89 Myocardial bridge	3.78000	.200000	3
	101 Right atrium	1.94500	.726476	4
	101 Myocardial bridges	2.34360	1.361020	5
	112 Myocardial bridges	3.08000	.478609	4
	Total	2.49740	1.024735	20
	13 cm CVRL	3.08250	.170367	4
	18.5 cm CVRL	2.52000	.917878	3
	52 Left atrium	2.50000	.842852	3
	89 Right atrium	1.69750	.012583	4
	89 Myocardial bridge	3.78000	.200000	3
	101 Right atrium	1.94500	.726476	4
	101 Myocardial bridges	2.34360	1.361020	5
	112 Myocardial bridges	3.08000	.478609	4
	Total	2.57793	.915777	30

Between-Subjects Factors

		Value Label	N
stage	1	Stage 1	10
factors	2	Stage 2	31
	3	Stage 3	45
	1	13 cm CVRL	10
	3	52 Left atrium	3
	4	60 CVRL Ventricular myocardium	5
	5	60 Left Atrium	4
	7	65 Left atrium	5
	8	65 Right atrium	4
	9	65 myocardial bridges	10
	10	89 Left atrium	10
	11	89 Right atrium	4
	12	89 Myocardial bridge	4
	13	101 Right atrium	4
	14	101 Myocardial bridges	4
	15	112 Left atrium	9
	16	112 Myocardial bridges	10

Descriptive Statistics

	stage	factors	Mean	Std. Deviation	N
Mitochondria Length	Stage 1	13 cm CVRL	1.12540	.285578	10
		Total	1.12540	.285578	10
	Stage 2	52 Left atrium	.51667	.100167	3
	Stage 3	60 CVRL Ventricular myocardium	.99060	.351914	5
	Total	60 Left Atrium	.76100	.136127	4
		65 Left atrium	1.03300	.645545	5
		65 Right atrium	.85300	.218637	4
		65 myocardial bridges	.98170	.284876	10
		Total	.90132	.357532	31
		89 Left atrium	.77410	.240441	10
		89 Right atrium	.41875	.129147	4
		89 Myocardial bridge	1.24475	.547446	4
		101 Right atrium	1.01575	.450046	4
		101 Myocardial bridges	.98475	.279983	4
		112 Left atrium	.77189	.183931	9
		112 Myocardial bridges	.93560	.217325	10
		Total	.86000	.328183	45
		13 cm CVRL	1.12540	.285578	10
		52 Left atrium	.51667	.100167	3

Descriptive Statistics

stage	factors	Mean	Std. Deviation	N
	60 CVRL Ventricular myocardium	.99060	.351914	5
	60 Left Atrium	.76100	.136127	4
	65 Left atrium	1.03300	.645545	5
	65 Right atrium	.85300	.218637	4
	65 myocardial bridges	.98170	.284876	10
	89 Left atrium	.77410	.240441	10
	89 Right atrium	.41875	.129147	4
	89 Myocardial bridge	1.24475	.547446	4
	101 Right atrium	1.01575	.450046	4
	101 Myocardial bridges	.98475	.279983	4
	112 Left atrium	.77189	.183931	9
	112 Myocardial bridges	.93560	.217325	10
	Total	.90576	.341021	86
	13 cm CVRL	.55010	.120050	10
	Total	.55010	.120050	10
	52 Left atrium	.42367	.064516	3
	60 CVRL Ventricular myocardium	.47200	.180357	5
	60 Left Atrium	.33600	.070071	4
	65 Left atrium	.43700	.032117	5
	65 Right atrium	.46925	.047020	4
	65 myocardial bridges	.83120	.227592	10
	Total	.55965	.242856	31
	89 Left atrium	.45290	.145974	10
	89 Right atrium	.37975	.099544	4
	89 Myocardial bridge	.91650	.258340	4
	101 Right atrium	.30025	.090515	4
	101 Myocardial bridges	.65225	.012093	4
	112 Left atrium	.47033	.219867	9
	112 Myocardial bridges	.73720	.174741	10
	Total	.55842	.240807	45
	13 cm CVRL	.55010	.120050	10
	52 Left atrium	.42367	.064516	3
	60 CVRL Ventricular myocardium	.47200	.180357	5
	60 Left Atrium	.33600	.070071	4
	65 Left atrium	.43700	.032117	5
	65 Right atrium	.46925	.047020	4
	65 myocardial bridges	.83120	.227592	10

Mitochondria Width Stage 1 Stage 2 Stage 3 Total

141

Descriptive Statistics

stage	factors	Mean	Std. Deviation	N
	89 Left atrium	.45290	.145974	10
	89 Right atrium	.37975	.099544	4
	89 Myocardial bridge	.91650	.258340	4
	101 Right atrium	.30025	.090515	4
	101 Myocardial bridges	.65225	.012093	4
	112 Left atrium	.47033	.219867	9
	112 Myocardial bridges	.73720	.174741	10
	Total	.55790	.228841	86

Between-Subjects Factors

		Value Label	N
stage	1	Stage 1	20
factors	2	Stage 2	56
	3	Stage 3	31
	1	13 cm CVRL	10
	2	18.5 cm CVRL	10
	3	52 Left atrium	10
	4	60 CVRL Ventricular myocardium	10
	5	60 Left Atrium	8
	6	60 Right atrium	4
	7	65 Left atrium	6
	8	65 Right atrium	8
	9	65 myocardial bridges	10
	10	89 Left atrium	4
	12	89 Myocardial bridge	7
	13	101 Right atrium	10
	15	112 Left atrium	6
	16	112 Myocardial bridges	4

Descriptive Statistics

Dependent Variable: Space between 2 Z lines 3000X

stage	factors	Mean	Std. Deviation	N
Stage 1	13 cm CVRL	1.05000	.201031	10
	18.5 cm CVRL	1.32500	.165814	10
	Total	1.18750	.228185	20
Stage 2	52 Left atrium	1.27930	.285317	10
	60 CVRL Ventricular myocardium	1.01800	.201713	10
	60 Left Atrium	1.32000	.169537	8
	60 Right atrium	2.68500	.269011	4
	65 Left atrium	.86400	.160568	6
	65 Right atrium	1.45750	.157094	8
	65 myocardial bridges	1.07760	.167570	10
	Total	1.28380	.474171	56
Stage 3	89 Left atrium	1.81000	.084063	4
	89 Myocardial bridge	1.23429	.159359	7
	101 Right atrium	1.75700	.246489	10
	112 Left atrium	1.83667	.286193	6
	112 Myocardial bridges	2.47500	.136991	4
	Total	1.75387	.416731	31
Total	13 cm CVRL	1.05000	.201031	10
	18.5 cm CVRL	1.32500	.165814	10
	52 Left atrium	1.27930	.285317	10
	60 CVRL Ventricular myocardium	1.01800	.201713	10
	60 Left Atrium	1.32000	.169537	8
	60 Right atrium	2.68500	.269011	4
	65 Left atrium	.86400	.160568	6
	65 Right atrium	1.45750	.157094	8
	65 myocardial bridges	1.07760	.167570	10
	89 Left atrium	1.81000	.084063	4
	89 Myocardial bridge	1.23429	.159359	7
	101 Right atrium	1.75700	.246489	10
	112 Left atrium	1.83667	.286193	6
	112 Myocardial bridges	2.47500	.136991	4
	Total	1.40199	.476881	107